University of Huddersfield Repository

Agbenorhevi, Jacob Kwaku

Phase Behaviour Of Oat β-Glucan/Sodium Caseinate Mixtures

Original Citation

Agbenorhevi, Jacob Kwaku (2011) Phase Behaviour Of Oat β-Glucan/Sodium Caseinate Mixtures. Doctoral thesis, University of Huddersfield.

This version is available at http://eprints.hud.ac.uk/id/eprint/17475/

PHASE BEHAVIOUR OF OAT β-GLUCAN/SODIUM CASEINATE MIXTURES

JACOB KWAKU AGBENORHEVI

A thesis submitted to the University of Huddersfield

in partial fulfilment of the requirements for the degree of

Doctor of Philosophy

December 2011

Acknowledgements

Abstract

Oat β-glucan is a water soluble polysaccharide which has been approved as a functional bioactive ingredient. In this thesis, β-glucan was successfully isolated from oat flour and samples of different molecular weights were produced. The structural features and molecular weights (Mw) were characterized by ^{13}C–NMR spectroscopy and high performance size-exclusion chromatography, respectively. The rheological properties and microstructure of aqueous oat β-glucan solutions were investigated by rheometry and atomic force microscopy (AFM), respectively. The samples with β-glucan content between 78-86 % on a dry weight basis had Mw, intrinsic viscosity ([η]) and critical coil overlap concentration (c*) in the range of 142 - 2800 x 10^3 g/mol, 1.7 - 7.2 dL/g and 0.25 - 1.10 g/dL, respectively. The flow and viscoelastic behaviour was highly dependent on Mw and on the concentration of the β-glucan solutions. AFM images revealed the formation of cluster or aggregates linked via individual polymer chains scattered heterogeneously throughout the system. The aggregate size was also dependent on molecular weight of the samples and influences the rheological behaviour of β-glucan solutions. The isothermal phase behaviour at 5 ^{o}C of β-glucan/sodium caseinate mixtures were investigated by means of phase diagram construction, rheometry, electrophoresis and fluorescence microscopy. Phase diagrams indicated that the compatibility of the β-glucan/sodium caseinate system increases as β-glucan Mw decreases. Images of the mixtures taken at various biopolymer concentrations revealed phase separation with the presence of β-glucan aggregates, whose size depends on Mw and concentration. At the same protein concentration in the mixtures, the viscosity increases with increasing Mw and concentration of β-glucan. However, the results also revealed that in the state of thermodynamic equilibrium with comparable polymer concentrations in mixture, the lower Mw samples yielded similar or higher viscosity. At equivalent hydrodynamic volume of β-glucan component in the mixture, all the samples exhibited similar viscosity/flow behaviour. A deviation dependent on the protein concentration was observed for the high Mw sample in the concentrated regime due to the size of the β-glucan aggregates formed. Results demonstrate that by controlling the structural features of β-glucan in mixture with sodium caseinate, informed manipulation of rheological properties in these systems can be achieved.

Contents

List of Figures

List of Tables

CHAPTER 1

1. INTRODUCTION

1.1 Context of the work

Oat (*Avena sativa L.*) and its products exhibit significant positive health effects including cholesterol lowering, modulation of glucose and insulin responses, weight management and improved gastrointestinal function. This is attributed to β-glucan, which has been accepted as a functional, bioactive ingredient (Braaten *et al.*, 1994a; Braaten *et al.*, 1994b; Behall *et al.*, 2004; Duss and Nyberg, 2004; Brennan and Cleary, 2005; Duss, 2005; Lazaridou and Biliaderis, 2007; Wood, 2007; Othman *et al.,* 2011).

β-Glucan either in the pure form or concentrated cereal fractions have been successfully incorporated into various products such as breakfast cereals, pasta, noodles and baked goods, as well as dairy and meat products (Cavallero *et al.*, 2002; Duss and Nyberg, 2004; Volikakis *et al.*, 2004; Izydorczyk *et al.*, 2005). The physical properties of β-glucan, such as solubility and rheological behaviour in the solution and gel states, are determined by the polysaccharide structure, molecular weight, temperature and concentration (Lazaridou *et al.*, 2003; Skendi *et al.*, 2003; Tosh *et al.*, 2004b; Vaikousi *et al.*, 2004; Papageorgiou *et al.*, 2005). It has been reported that when β-glucan is incorporated into various food products, attributes such as thickening ability, water binding and emulsion stabilising capacity, texture, and appearance are often related to the concentration, molecular weight and structure of the polysaccharide. The physiological effects of β-glucan, such as lowering blood cholesterol levels and regulating postprandial glucose and insulin responses, are also correlated with the amount and molecular weight of the solubilised β-glucan (Lazaridou and Biliaderis, 2007; Wood, 2007).

Increased interest in β-glucans has stimulated new product development activity over the years (Brennan and Cleary, 2005). Incorporation of *β*-glucans into milk and dairy products presents potential application of this polysaccharide to confer the associated health benefits to consumers. However, the recommended amount (≥ 0.75 g/serving, 3g/day) by the Food and Drug Administration (FDA) and the Joint Health Claims Initiative (JHCI) for health claims (lowering serum cholesterol levels to reduce the risk of heart disease) (FDA, 1997; JHCI, 2004) presents some challenges in the development of food formulations. At this quantity, *β*-glucan exhibits thermodynamic incompatibility when mixed with milk proteins (Kontogiorgos *et al.*, 2009a; Kontogiorgos *et al.*, 2009b).

The nature and strength of the protein-polysaccharide interactions determines the miscibility/stability, structural, rheological and textural characteristics of food products. The phase behaviour of protein-polysaccharide mixtures is also dependent on the molecular characteristics (molecular weight, conformation, charge density) and the concentration of the biopolymers as well as the mixing conditions (Tolstoguzov, 1997; Schmitt *et al.*, 1998; Doublier *et al.*, 2000; Tolstoguzov, 2000; de Kruif and Tuinier, 2001; Tolstoguzov, 2003; Turgeon *et al.*, 2003; Tolstoguzov, 2006; Perez *et al.*, 2009). Therefore, understanding of the phase behaviour of *β*-glucan with milk proteins will be useful in the design of products with desired flow, structure and texture.

The general aim of this thesis, therefore, is to characterize the physical properties of oat *β*-glucan varying in molecular weight and the phase behaviour when mixed with milk proteins.

1.2 β-Glucan

1.2.1 Definition and structural features

Glucans are polysaccharides that only contain D-glucose monomers linked by glycosidic bonds. *β*-Glucans (*beta-glucans*) found in cereals are linear homopolysaccharides of consecutively linked (1→4)-*β*-D-glucopyranosyl residues that are separated by single (1→3) linkages (Figure 1.1). The polysaccharide is neutral and made up of approximately 70% *β*-(1→4) and 30 % *β*-(1→3)-linkages (Wood *et al.*, 1994b). The (1→4)-linkages occur mostly in groups of two or three whereas (1→3)-linkages occur individually. The resulting polysaccharide structure is built mainly from *β*-(1→3)-linked cellotriosyl (58–72%) and cellotetraosyl (20–34%) units, but sequences with consecutive (1→4) linkages longer than the tetraose type and up to 14 glucosyl units are also known to exist in minor amounts. Significant structural differences in cereal *β*-glucans, as indicated by the trisaccharide to tetrasaccharide ratios, have been reported between different genera of cereals (oat, rye, barley, and wheat). This has been shown through quantitative analysis of lichenase released oligosaccharides. The enzyme lichenase, a (1→3)(1→4)-*β*-D-glucan-4-glucanohydrolase (EC 3.2.1.73), specifically cleaves the (1→4)-glycosidic linkages of the three-substituted glucose residues in *β*-glucan, yielding oligomers with different degrees of polymerisation (DP) (Figure 1.2) (Lazaridou and Biliaderis, 2007).
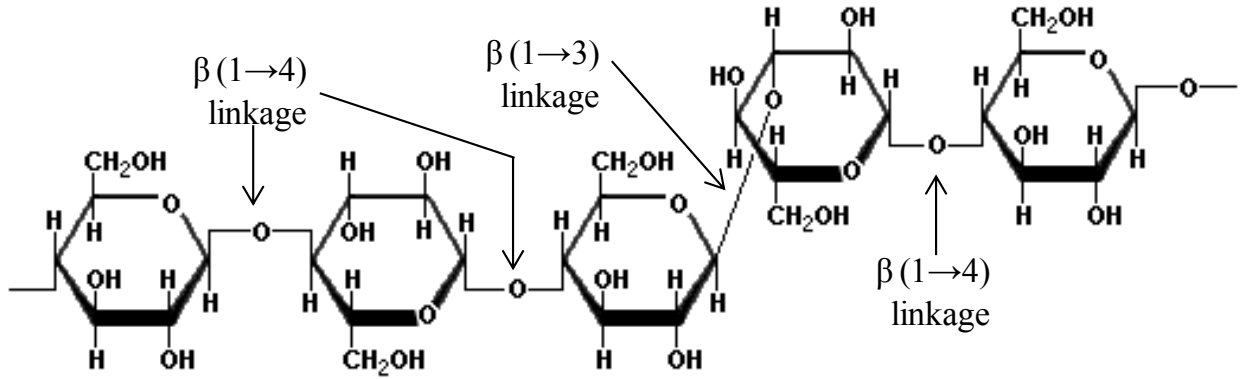
Figure 1.1: Chemical structure of cereal β-glucan
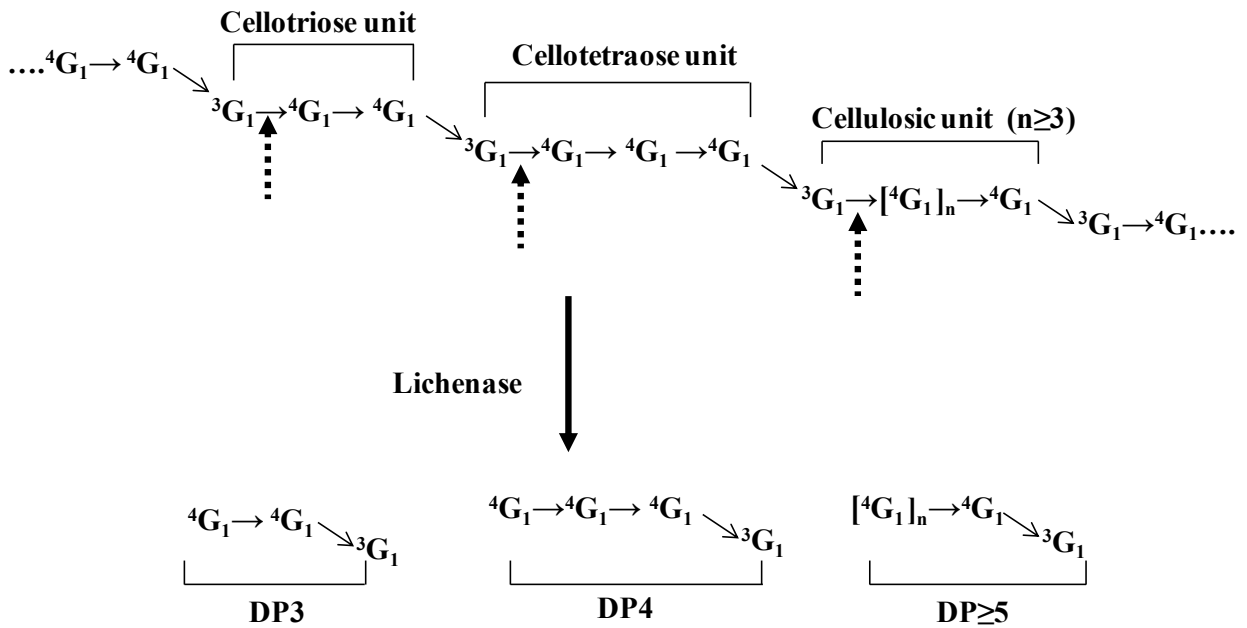
Figure 1.2: Generalised structure of cereal β-glucan and debranching with lichenase (adapted from Lazaridou and Biliaderis, 2007).

The majority of hydrolysis products of cereal β-glucans are 3-O-β-cellobiosyl-D-glucose (DP3) and 3-O-β-cellotriosyl-D-glucose (DP4), but cellodextrin-like oligosaccharides (DP$\geq$5) are also released in smaller amounts (5–10%) from the polymer regions containing more than three consecutive 4-O-linked glucose residues. The DP of the long cellulose-like fragments varies

15

between 5-20, with DP 5, 6, and 9 being the most common (Wood *et al.*, 1994b; Izydorczyk *et al.*, 1998; Lazaridou *et al.*, 2004). It has been shown that the cellotriosyl and cellotetraosyl segments are distributed in a random pattern in the polymer. The relative amount of DP3 in the *β*-glucans decreases from wheat (67–72%), to barley (52–69%) and oats (53–61%), whereas that of DP4 follows the opposite trend, i.e. increases from wheat (21–24%), to barley (25–33%) and oats (34–41%). But, the collective tri- and tetrasaccharides components are similar among *β*-glucans from different cereal genera, resulting in similar total amount of cellulose-like oligomers with DP≥5. The differences in the proportions of tri- and tetrasaccharides observed among different *β*-glucans from various sources are also reflected in the molar ratio of cellotriose to cellotetraose units (DP3:DP4), following the order of wheat (3.0–4.5), barley (1.8–3.5), rye (1.9–3.0) and oats (1.5–2.3). This ratio is considered to be a fingerprint of the structure of cereal *β*-glucans. It is also known that there some differences exist in the ratio of DP3:DP4 within the same genera, due to genotypic and environmental factors (Lazaridou and Biliaderis, 2007).

1.2.2 Molecular weight

Molecular weight (Mw) values for *β*-glucans in the range of 20–3100 $\times 10^3$, 31–2700 $\times 10^3$, 21–1100$\times 10^3$, and 209–487$\times 10^3$ g/mol have been reported for oats, barley, rye, and wheat, respectively. The differences in the Mw estimates of *β*-glucans are attributed to the botanical source, environmental factors, extraction/isolation protocols, and the analytical methodology used in the determination of these values (Cui and Wood, 2000; Izydorczyk and Biliaderis, 2000; Lazaridou *et al.*, 2003; Lazaridou and Biliaderis, 2007; Andersson and Börjesdotter, 2011).

1.2.3 Occurrence

β-Glucan in cereals (oats, barley, rye and wheat) is the predominant component of the endosperm cell walls of the grains. Oat *β*-glucan is located throughout the starchy endosperm and is concentrated in the aleurone and sub-aleurone layer (Figure 1.3). The content of *β*-glucan, ranges from 1 % in wheat grains to 3–9 % in oats, and 5–11 % in barley (Skendi *et al.*, 2003; Warrand, 2006).
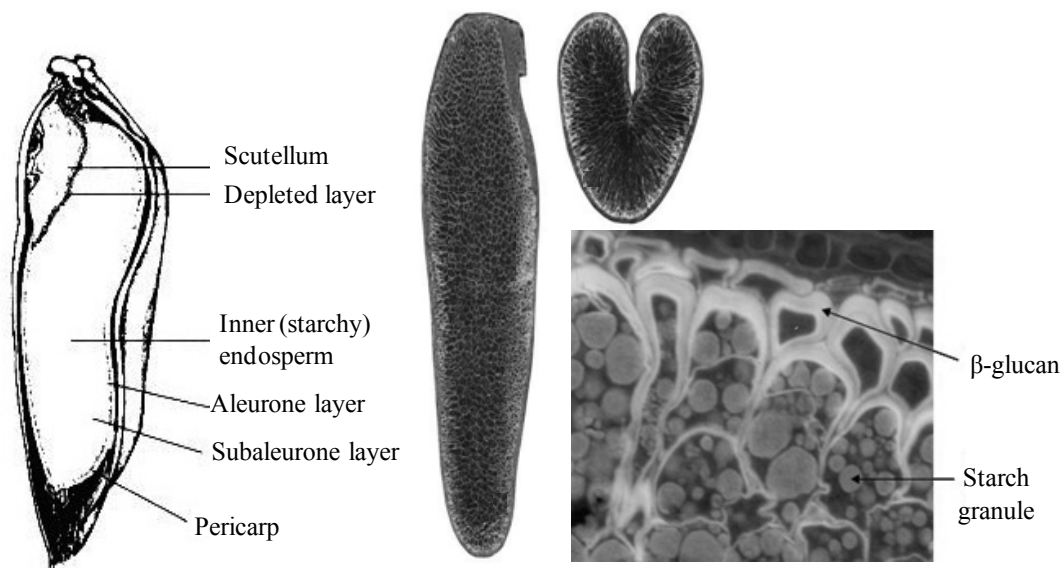
Figure 1.3: Structure of oat grain and locations of *β*-glucan (adapted from Webster, 1986; Oats and Health, 2007).

1.2.4 Solution properties

β-Glucans are water soluble and have the capacity to form highly viscous solutions. The mixed linkages that form the *β*-glucan structure as well as the arrangement of the cellotriosyl and cellotetraosyl units in the polymer chain are believed to be important determinants of the solution properties of *β*-glucans (Böhm and Kulicke, 1999b; Cui *et al.*, 2000; Tosh *et al.*, 2004a; Lazaridou and Biliaderis, 2007). The presence of two types of linkages prevents compact folding of the *β*-glucan chains, making them soluble in water. Thus the *β*-(1→3) linkages break up the

regularity of the β-(1→4) linkage sequence, making the molecule soluble and flexible. It has been suggested that non-consecutive occurrence of β-(1→3) linkages along the polymeric chain contribute to solubility and flexibility of (1→3),(1→4)-β-glucans whilst the regularity of the (1→4) linkages is considered to be responsible for insolubility and aggregation phenomena (Buliga *et al.*, 1986; Woodward *et al.*, 1988). Two possible aggregation mechanisms have been suggested (Figure 1.4). The first suggestion was that hydrogen bonds would form between the long cellulose-like segments (β-(1→4) linked D-glucopyranosyl units) of two or more neighbouring polymer chains and form stable zones, hence formation of aggregates (Woodward *et al.*, 1983; Varum and Smidsrod, 1988; Doublier and Wood, 1995). The second proposal was that hydrogen bonds could form between consecutive cellotriosyl units and form stable junction zones (Böhm and Kulicke, 1999b; Cui *et al.*, 2000; Tosh *et al.* 2004a, b) (Figure 1.4).
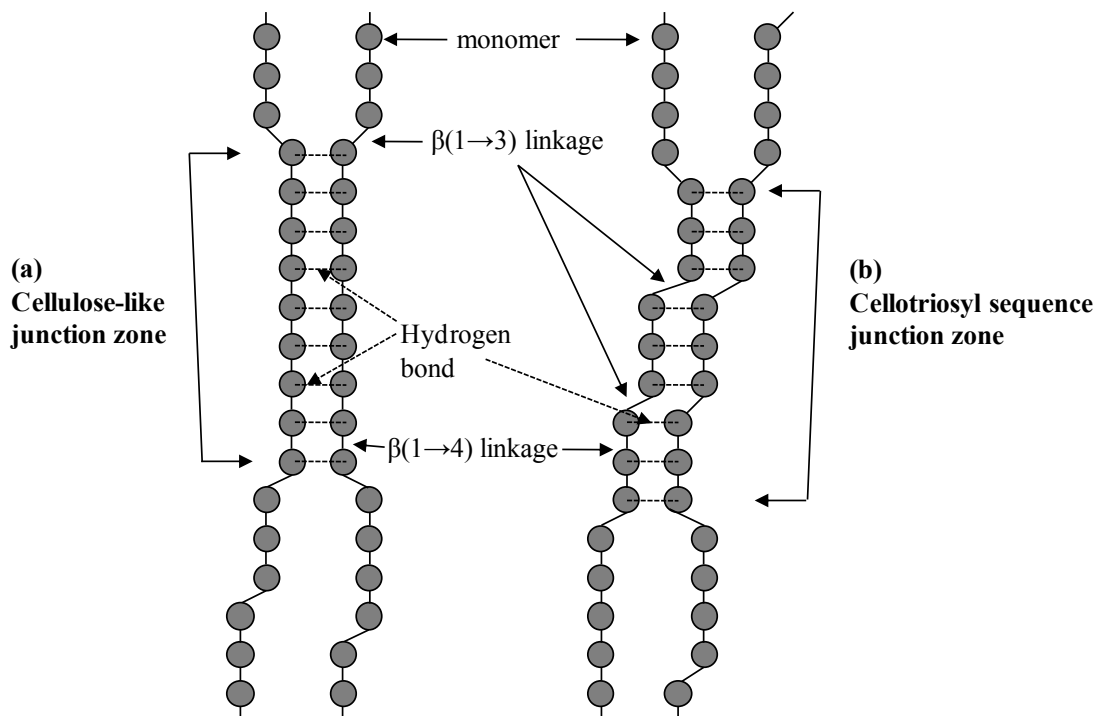
Figure 1.4: Schematic diagrams of interactions that may form junction zones between (1→3)(1→4)-β-D-glucan molecules. (a) Interaction between cellulose-like sections of the polymer and (b) interaction between sequential cellotriosyl units (adapted from Tosh *et al.*, 2004a).

It has been shown from rheological measurements that solutions of cereal *β*-glucans exhibit behaviour typical of non-interacting disordered polysaccharides with chain entanglements in the concentrated state. Intrinsic viscosity values, which depend largely on the molecular weight of the isolated polysaccharides in the range of 0.28 - 9.6 dL/g have been reported for *β*-glucans (Lazaridou and Biliaderis, 2007). Some studies have shown that the viscosity and viscoelastic properties are also dependent on the molecular weight and concentration. With increasing molecular weight and/or concentration of polysaccharide, there is an increase in viscosity as well as in the shear thinning and viscoelastic properties of aqueous *β*-glucan solutions (Irakli *et al*.,2004; Lazaridou *et al*., 2003, 2004; Skendi *et al*., 2003;Vaikousi *et al*., 2004). Doublier and Wood (1995) reported that unhydrolysed *β*-glucan behaves like a non-interacting polysaccharide whereas the hydrolyzed *β*-glucans aggregate and exhibit gel-like behaviour. Tosh *et al.* (2004b) studied the gelation of *β*-glucans partially hydrolyzed by acid, lichenase and cellulase. They showed that the method of hydrolysis had an effect on gel formation and concluded that it is the (1→3)-linked cellotriose segments that form the junction zones needed for gelation rather than the cellulose-like sequences. Lazaridou *et al*. (2003) found that the gelation rate decreased and the gelation time increased with increasing molecular weight. The hypothesis for this phenomenon is that small molecules have higher mobility (i.e. less restriction of diffusion) than the larger ones, thus more readily interact with each other to form a stable junction zone and consequently form aggregates. Increased aggregation leads to the formation of the three-dimensional gel networks at the concentrated solution regime. Li *et al*. (2011) studied the aggregation behaviour using static and dynamic light scattering and found that the structural features of cereal *β*-glucans played an important role on their aggregation behaviour. As molecular weight increased the degree of aggregation decreased due to the lower diffusion rate

of large molecules. For the more rigid conformation (lower diffusion rate) of *β*-glucans with higher tri/tetra ratio, their degrees of aggregation were lower. Their results suggested that the aggregation process was diffusion limited.

1.2.5 Physiological effects

The United States Food and Drug Administration (FDA) and the United Kingdom Joint Health Claims Initiative (JHCI) have allowed a cholesterol-lowering health claim in which it is recommended that a daily intake of 3 g of soluble oat *β*-glucan can lower the risk of coronary heart disease (FDA, 1997; JHCI, 2004). A number of studies have shown that oat and barley *β*-glucans exhibit physiological effects, including lowering cholesterol levels and attenuating postprandial glycemic response (Wood *et al.*, 1990; Ripsin *et al.*, 1992; Kahlon *et al.*, 1993. Wood *et al.*, 1990; Braaten *et al.*,1994b; Tappy *et al.*, 1996; Bourdon *et al.*,1999; Kalra and Jood , 2000; Cavallero *et al.*, 2002, Wood, 2007). Oat *β*-glucan is also known to demonstrate other physiological effects. According to Mälkki and Virtanen (2001) oat fibre prolongs satiety after meals and alleviates constipation. In the large bowel, oat fibre also acts as a substrate for fermentation by probiotic bacterial strains enhancing the formation of short-chain fatty acids (acetic, propionic and butyric acids) which enhance the growth of normal colonic cells – thus reduce the risk of colon cancer.

Different mechanisms by which *β*-glucans exert the associated physiological effects have been proposed. The most common hypothesis is that *β*-glucans exert their effects mainly by increasing the viscosity in the small intestine. It has been suggested that *β*-glucans decrease the absorption and reabsorption of cholesterol, bile acids, and their metabolites by increasing the viscosity of the gastrointestinal tract contents as well as delaying gastric emptying and the intestinal absorption of nutrients, such as digestible carbohydrates, and hence reducing postprandial blood glucose and insulin secretion. It has also been suggested that the viscous oat

β-glucans encapsulate bile acids and cause their excretion in faeces. The synthesis of new bile acids requires cholesterol, which the liver extracts from the blood, decreasing the blood cholesterol levels (Bourdon *et al.*, 1999; Mälkki and Virtanen, 2001; Dikeman and Fahey, 2006; Lazaridou and Biliaderis, 2007; Othman *et al.,* 2011).

Wood *et al.* (1994a) showed that there is a highly significant ($p < 0.0001$) inverse linear relationships between viscosity of β-glucan and the plasma glucose and insulin responses (Figure 1.5). According to their findings, viscosity accounted for 79-96% of the changes in plasma glucose and insulin response tested.
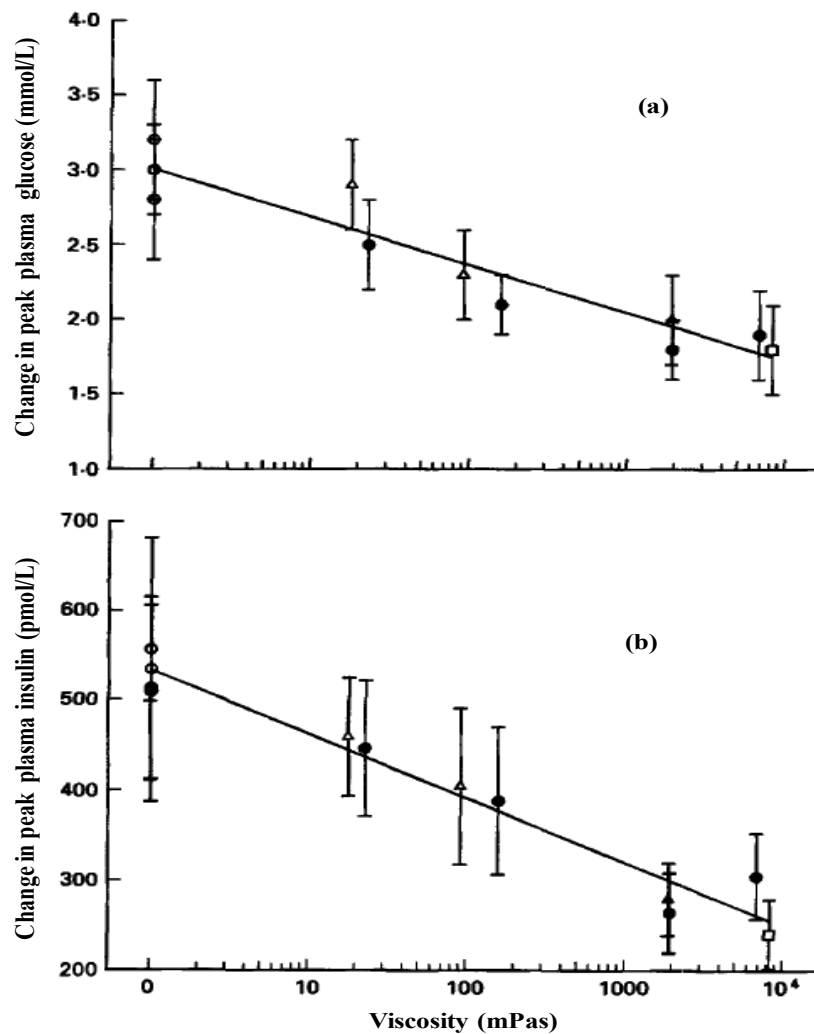
Figure 1.5: Relationship in increment in (a) peak plasma glucose and (b) peak plasma insulin to log [viscosity] (adapted from Wood *et al.,* 1994a).

21

Wood *et al.* (2000) also found a significant inverse relationship between changes in peak blood glucose and a combination of logarithm of the concentration and logarithm of molecular weight of *β*-glucans consumed in a drink (Figure 1.6).
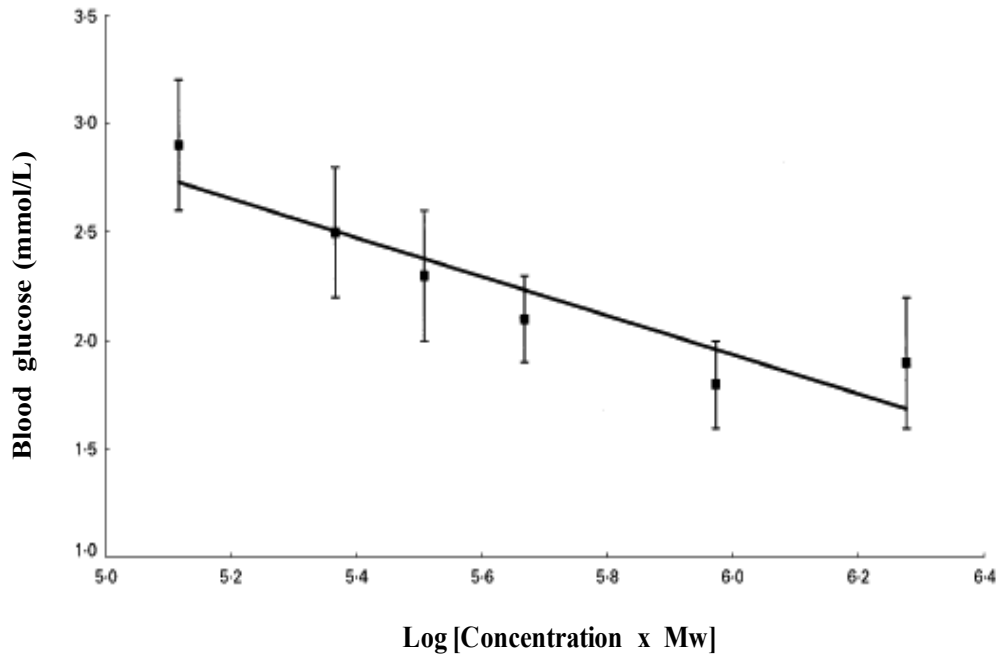
Figure 1.6: Relationship of peak blood glucose increment to log [concentration and molecular weight] of β-glucan consumed (adapted from Wood *et al.*, 2000).

Cavallero *et al.* (2002) studied the effect of barley *β*-glucan on human glycemic response and found a decrease in glycemic index with increasing *β*-glucan content of bread. Tosh *et al.* (2008) measured the glycemic response elicited by oat bran muffins containing *β*-glucans of different molecular weight in healthy subjects and found a significant correlation ($r^2 = 0.729$, $P < 0.001$) between the peak blood glucose and the product of the extractable *β*-glucan content and the molecular weight of the *β*-glucan extracted.

The solubility and viscosity properties of *β*-glucans are known to be affected by their structural features, concentration and molecular weight and these factors are believed to play a role on their physiological effect. However, the role of viscosity of *β*-glucans has not been

directly demonstrated for lowering of serum cholesterol levels, and not all studies reported a statistically significant lowering (Wood, 2007). For instance, in a recent study by Immerstrand *et al.* (2010), the cholesterol lowering effect of oat bran preparations differing in molecular weight of *β*-glucans was evaluated. It was shown that all the oat bran preparations investigated significantly reduced the plasma cholesterol regardless of molecular weight of *β*-glucan. It was also found that the difference in the viscous properties between the processed oat bran preparations (from 0.11 to 17.7 dL/g) did not play a major role in the cholesterol lowering properties. Bae *et al.* (2009) prepared oat *β*-glucan samples of different molecular weights (1450, 730, 370×10^3 g/mol) by enzymatic hydrolysis and evaluated their physicochemical, hypocholesterolemic, and weight-reducing characteristics. They showed that a decrease in the molecular weight resulted in reduced viscosity which also affected swelling power and bile acid/fat binding capacities. When mice were fed high-fat diet supplemented with *β*-glucans of different molecular weights, the diets treated with *β*-glucans significantly reduced the body weight of the mice. However, the molecular weight of *β*-glucans did not significantly affect the serum lipid profile and no linear correlations between molecular weight and in vitro bile acid/fat binding capacity were observed. Their findings showed that the molecular weight of *β*-glucan was not a sole factor contributing to the lipid profile in serum since the molecular weight of oat *β*-glucan was not always positively correlated with weight gain and lipid profile of mice. According to their study, partially hydrolyzed oat *β*-glucan was shown to have great potential to be used in a wider range of food applications without significant loss in biological functions since it can impart suitable viscosity to foods.

Bae *et al.* (2010) also evaluated the *in vivo* hypocholesterolemic effects in rats fed with high-cholesterol diets. Supplements with *β*-glucan hydrolysate as well as native *β*-glucan

significantly reduced the levels of low-density lipoprotein (LDL) cholesterol in serum and further improved the lipid profile in liver. They observed greater faecal bile acid excretion when rats were fed high-cholesterol diets supplemented with the *β*-glucan hydrolysate, which could be favourably correlated to *in vitro* bile acid binding capacity. They also found that the hydrolysate was more effective at increasing the excretion of faecal cholesterol and triglyceride than the native *β*-glucan, showing its effectiveness in improving the lipid profile.

It is also known that the food matrix may also influence the physiological effects though this is still not fully understood. For instance, liquid food fibre preparations have been shown to be more effective physiologically than solid food counterparts. It has been reported that orange juice enriched with oat *β*-glucans gave a lower total and LDL-cholesterol in a mildly hypercholesterolemic subjects than the same preparation of *β*-glucan when added to bread and cookies. These results, however, may also be due to the effect of food processing on the *β*-glucans. Also, in the gastrointestinal tract there are a number of factors which may influence the viscosity, solubility and molecular weight and thus the efficacy of the *β*-glucan enriched foods (Kerckhoffs *et al.*, 2003; Brennan and Cleary, 2005; Lazaridou and Biliaderis, 2007; Cui and Roberts, 2009).

1.2.6 Applications of *β*-glucans

β-Glucans from cereals have gained much public and research interests largely due to the acceptance as a functional, bioactive ingredient (Cui and Wood, 2000). The approvals in the EU, UK and USA of health claims for oat *β*-glucan have stimulated new product development activity and worldwide application of *β*-glucans in the food and nutraceutical industries (Duss and Nyberg, 2004; Cui and Roberts, 2009). *β*-Glucans can impart high viscosity to aqueous solutions due to their high molecular weight, conformation, and interactive properties. The

structural and molecular features of β-glucan are important determinants of their physical properties and functionality when utilized as ingredients in cereal-based foods and other formulated products. The potential use of β-glucan as food hydrocolloid has also been proposed based on their rheological characteristics (Lazaridou *et al.*, 2003). Because of formation of high viscosity solutions, β-glucan could be utilized as thickening agent in sauces, salad dressings, or in ice cream formulations. As an active component in oat products (such as whole oats, oat bran, oatmeal, etc.), β-glucans have been used in various reduced-fat and soluble fibre-enriched foods, mostly in breakfast cereals and snack foods (Cui, 2000; Brennan and Cleary, 2005).

Several oat and barley β-glucan rich products have emerged and are available as food ingredients. Some of these include: Glucagel™ from barley β-glucan prepared by extraction and partial hydrolysis, Oatwell®, Nutrim and Oatrim (oat β-glucan amylodextrins) made from oats by treating oat bran or flour with thermostable α-amylase at high temperatures, and Viscofiber® made from both oats and barley by water-alcohol treatment of the flours with or without enzymes. Glucagel™ has gelling and fat mimetic properties, and is used as fat substitutes in dairy products, bakeries, dressings and edible films. The use of Oatrim in foods includes bakery products, frozen desserts, processed meats, sauces and beverages. Oatrim is also used as a fat replacer (Inglett, 1990; Lee *et al.*, 2005). Nutrim and Viscofiber® are also available as dietary supplements (Cui and Roberts, 2009).

1.3 Milk Proteins

Bovine milk proteins are divided into two major categories: caseins (~ 80 wt%) and whey proteins (~20 wt%). The main whey proteins are β-lactoglobulin (~50 wt%), and α-lactalbumin (~20 wt%). Both proteins have globular conformations and molecular weights of ~18 kDa and

~14 kDa, repectively. They represent approximately 70% of the total whey proteins and are responsible for hydration, gelling, and surface-active properties (emulsifying and foaming properties) of whey protein ingredients. The remaining whey proteins are bovine serum albumin (~ 66 kDa, ~5 wt%), immunoglobulins (148–1000 kDa, ~13 wt%), lactoferrin (80–92 kDa, ~3% wt) and other minor proteins (proteose–peptones) (Wong *et al.*, 1996; Cayot and Lorient, 1997).

Four main caseins present in bovine milk are α_{s1}-, α_{s2}-, β-, and κ-caseins in the approximate ratio of 4:1:4:1. The characteristic features of caseins are summarized in Table 1.1.

Table 1.1: Some characteristics of caseins in bovine milk

Protein	% in Total Casein	Molecular Weight (~kDa)	Amino Acid Residues			Phosphate Groups
			Total	Proline	Cysteine	
α_{s1}-casein	40-45	23	199	17	0	8-9
α_{s2}-casein	10	25	207	10	2	10-13
β-casein	35-40	24	209	35	0	5
κ-casein	9-15	19	169	20	2	1-2

(adapted from Dalgleish, 1997; Fox and Kelly, 2006).

The major caseins (α_{s1}-, and β-caseins) contain neither cysteine nor cystine and therefore lack the capacity to form inter- or intramolecular disulfide bonds. The minor caseins (α_{s2}-, and κ-caseins), however, each contain two cysteinyl residues and these are known to form intermolecular disulfide bonds. These proteins do not possess well defined tertiary structures, and they have phosphoseryl residues that bind to calcium phosphate. The exception to this behaviour is κ-casein, which has only one or rarely two phosphoseryl residues and binds little Ca^{2+}, and are very resistant to calcium precipitation, stabilizing other caseins. Rennet cleavage

26

occurs at the Phe105-Met106 bond and this eliminates the stabilizing ability, leaving a hydrophobic portion, *para*-κ-caseins, and a hydrophilic portion called caseinomacropeptide (CMP) (Dalgleish, 1997; Corredig *et al.*, 2011).

The various caseins are assembled together in aggregated structure as spherical colloidal particles called casein micelle, with a mean diameter of about 120 nm (range, 50-600 nm) and an average particle mass of 10^5 kDa (i.e., an average micelle contain about 5000 molecules) (Fox and Kelly, 2006). A casein micelle is regarded as a core consisting of a mixture of α_s- and β-caseins stabilized by a surface coat of κ-casein (Figure 1.7) and the proteins are held together by calcium phosphate nanoclusters, hydrophobic interactions, hydrogen bonding and van der Waals interactions.

Casein micelle

Casein submicelle

hydrophobic core

κ-casein enriched surface

CMP hairy layer

calcium phosphate
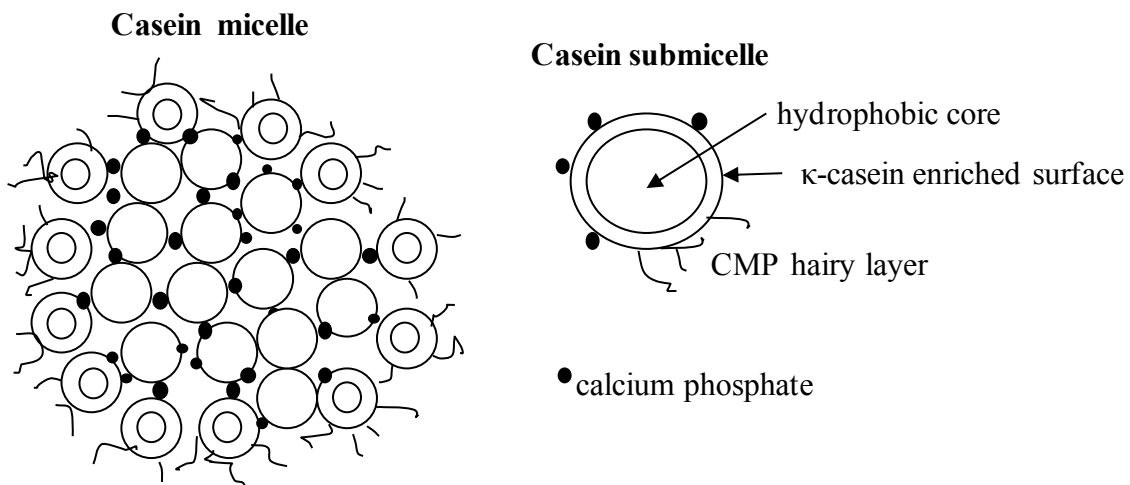
Figure 1.7: Structure of casein micelle (adapted from Goff, 1995; Fox and Kelly, 2006).

Majority of κ-casein is located on the surface of the casein micelle, where it imparts steric stability, by protruding into the serum phase with its hydrophilic glycosylated portion. The uneven, rough surface of the casein micelles is believed to influence the interactions with other biomolecules, such as polysaccharides. The interior of micelles will not be accessible to large

molecules, and so the polyelectrolyte layer of κ-casein is what drives the polysaccharide molecules to attraction or repulsion at close distance (Corredig *et al*., 2011).

Unlike whey proteins which unfold and denature at temperatures above 60 °C, casein micelles are mostly unaffected by heating at temperatures below 100 °C. Gelation occurs in milk by acid coagulation, enzymatic hydrolysis, heating and even during storage. During rennet coagulation the release of CMP reduces steric repulsion of the casein micelles thus enhancing interactions and resulting in aggregation. Thus caseins form a gel when more than 85% of κ-casein is hydrolyzed. During acidification or fermentation, destabilization of the micelles occurs near the isoelectric point of the caseins. The decrease of pH causes shrinking of casein micelle size, which is attributed to the collapse of the polyelectrolyte layer of κ-casein on the surface of the micelle. This reduces the steric repulsion and promotes the interactions between the particles, leading to aggregation. The caseins in unheated milk show a gelation pH of about 4.9 whereas in heated milk, gelation occurs at a higher pH, because of the presence of whey protein aggregates, bridging between the casein micelles (Corredig *et al*., 2011). These phenomena have also been reported by Schorsch *et al.* (2001) that the gelation kinetics of casein-whey mixtures and gel properties are influenced by the nature of heat treatment. When they co-heated casein/whey mixtures above 60 °C, the resulting gels had increased firmness (i.e., were stronger) in comparison to gels made from unheated or low heated (<60 °C) mixtures. At high temperature the gelation time also decreased. It was also shown that when whey proteins were pre-heated alone at 80 °C and added to casein micelles prior to acidification, gel formation begins when pH starts to decrease from 6.0. When the pre-heated sample was then co-heated a lag time was evident in the gelation profile and gelation did not start until pH ≈ 5.3. The resulting gels from heat-treatment of mixture of pre-heated whey protein with casein micelles were found to be

heterogenous in nature due to particulates from casein micelles which are complexed with denatured whey proteins and also from separate whey aggregates. Therefore, the explanation is that, for unheated samples gel formation results mainly from casein micelles, with 'native' whey proteins acting only as 'inactive' filler. Heat treatment causes denatured whey proteins to complex with the casein micelles surface via κ-casein-whey protein sulphydryl interchange which makes the whey able to form bridges between the micelles. The isoelectric point (pI) of whey protein (e.g., pI of β-lactoglobulin = 5.3) is higher than that of caseins and possibly explains why gelation occurs at higher pH (Lucey *et al.,*1998; Schorsch *et al.,* 2001).

1.3.1 Caseinates

Acidification of milk (casein micelles) to a pH of 4.6 causes calcium phosphate to dissolve and the casein proteins to precipitate. At this pH caseins are the only proteins that precipitate and can be collected and redissolved by neutralization to make caseinates. Thus caseinates are produced by neutralization of acid casein curd to ~ pH 6.7, using calcium, sodium, potassium or magnesium hydroxide. Caseins become soluble and reassociate randomly**.** Sodium caseinate is produced by acid coagulation of the casein in bovine milk, followed by neutralization with sodium hydroxide, and spray drying (Wong *et al.*, 1996; Dalgleish, 1997).

Sodium caseinate is completely soluble and forms viscous and translucent solutions, while calcium caseinate exists as an opaque dispersion of relatively low viscosity in water. The use of calcium hydroxide to neutralize acid casein curd causes cross-linking of phosphate esters *via* calcium ions. A calcium caseinate solution is destabilized by heat, especially at low pH, where calcium phosphate starts to solubilise. Sodium caseinate has a less rigid structure and exhibits excellent emulsifying capacity, foam stability, heat resistance, and water-binding properties. It is widely used in industry, in the manufacture of various products such as whipped toppings, coffee

creamers, bakery goods, instant breakfasts, emulsified meats and formulated blends of proteins used for cereals, frozen desserts, and nutritional beverages (Kinsella and Morr, 1984; Wong *et al.*, 1996).

κ-Casein is known to contribute to the surface rheology of the caseinate film. Caseinate fractions enriched with *β*-caseins exhibit enhanced solubility, surface activity, and emulsifying capacity, but a decrease in film viscosity and stability. Fractions enriched with α_s-/κ-caseins are known to show lower surface activity and emulsifying capacity, but greater film stability (Wong *et al*., 1996).

Lucey *et al.* (2000) characterized various sodium caseinate samples by using a multiangle laser light scattering (MALLS) and size-exclusion chromatography (SEC). They reported molecular weight (Mw) values in the range of 1200-4700 kDa and z-average root-mean-square radius (Rg) values ranged from ~50 to 120 nm for sodium caseinate solutions analyzed using only the MALLS system. Following untracentrifugation of the solutions at 90000 g for 1h, and the subnatant analyzed by SEC-MALLS, the Mw values obtained were in the range ~30-575 kDa whereas Rg values ranged from ~22 to 49 nm. It was shown that during SEC, the MALLS system detected some very large-sized material that eluted close to the void volume but its intensity of light scattering, however, decreased significantly in the subnatant. Two main peaks with Mw of ~420-750 kDa and 39-69 kDa, respectively were observed from SEC of sodium caseinate samples. The Rg values determined were extremely large for a protein molecule, and based on their estimations it was suggested that the shape of caseinate molecules may be highly elongated.

1.4 *Mixed biopolymer systems*

1.4.1 Polysaccharide-protein interactions

Mixtures of polysaccharides and proteins constitute important ingredients of wide range of colloidal food systems. Basically, proteins serve as emulsion forming and stabilizing agents while polysaccharides act as thickening and water holding agents among other functions. The phase behaviour of protein-polysaccharide mixtures contributes significantly to the stability, structural, rheological and textural characteristics of food products. Thus stability and texture of colloidal food systems partly depend on the nature and strength of the protein-polysaccharide interactions (Dickinson, 1995; Tolstoguzov, 1997).

When a polysaccharide and a protein are mixed in a solution, interaction of the two may be segregative or associative (de Kruif and Tuinier, 2001). For very dilute solutions the mixture is stable since mixing entropy dominates and protein and polysaccharide are co-soluble. Upon increasing concentration of the biopolymers, association or segregation phenomena can occur. These possibilities are illustrated in Figure 1.8.
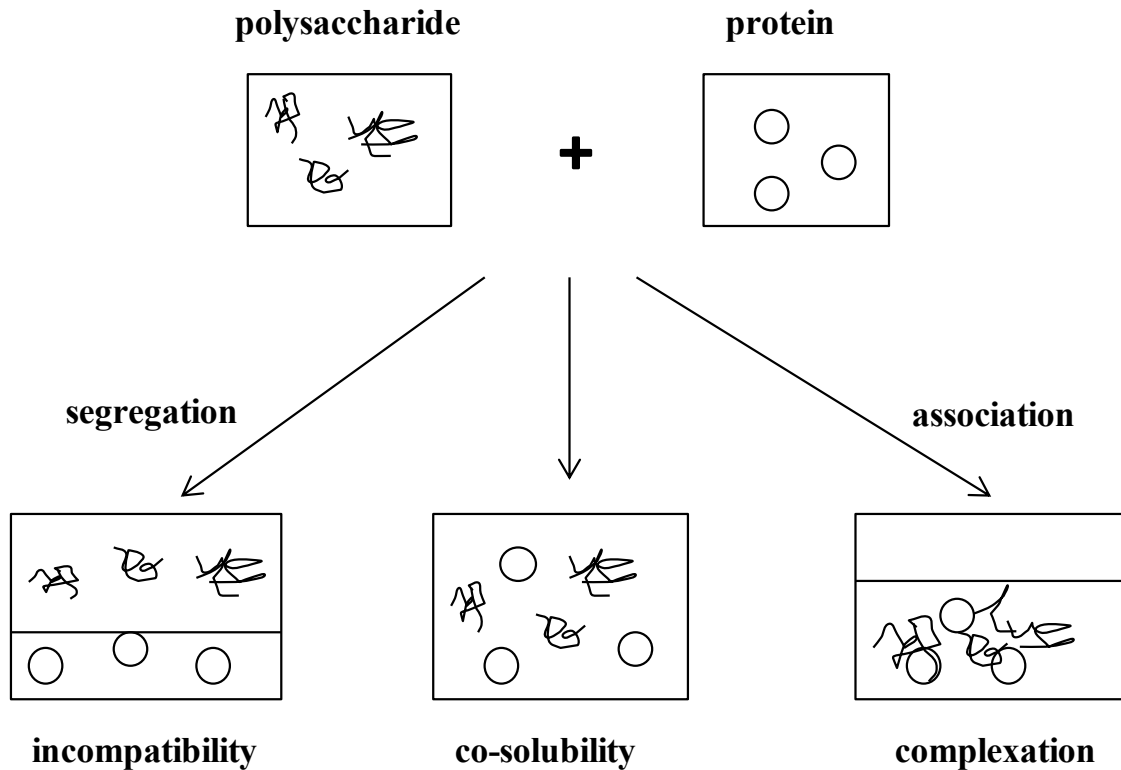
Figure 1.8: Phase behaviour of protein-polysaccharide mixtures (adapted from de Kruif and Tuinier, 2001).

Thus polysaccharide-protein interactions may result in phase separation through thermodynamic incompatibility (biopolymers being mutually segregated one from the other), co-precipitation or complex coacervation (biopolymers associate, excluding solvent from their vicinity) (Turgeon *et al.*, 2003). Phase separation is known to occur depending on the molecular characteristics of biopolymers (molecular weight, conformation, charge density) as well as the mixing conditions or parameters such as pH, ionic strength, solvent quality, mixing ratio, relative concentration of both biopolymers, mixing temperature and cooling rate, etc.) (Schmitt *et al.*, 1998; Syrbe *et al.*, 1998; Doublier *et al.*, 2000; Tolstoguzov, 2000; de Kruif and Tuinier, 2001; Norton and Frith, 2001; Tolstoguzov, 2003; Turgeon *et al.*, 2003; Neirynck *et al.*, 2007; Perez *et al.*, 2009).

Attractive interactions between protein and polysaccharide may result to the formation of soluble and/or insoluble complexes. The formation of insoluble complexes gives rise to phase separation occurrence known as coacervation or associative phase separation (Schmitt *et al.*, 1998). The associative phase separation results in the formation of primary soluble macromolecular complexes that interact to form electrically neutralized aggregates, that ultimately sediment to form the coacervate phase containing both biopolymers (Doublier *et al.*, 2000). Two coexisting phases are formed; one loaded with both complexed biopolymers whereas the other is solvent-rich depleted of biopolymers (Figure 1.6). Protein-polysaccharide association is of physical origin, arising from ionic, hydrogen bonding or hydrophobic interactions. The contribution of electrostatic interactions is prevalent in mixtures of positively charged proteins (pH < pI) and negatively charged polysaccharides, consequently forming strong electrostatic complexes. Weaker reversible complexes are likely to be formed between anionic polysaccharides and proteins with zero net charge (pH = pI) or a net negative charge (pH > pI) (Rodríguez Patino and Pilosof, 2011). Examples of systems in which associative interactions or complex coacervation have been observed include pectin-casein micelles (Maroziene and de Kruif, 2000), *β*-lactoglobulin and acacia gum (Schmitt *et al.*, 1999), gelatin–κ-carrageenan systems (Antonov and Goncalves, 1999) and whey protein concentrate (WPC)/λ-carrageenan (Perez *et al.*, 2009).

Thermodynamic incompatibility occurs as a result of unfavourable repulsive interactions between biopolymers in solution which leads to the mutual exclusion of each biopolymer from the local vicinity of the other. At a sufficiently high biopolymer concentration, the net repulsion between the two biopolymers at the molecular level causes the system to phase separate spontaneously into two distinct phases and each of them is mainly loaded with only one

biopolymer species. Thermodynamic incompatibility usually occurs at pH > pI of the protein and/or at high ionic strengths. Phase separation of protein-polysaccharide mixtures occurs above a critical concentration. At lower concentrations, the protein and the polysaccharide co-exist in a single phase containing the biopolymers in domains in which they mutually exclude one another so that increases the thermodynamic activity of a protein and influences the functional properties (Grinberg and Tolstoguzov, 1997; Tolstoguzov, 1997; Rodríguez Patino and Pilosof, 2011). Thermodynamic incompatibility has been reported for mixed systems such as *β*-glucans/whey protein isolate (Kontogiorgos *et al.,* 2009a,b), casein/exopolysaccharides from lactic acid bacteria at pH near neutral (Tuinier and De Kruif, 1999; Tuinier *et al*., 1999), casein and guar gum (Antonov *et al.*, 1999; Bourriot *et al.*, 1999b), pectin-caseinate mixtures at pH > 6 (Rediguieri *et al*., 2007) and many other systems. Linear polysaccharides are normally more incompatible with proteins than branched polysaccharides. Thermodynamic incompatibility is observed when the solvent-biopolymer interactions are favoured compared to biopolymer-biopolymer interactions (Grinberg and Tolstoguzov, 1997).

The molecular weight (Mw) of biopolymers in a mixture is also known to have significant influence on the miscibility or phase behaviour of the system. Higher Mw polymers usually have a smaller entropic term and thus increasing the Mw will have the effect of increasing the concentration of the polymer in its enriched phase. On the other hand, the polymer with lower Mw will have a greater tendency to mix with the other components in solution. Thus in mixed systems that form two liquid phases, when one or both of the biopolymers in solution have a broad Mw distribution, the high Mw portion of the polydisperse species will concentrate more in one phase than the other, compared to the low Mw portion of the same species (Frith, 2010). Loret *et al.* (2005) used fourier transform infrared (FTIR) spectroscopy in combination with

multivariate curve resolution to determine the phase compositions of bulk separated agarose/maltodextrin mixtures. They found higher concentrations of maltodextrin in the agarose rich phases than would be expected from the cloud point curve determined for this system. High performance size exclusion chromatography measurements on the separated phases showed that this behaviour was due to fractionation in Mw of maltodextrin during the phase separation. Edelman *et al.* (2003) also reported the effects of phase separation of aqueous mixtures of gelatin and dextran on the fractionation in Mw of the two biopolymers. They investigated the Mw distributions in coexisting phases by using size exclusion chromatography with multi-angle laser light scattering and found a strong fractionation in Mw for both components which was depended on only the Mw and concentration of the native material.

Einhorn-Stoll *et al*. (2010) showed that the thermodynamic compatibility of sodium caseinate and pectins increased with decreasing pectin molecular weight. The pectins varying in molecular weight were obtained by systematic mechanolysis of high methoxyl pectin (HMP) using a vibration mill. When the molecular weight of the caseinate was reduced by enzymatic partial hydrolysis (with varying degree of hydrolysis up to 10 %), the thermodynamic compatibility with HMP also increased. They also found that whey protein was completely compatible with all pectins, and conjugates with excellent emulsifying properties were formed with pectins of reduced molecular weight.

Tuinier *et al*. (2000) studied the effect of depolymerised guar gum on the stability of skim milk. They degraded native guar gum by heating its solutions at low pH for various heating times which yielded samples of lower molecular weights. According to their findings, mixing guar gum with casein micelles resulted in phase separation whereby the polymer concentration at the phase boundary increased with decreasing guar chain. Phase separation was attributed to

depletion interaction resulting in effective attraction between the casein micelles by non-adsorbing guar. It was speculated that maximum achievable viscosity of the guar solution in the one-phase region increases with decreasing guar chain length.

1.4.2 Phase diagram

The incompatibility of protein-polysaccharide mixed system is described quantitatively by phase diagrams (Tolstoguzov, 1997; Tolstoguzov, 2006; Rodríguez Patino and Pilosof, 2011). Figure 1.9 depicts a typical phase diagram of a protein-polysaccharide system exhibiting thermodynamic incompatibility. The solid curve is the binodal. The binodal curve (also called solubility curve) shows the co-solubility profile of biopolymers in a given medium. The binodal curve separates the region of co-solubility from the region of phase separation. Systems with composition below the binodal remains as a single homogeneous phase at the macroscopic scale. At the molecular scale, however, each biopolymer domain will exclude the other biopolymer (thermodynamic unfavourable interactions). Thus the region below the binodal is a region of limited thermodynamic compatibility. Systems with compositions above the binodal curve will spontaneously separate into two phases, one enriched in protein and the other enriched in polysaccharide.
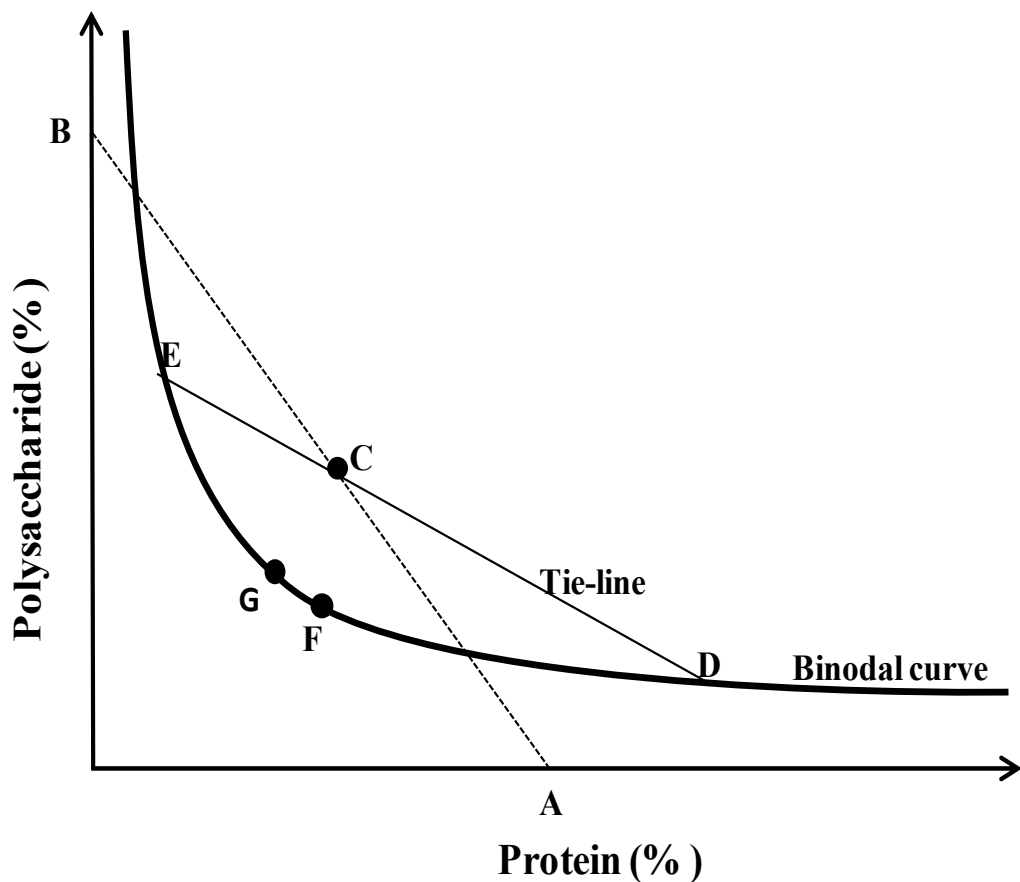
Figure 1.9: Phase diagram typical of protein-polysaccharide mixed system (adapted from Tolstoguzov, 1997).

As shown in Figure 1.9, mixing solution A and B in the volume proportion BC/AC, gives an initial mixture C. After phase separation, the mixed solution C breaks down into two liquid phases D (protein-rich phase) and E (polysaccharide-rich phase). The line ED is the tie-line which connects the binodal points corresponding to the composition of the co-existing phases. A point on the tie-line corresponds to the composition of the systems breaking down into two phases, each with the same composition as those of D and E. The length ratio of tie-line segments EC/ CD represents the volume fractions of D and E. Point F on the binodal represents the critical point, where the two co-existing phases are of the same composition and volume. At the critical point the composition of the phases are equal to that of the initial system. Point G is

the phase separation threshold (i.e. the minimum total concentration of biopolymers required for phase separation to occur) for a given biopolymer pair (Tolstoguzov, 1997; Tolstoguzov, 2006).

1.4.3 Thermodynamics of mixing biopolymers

The condition necessary for mixing one or more biopolymers with a solvent to form a single-phase is that the resulting free energy of mixing, ΔG_{mix}, must be negative:

$$\Delta G_{mix} = \Delta H_{mix} - T\Delta S_{mix} < 0 \qquad\qquad (1)$$

where ΔH_{mix} and ΔS_{mix} are the enthalpy and entropy of mixing, respectively, and T is the absolute temperature (Schmitt *et al.*, 1998; Rubinstein and Colby, 2003; Sperling, 2006).

ΔH_{mix} is usually positive and consequently favours demixing of two solutes in solution, however, for low molecular weight solutes, ΔS_{mix} is often sufficiently large and positive so that the two solutes will mix. For polymeric solutes, ΔS_{mix} is negligible, and thus the ΔH_{mix} term dominates favouring two polymeric solutes in a common solvent to demix (Frith, 2010). For charged biopolymers, the type and degree of charge on the two polymers will determine the nature of interactions in solution. In the mixed system where two polymers are either uncharged or have similar charge, the tendency is for the system to form two phases but where the two polymers have opposite charge, the tendency is for the two species to interact strongly, and form a complex that will form a separate phase or a precipitate. In the case where only one of the polymers is charged, the entropy of the counterions becomes a strong driving force for mixing of the two systems, since it is much greater than that of the polymers themselves. It is also known that the probability of phase separation to occur is highly dependent on the ionic strength of the aqueous solvent in which the two polymers are dissolved. When charged and neutral polymers are mixed in a low ionic strength solution, the counterion entropy will often dominate, and lead

to the formation of a homogenous solution. Addition of salt to such a system will raise the ionic strength and as a result the counterion entropy effect will be masked by that of the added salt, and the mixture will phase separate (Frith, 2010).

On the whole, the stability of mixed biopolymer systems depends on three thermodynamic effects: the combinatorial entropy of mixing, the intermolecular interactions arising from the different forces surrounding the macromolecules, and the free volume effect (Schmitt *et al.*, 1998). These are explained by their thermodynamical relations in the following sections.

1.4.3.1 Combinatorial entropy of mixing

The combinatorial entropy of mixing, ΔS_{mix}, represents the number of possible permutations of the molecules present in the mixing (solvent-biopolymer) among all sites of the system in its "quasilattice-state", which is the positional disorder of the system. ΔS_{mix} can be defined as (Schmitt *et al.*, 1998):

$$\Delta S_{mix}/RV = [(\varphi_1 \ln \varphi_1)/V_1 + (\varphi_2 \ln \varphi_2)/V_2] \tag{2}$$

where,

φi: the volume fraction of the component *i* in the mixture,

$V i$: the molar volume of the component *i*,

R: the gas constant (8.3144 J.mol^{-1}.K^{-1}) and

$\Delta S_{mix}/RV$: the combinatorial entropy variation per total volume, *V*, of solution.

Since φ_i is always less than 1, ΔS_{mix} is positive and contributes negatively to ΔG_{mix}. Thus the mixing stability through combinatorial entropy decreases with larger macromolecules because of the higher *Vi* values (Schmitt *et al.*, 1998).

1.4.3.2 Interactional contribution

The interactional contribution or heat of mixing, ΔH_{mix}, is based on the existence of repulsive (hydration, steric) or attractive forces (electrostatic, hydrophobic, van der Waals) surrounding every atom and molecule. It can be defined as (Schmitt *et al*., 1998):

$$\Delta H_{mix} = V_m (\delta_1 - \delta_2)^2 \varphi_1 \varphi_2 \qquad (3)$$

$$\text{and } \delta_i = (\Delta E/V_i)^{1/2}$$

V_m: the total volume of the mixture,

ΔE: the energy of vaporization to a gas at zero pressure,

V_i: the molar volume of the component *i,*

$\Delta E_i/V_i$: the cohesive energy density,

δ_i: the solubility parameter.

It has been shown that dispersion forces (random dipole-induced dipole interactions) always lead to a positive contribution to ΔG_{mix} ($\Delta H_{mix} > 0$). Thus, it cannot contribute to biopolymer compatibility in solution. Rarely, specific weak interactions contribute negatively to ΔG_{mix} ($\Delta H_{mix} < 0$). These specific interactions are usually associated with charge transfer or hydrogen bonding between the components.

The enthalpy of mixing, ΔH_{mix}, can also be expressed as follows:

$$\Delta H_{mix} / RTV = [(z\Delta\omega_{12})kTV_s] \, \varphi_1\varphi_2$$

$$= (\chi_{12}/V_1)\varphi_1\varphi_2 \qquad\qquad (4)$$

with z: the lattice coordination number,

V_s: the molar volume of a segment,

k: the Boltzmann Constant (1.38×10^{-23} J.K^{-1}) and

$\Delta\omega_{12}$: the energy of interaction of the system associated with the creation of a new contact of type

(1–2) in the mixture between segment of types 1 and 2 (corresponding to the species in solution, i.e.

solvent and biopolymer)

χ_{12}: the interactional parameter between the solvent and the biopolymer as defined by

Flory- Huggins equation:

$$\chi_{12} = (z\Delta\omega_{12} \, r_1)/kT \qquad\qquad (5)$$

where r_1 is the number of segments contained by the whole molecule of component 1.

A combination of equations 2 and 4 gives for ΔG_{mix}:

$$\Delta G_{mix}/RTV = (\varphi_1\ln\varphi_1)/V_1 + (\varphi_2\ln\varphi_2)/V_2 + (\chi_{12}/V_1)\varphi_1\varphi_2 \qquad (6)$$

For two high molecular weight biopolymers, the two first terms of equation 6 are negligible (V_1

and V_2 tend to infinity), thus χ_{12} determines the mixing stability. Because χ_{12}/V_1 is a function of

1/T, it increases positively by decreasing the temperature. As a result, χ_{12} will tend to be more

positive, giving rise to greater dispersion forces and decreasing solution stability (Schmitt *et al.*,

1998).

1.4.3.3 Free volume effect

The free volume effect arises from a volume change in the solution after mixing of the biopolymers. It represents the influence of the difference in free volumes of the solvent and of the biopolymer. It is believed that the free volume of the biopolymer is smaller than that of the solvent, because of the large molecule size difference. As a result, it brings the molecules of the system closer and causes negative contributions to ΔS_{mix} and ΔH_{mix}. This free volume effect is, by convention, part of the χ_{12} interaction parameter. The critical value of χ_{12} is given as:

$$(\chi_{12}/V_1)_{crit} = \tfrac{1}{2} \left[1/V_1^{\tfrac{1}{2}} + 1/V_2^{\tfrac{1}{2}} \right]^2 \qquad\qquad (7)$$

For an ideal solution, the solvent/solvent interactions and the biopolymer/solvent interactions are equal, the limiting value of χ_{12} is then 0.5, resulting in a zero value for ΔH_{mix}. For χ_{12} values lesser or greater than 0.5, the solvent is qualified as "good" and "poor", respectively. In a mixed system of a solvent and two biopolymers (such as polysaccharides and proteins dispersed in water), three different Flory-Huggins interactional parameters must be defined:

• χ_{12} and χ_{13}, accounting for the interactions between the solvent and the two biopolymers.

• χ_{23}, accounting for the two biopolymers interactions (attractive or repulsive).

As the size of the biopolymers is greater than that of the solvent, χ_{23} tends to control the mixture stability. It mainly determines the conditions for the system to phase separate. When χ_{23} is positive (indicating a net repulsion between the biopolymers), thermodynamic incompatibility or segregative phase separation is observed. Coacervation or associative phase separation takes place when χ_{23} is negative - thus the interactions between the two biopolymers are favoured (Schmitt *et al.*, 1998).

The thermodynamics of interaction of biopolymers with the solvent and with each other may be quantitatively determined and described by the values of the second virial coefficient (A_{12} and A_{13}) and the cross-second virial coefficient, A_{23} (or interaction parameter) using a light scattering technique. The inequality: $(A_{23})^2 > A_{12}A_{13}$ is a general rule employed for the prediction of phase separation. A positive value of the cross-second virial coefficient ($A_{23} > 0$) is indicative of exclusion of the molecules of one biopolymer from the solution volume occupied by the molecules of the other biopolymer, and the negative is indicative of mutual miscibility of the two biopolymers (Tolstoguzov, 1997; Syrbe *et al.*, 1998; Doublier *et al.*, 2000; Semenova, 2007). The excluded volume effect arises when the molecules of one of the biopolymers cannot have access to the volume occupied by another incompatible biopolymer. This results in lowering of the entropy of mixing. The excluded volume effect determines the solution space occupancy by the biopolymers and their phase separation threshold. The excluded volume effect increases with an increase in the rigidity and size of the macromolecules (Tolstoguzov, 1997; Tolstoguzov, 2006). According to Semenova (2007), an increase in the strength of the thermodynamically unfavourable interactions between biopolymers can be caused by the following main factors: (i) an increase in their size; (ii) lowering of the degree of accessibility of space occupied by one of the biopolymers for the others due to higher biopolymer flexibility; (iii) the rise in the stiffness of the interacting biopolymer molecules that has been followed by an increase in their size and consequently excluded volume; and (iv) the availability of the like net charge on the interacting biopolymers.

1.5 Viscometry

Viscosity is a measure of resistance of a fluid to flow. It is the ratio of the applied shear stress to the resulting strain rate. Several methods exist for characterizing the solution viscosity, or more specifically, the capacity of the solute to increase the viscosity of the solution. Given that η_o is the viscosity of the pure solvent whereas η is the viscosity of a solution using that solvent and c is the concentration (expressed in g/dL), most common solution viscosity terms are expressed as follows (Rao, 2007):

$$\text{Relative viscosity, } \eta_r = \frac{\eta}{\eta_o} \tag{8}$$

$$\text{Specific viscosity, } \eta_{sp} = \frac{\eta - \eta_o}{\eta_o} = \eta_r - 1 \tag{9}$$

$$\text{Inherent viscosity, } \eta_i = \frac{\ln \eta_r}{c} \tag{10}$$

$$\text{Intrinsic viscosity, } [\eta] = \lim_{c \to 0} \frac{\eta_{sp}}{c} \tag{11}$$

$$\lim_{c \to 0} \frac{\ln \eta_r}{c} = \lim_{c \to 0} \frac{\ln (1+\eta_{sp})}{c} = \lim_{c \to 0} \frac{\eta_{sp}}{c} = [\boldsymbol{\eta}] \tag{12}$$

Specific viscosity expresses the increase in viscosity due to the presence of the polymer in the solution. Normalizing η_{sp} to concentration gives η_{sp} /c which expresses the capacity of a polymer to cause the solution viscosity to increase i.e., the incremental viscosity per unit concentration of polymer. The extrapolated value of η_{sp} /c at zero concentration is known as the intrinsic viscosity, $[\eta]$. Like η_{sp}, $ln\ \eta_r$ is zero for pure solvent and increases with increasing concentration, thus $\ln \eta_r$ also expresses the incremental viscosity due to the presence of the polymer in the solution. Normalizing $ln\ \eta_r$ to concentration or $ln\ \eta_r/c$ gives the inherent viscosity.

In the limit of zero concentration, η_i extrapolates the same as η_{sp}/c and becomes equal to the intrinsic viscosity. Thus $[\eta]$ can be found be extrapolating either η_i or η_{sp}/c to zero concentration. The units of $[\eta]$ are inverse concentration and usually expressed as dL/g. The most useful and simple approach to determine $[\eta]$ is through the use of the "suspended level" or Ubbelohde capillary viscometer (Rao, 2007).

1.5.1 Capillary viscometry

The time it takes a volume of dilute polymer solution to flow through a thin capillary is compared to the time for a solvent flow. The flow time is proportional to the viscosity, and inversely proportional to the density (Harding, 1997; Russo, 2008).

$$t_{solvent} = \frac{\eta_{solvent}}{\rho_{solvent}} \tag{13}$$

$$t_{solution} = \frac{\eta_{solution}}{\rho_{solution}} \tag{14}$$

Since r*elative viscosity* is defined as the ratio $\eta_{solution} / \eta_{solvent}$ and for most polymer solutions at the concentrations of interest, $\rho_{solution} / \rho_{solvent} \approx 1$, therefore, by approximation the relative viscosity is a simple time ratio:

$$\eta_r = t_{solution} / t_{solvent} \tag{15}$$

Specific viscosity is also defined as the fractional change in viscosity upon addition of polymer:

$$\eta_{sp} = \frac{\eta_{solution} - \eta_{solvent}}{\eta_{solvent}} = \frac{t_{solution} - t_{solvent}}{t_{solvent}} = \eta_r - 1 \tag{16}$$

Hence relative viscosity and specific viscosity can be calculated by comparing the flow time of the solution to the flow time of the pure solvent at several different concentrations and

45

extrapolating to zero concentration to determine intrinsic viscosity, [η]. The extrapolation of experimental viscometric data (at a constant temperature e.g., 20°C) to zero concentration can be done according to the Huggins equation (Huggins, 1942):

$$\eta_{sp}/c = [\eta] + k'\,[\eta]^2 c \qquad (17)$$

or the Kraemer's equation (Kraemer, 1938):

$$\text{In } \eta_r/c = [\eta] + k''\,[\eta]^2 c \qquad (18)$$

$$k' \approx k'' + 0.5 \qquad (19)$$

where k′ is the Huggins' constant and k″ is the Kraemer's constant.

The plots of both η_{sp}/c vs. c and $ln\ \eta_r/c$ vs. c (as shown in Figure 1.10) should be linear and extrapolate to intercept [η] at zero concentration though their respective slopes, k′[η]² and k″ [η]², will be different (Harding, 1997; Rao, 2007).
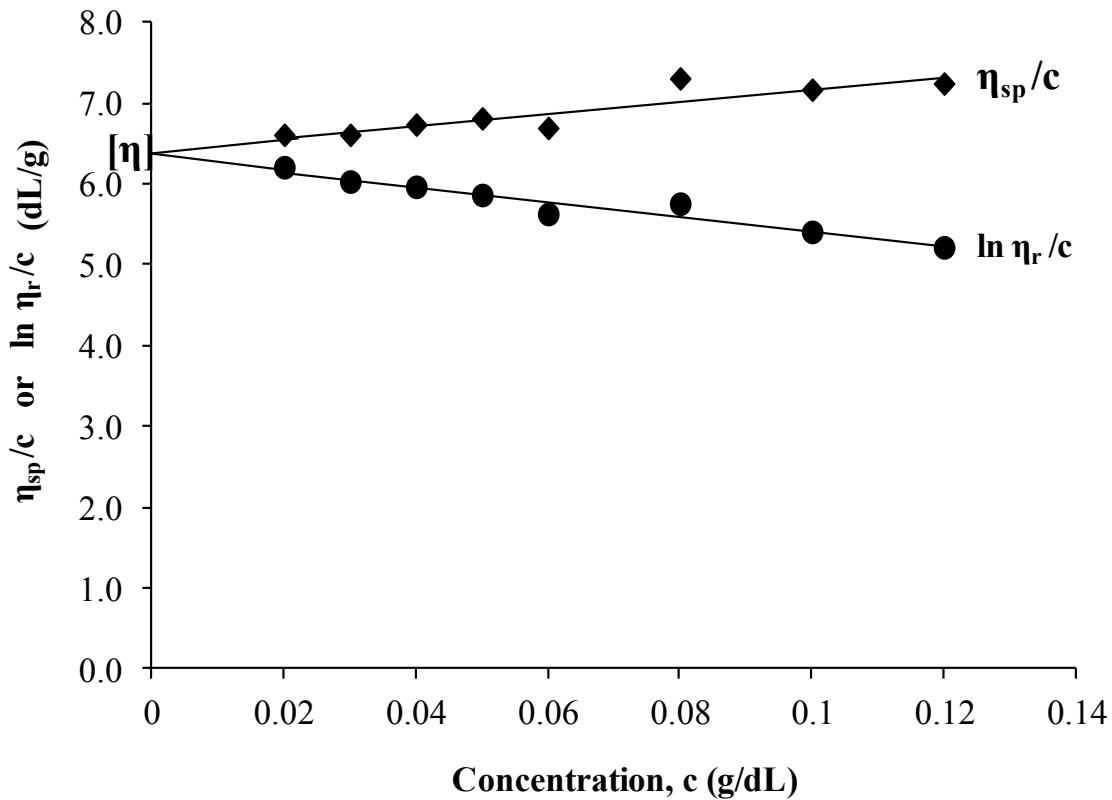
Figure 1.10: Plots of η_{sp}/c and $ln\ \eta_r/c$ as a function of concentration.

The intrinsic viscosity [η] is also a unique function of molecular weight (for a given polymer-solvent pair) and measurements of [η] can be used to estimate molecular weight. For polymer-solvent systems, the intrinsic viscosity is directly related to the molecular weight according to the Mark-Houwink relationship:

$$[\eta] = K \, (\overline{M}_v)^{\alpha} \tag{20}$$

where K is a constant, α is the Mark-Houwink exponent, and $\overline{M}_v$ is the viscosity-average molecular weight. K and α are related to the degree of molecular expansion and depend on the local stiffness of the polymer backbone and polymer-solvent interactions. The magnitude of α generally ranges between 0.5 and 0.8 when for random coiled polymers whereas α < 0.5 for polymers that assume compact conformations and α > 0.8 when hydrodynamic interactions are absent (when the conformations are elongated and rigid or rod-like polymers) (Harding, 1997; Eliasson, 2006; Rao, 2007; Foster and Wolf, 2011).

The flow characteristics of a material can be shown by plotting shear stress or viscosity *versus* shear rate, a graph known as a *flow curve*. Two common flow behaviour exhibited by polysaccharides when sheared are: *Newtonian behaviour* (viscosity remains constant and independent of the shear rate) and *shear thinning (pseudoplastic) behaviour* (viscosity decreases as shear rate is increased). The shear thinning behaviour can be described by the power law model (Ostwald-de Waele equation):

$$\eta = k \, (\dot{\gamma})^{n-1} \tag{21}$$

where *k* is the flow coefficient (or consistency constant), $\dot{\gamma}$ is the shear rate and *n* is the power law index. For n = 1, the flow is Newtonian, and *k* equals the viscosity of the solution, for n < 1, indicates shear thinning and n > 1, indicates the solution is shear thickening (i.e., viscosity increases as shear rate is increased) (Rao, 2007; Foster and Wolf, 2011).

1.6 Viscoelastic characterization

A viscoelastic sample, as the name suggests, has both viscous (liquid) and elastic (solid) properties. Dynamic or oscillatory tests are usually performed to study the viscoelastic properties of a sample.

1.6.1 Mechanical spectroscopy (Oscillatory tests)

Mechanical spectroscopy is a technique used to study and characterize materials and is most useful for studying the viscoelastic behaviour of polymers. An oscillatory test is performed (using a rheometer) by exposing the material to a sine-wave-shaped input of either stress or strain and the resulting sinusoidal strain or stress output is then resolved (i.e., separated) into a certain amount of solid-like response, which is in phase with the input, and a corresponding amount of liquid-like response which is $\pi/2$ (i.e., 90°) out of phase with the input. The solid-like component at any particular frequency is characterised by the *storage (elastic) modulus*, *G′*, and the liquid-like response is described by the complementary *loss (viscous) modulus*, *G′′*. The storage modulus describes the elastic storage of energy in the material while the loss modulus describes the viscous dissipation (loss) of energy through permanent deformation in flow. The units of both moduli are pascals (Pa or N/m^2). The magnitude of both parameters vary with temperature, strain and applied angular frequency, ω (rads/s), which is given by $2\pi f$, where *f* is the frequency in hertz (Hz). However, for strain values within the linear domain, *G′* and *G′′* are independent of strain (Barnes, 2000; Rao, 2007).

G′ is defined as the ratio of the stress in phase with the strain to the strain and G′′ is defined the ratio of the stress 90° out of phase with the strain to the strain. The frequency dependence of *G′* and *G′′* is called the mechanical spectrum (Barnes, 2000; Rao, 2007; Clark and Ross-Murphy, 2009; Miri, 2011).

The sum of G' and G'' referred to as complex modulus, G*, is a measure of materials overall resistance to deformation. It is obtained from the ratio of the stress amplitude to the strain amplitude.

$$G* = \frac{\sigma}{\gamma} = G' + iG'' \tag{22}$$

$$G* = \sqrt{G'^2 + G''^2} \tag{23}$$

By measuring the ratio of the stress to the strain (G*) as well as the phase difference (delta, δ) between the two, the G' and G'' are defined in terms of sine and cosine functions as follows:

$$G' = G* \cos \delta \tag{24}$$

$$G'' = G* \sin \delta \tag{25}$$

The phase angle ($\tan \delta = G''/G'$) is associated with the degree of viscoelasticity of the sample. A low value in $\tan \delta$ or δ indicates a higher degree of elasticity (more solid-like). Thus phase angle δ can also be used to describe the properties of a sample. Basically, for purely elastic sample $\delta = 0^o$ and for purely viscous material $\delta = 90^o$. For a viscoelastic sample, $0^o < \delta < 90^o$: where $\delta > 45^o$, $G'' > G'$ (i.e., $\tan \delta > 1$) implies liquid-like sample whereas $\delta < 45^o$, $G' > G''$ (i.e., $\tan \delta < 1$) implies solid-like sample.

The viscosity functions are defined as: $\eta' = G''/\omega$ and $\eta'' = G'/\omega$; where η' represents the viscous or in-phase component between the stress and strain rate, while η'' represents the elastic or out-of-phase component. The complex viscosity $\eta*$ is given by (Barnes, 2000; Dogan and Kokini, 2007; Rao, 2007):

$$\eta* = \sqrt{(G'/\omega)^2 + (G''/\omega)^2} = G*/i\omega \tag{26}$$

$$|\eta*| = |G*|/\omega \tag{27}$$

Rheometers are usually supported with computer software for the determination of these viscoelastic parameters during the oscillatory measurements. The measuring systems or

geometries are of three categories namely: cone and plate, parallel plates, and cup and bob geometries. The choice of measuring geometry is subject to the nature of sample to be tested and also experimental conditions or preferences. For instance, thick materials can be tested with a cone and plate unless they contain particulate matter, in which case a parallel plate can be a better option. Due to variations in gap with thermal expansion of the measuring system, a parallel plate is preferred to cone and plate when performing a temperature sweep. A cup and bob geometry (e.g., a double concentric cylinder for maximum sensitivity) is suitable for low viscosity materials and mobile suspensions. The cup and bob or parallel plate produces optimum test conditions when performing oscillatory measurements at high frequencies on low viscosity materials (Rao, 2007; Miri, 2011).

1.6.2 Cox-Merz rule

The steady shear rheological properties and the small amplitude oscillatory properties of polymer solutions can be related. According to the Cox-Merz rule, the complex dynamic viscosity η^* (as a function of angular frequency, ω, rad/s) is identical to the plot of shear viscosity as a function of shear rate (1/s). Thus according to Cox and Merz (1958):

$$|\eta*(\omega)|_{\omega \to 0} = |\eta\ (\dot{\gamma})|_{\gamma \to 0} \qquad\qquad (28)$$

The Cox-Merz rule if correctly applied can be used to predict $|\eta(\dot{\gamma})|$ from oscillatory measurements or to predict $|\eta*(\omega)|$ from steady state viscosity data. It is also useful for analytical description of the microstructure of materials from the degree to which they obey the rule. Thus a direct relationship exists between the rheological response to non-destructive and destructive deformation whereby the oscillatory and shear flow curves should be identical if the polymer solutions are free from high-density entanglements or aggregates. Some previous studies have shown that polymer solutions follow the Cox-Merz rule at low concentrations but deviations

occur at high concentrations whereby η* was higher than η at high frequencies or shear rates (Morris *et al.*, 1981; Jacon *et al.*, 1993; Böhm and Kulicke, 1999a; Lazaridou *et al.*, 2003; Skendi *et al.*, 2003; Vaikousi *et al.*, 2004).

1.7 Aims of the study

The general aim of this study is to investigate the phase behaviour of oat *β*-glucan isolates of different molecular weights in mixed systems with milk proteins.

The specific objectives were:

1. To isolate *β*-glucan from oat flour and generate samples of different molecular weights.

2. To characterize the purity, molecular weight and the structural features of the *β*-glucan samples (Chapter 2).

3. To investigate the relationship between the rheological properties and microstructure of aqueous oat *β*-glucan solutions as a function of molecular weight by rheometry and atomic force microscopy (Chapter 3).

4. To optimize the effect of protein removal from protein-polysaccharide mixtures on the determination of polysaccharide concentration using phenol-sulphuric acid method for phase-diagram construction by response surface methodology (Chapter 4).

5. To investigate the phase behaviour of mixtures of sodium caseinate with oat *β*-glucan isolates varying in molecular weight by means of phase diagram construction, rheometry, electrophoresis and fluorescence microscopy (Chapter 5).

CHAPTER 2

EXTRACTION AND CHARACTERIZATION OF β-GLUCAN[*]

2.1 Introduction

The extraction of β-glucan from cereal grains generally involves: (1) inactivation of endogenous enzymes that cause β-glucan degradation, (2) extraction and (3) precipitation of the β-glucan (Brennan and Cleary, 2005). The sample is usually refluxed with aqueous ethanol or treating the flour with dilute aqueous ethanol at temperatures above 60 $^{\circ}$C to inactivate the endogenous enzymes and to remove most of the lipids. When the temperature of extraction rises above 60 $^{\circ}$C, starch polymers may also be co-extracted with the β-glucan and thus needs to be removed from the extracts. This is usually achieved by enzyme hydrolysis using alpha-amylase. Different procedures have been employed in the extraction of β-glucan in cereals. The extraction method is also known to affect the yield, purity, structural conformation and molecular weight of the isolated β-glucan due to the effect of factors such as solvent and temperature of extraction (Beer *et al.*, 1996; Storsley *et al.*, 2003; Wang *et al.*, 2003; Brennan and Cleary, 2005). Wood *et al.* (1989) studied the effects of particle size, temperature, pH and ionic strength on β-glucan yield on the laboratory scale, and prepared an oat gum fraction (from oat bran) by extracting hot 75% ethanol-inactivated oat bran with a sodium carbonate solution at pH 10 to give a preparation containing 78% β-glucan. McCleary (1988) also demonstrated that sequential water extractions at 40, 65, and 95 $^{\circ}$C, increased the extraction rate of barley β-glucans to 90%. It has been shown that optimum recovery of barley and oat β-glucans with retention of viscosity

characteristics could be obtained using 1 M NaOH but the extract was impure as a result of contamination with considerable amounts of starch and protein (Bhatty, 1993). Saulnier *et al*. (1994) used a thermostable alpha-amylase in the hot water extraction procedure to minimize the contamination from starch, and to optimize the purification of the *β*-glucan material. Morgan and Ofman (1998) obtained *β*-glucans from barley grains by hot water extraction procedure followed by freezing and thawing of the extract. The commercial product obtained (Glucagel[TM]) had between 89 and 94% *β*-glucan, depending on the duration of the initial extraction. Temelli (1997) demonstrated that *β*-glucan extraction increased with temperature. Carr *et al*. (1990) observed that the use of NaOH for complete extraction resulted in partial depolymerisation of the *β*-glucan. Knuckles *et al*. (1997) included sodium borohydride in NaOH extraction at 65 ^{o}C to prevent alkaline depolymerisation but found that molecular weight of the extracted *β*-glucan was lower than with water at 100 ^{o}C. Beer *et al.* (1997) also observed that the Mw of *β*-glucan extracted from oats and barley with NaOH was lower than that extracted with hot water. It has also been shown that the temperature used for sequential water extractions affect molecular weight, the ratio of (1→4) to (1→3) linkages, and the amount of cellulosic regions on the *β*-glucan chain (Knuckles *et al.*, 1997; Storsley *et al.*, 2003). Symons and Brennan (2004) also evaluated extraction procedures and showed that extraction with thermostable alpha-amylase yielded the purest *β*-glucan fraction. The use of thermostable alpha-amylase (Termamyl 120L) has been employed by many researchers for degrading the starch component in the *β*-glucan extracts whereas protein is usually removed by pH adjustment to 4.5 to precipitate the proteins or digestion with protease/pancreatin. Exhaustive dialysis in water is carried out to get rid of smaller molecules (glucose, amino acids/peptides) resulting from starch and protein breakdown procedures. The *β*-glucans are precipitated using ethanol (95% v/v) or ammonium sulphate (20-

50% v/v) and with propan-2-ol (100% v/v) exchange followed by drying (Lazaridou *et al.*, 2003; Skendi *et al.*, 2003; Irakli *et al.*, 2004; Vaikousi *et al.*, 2004; Li *et al.*, 2006).

The objectives of this work are to isolate *β*-glucan from oat flour and generate samples of different molecular weights, and to characterize the purity, molecular weight and the structural features of the *β*-glucan samples.

2.2 Materials and methods

2.2.1 Materials and chemicals

The Megazyme mixed-linkage beta-glucan assay and Quick Start[TM] Bradford protein assay kits were purchased from Megazyme International Ltd. (Bray, Ireland) and Bio-Rad Laboratories Inc. (Hertfordshire, UK), respectively. Sodium azide (NaN$_3$), dialysis membrane tubing (MwCO 12000) and closures were purchased from Sigma-Aldrich (Poole, Dorset, UK) whereas ethanol and isopropanol were obtained from Fisher Scientific (Loughborough, UK). Termamyl 120L Type L (heat-stable alpha-amylase) was purchased from Univar (Bradford, UK). Oat flour (Oatwell® 28%, oat bran with 28% *β*-glucan content) was obtained from CreaNutrition (Swedish Oat fibre, Sweden). Distilled water was used throughout the experiments. All chemicals used were analytical grade reagents.

2.2.2 Extraction of *β*-glucan

Extraction of oat *β*-glucan from oat flour was performed by adapting previously published isolation protocols with slight modifications (Lazaridou *et al.*, 2003; Skendi *et al.*, 2003; Vaikousi *et al.*, 2004). Figure 2.1 presents a schematic diagram of the extraction procedures employed for the isolation and purification of *β*-glucan. The extraction resulted in the initial *β*-glucan isolate that was denoted as OBG.

A 100 g of oat flour (OatWell) was dispersed into 3 L of distilled H_2O (with 0.2 % w/v NaN_3). The flour suspension was heated on water bath at 45 ^oC for 1 h while shaking periodically. The addition of NaN_3 was to inactivate microorganisms that might be present so as to prevent degradation of β-glucans by microbial growth. Solubilisation at 45 ^oC prevents starch gelatinization. The pH was adjusted to 4.5 using 2 M HCl and then 60 ml of Termamyl 120L (a thermostable alpha-amylase) was added to breakdown starch to glucose. This was carried out for 3 h while the temperature was raised to 75 ^oC and shaking vigorously from time to time. The elevated temperature facilitates starch gelatinization and digestion by the amylase as well as solubilization and hence extraction of β-glucan. After extraction, the system was cooled and then centrifuged at 4000 rpm for 15 min at 30 ^oC using Alergra X-15R centrifuge (Beckman Coulter Inc.). The supernatant was collected and 2 M HCl added to bring the pH to 4.5 so as to precipitate the proteins. The resulting mixture was centrifuged again as above. The supernatant was put in dialysis membrane tubes (made with cellulose, 76 mm in diameter) and dialysed exhaustively for 3 days in a bucket containing distilled water which was replaced daily. The sample was then concentrated under vacuum at 80 ^oC using a rotary evaporator (Büchi Rotapor R-114). The concentrate was then precipitated with 95% ethanol, twice the volume. This was left overnight, decanted and 95% isopropanol added and stirred thoroughly to further precipitate the β-glucans. The precipitate was filtered, frozen using liquid nitrogen and then freeze-dried. The freeze-dried samples were ground/milled into powder of 600 μm mesh size and stored in tightly closed plastic containers for use. The extraction procedures are summarized in Figure 2.1.

2.2.3 Acid hydrolysis

Three more samples (H05, H10, H15) were obtained from the initial isolate (OBG) by controlled acid hydrolysis. The β-glucan sample was dispersed in double-distilled water (1.5%

w/v) at 80 °C under continuous stirring in a sealed vial. When the polysaccharide was fully dispersed, the temperature was lowered to 70 °C and concentrated HCl added to bring the concentration to 0.1 M (HCl). The polysaccharide was hydrolysed for 0.5, 1, or 1.5 h. Immediately after the end of hydrolysis, the solutions were cooled in running water to room temperature, and the pH was adjusted to 7.0 with 5 M NaOH. The hydrolysates were precipitated with three volumes of 95% v/v ethanol and left standing for 1 h at 4 °C. The precipitate was collected by filtration, washed with isopropyl alcohol, freeze dried and ground to a powder of 600 μm mesh size.

Aqueous Oat Flour Suspension
[100g flour - 3 L H_2O (0.2% w/v NaN_3), 45 °C – 1h]

Termamyl 120L, 1% v/v
(pre-heated, 75 °C /30min)
pH 4.5, 75 °C – 3h
Centrifugation (4000 rpm/15 min)

Supernatant

Protein precipitation.
pH 4.5 (2.0 M HCl)
Centrifugation (4000 rpm/15 min)

Supernatant

Dialysis
(distilled H_2O, 3 days)

Concentration under vacuum, 80 °C

Precipitation
(2 vol – 95% v/v EtOH)

Propanol exchange
(1 vol – 95% propan-2-ol)

Filtration

Freeze drying

Oat β-glucan (**OBG**)

Acid Hydrolysis,
pH 1.0, conc. HCl,
80 °C/0.5, 1.0, 1.5 h
Cooling, 20 °C
Adjustment of pH to 7.0

H05, H10, H15

Figure 2.1: Extraction and purification of *β*-glucan from oat flour

2.2.4 *β*-Glucan assay

The *β*-glucan content of the obtained isolates was determined by the McCleary method using the Megazyme mixed-linkage *β*-glucan assay kit (McCleary and Glennie-Holmes, 1985). The mixed linkage *β*-glucan test kit was obtained from Megazyme International Ltd (Bray, Ireland).

Principle: Samples are suspended and hydrated in a buffer solution of pH 6.5 and then incubated with purified lichenase enzyme and filtered. An aliquot of the filtrate is then hydrolysed to completion with purified *β*-glucosidase. The D-glucose produced is assayed using a glucose oxidase/peroxidase.

$$\text{Mixed-linkage}\,\beta\text{-glucan} \xrightarrow{\;+\,\text{Lichenase}\;} \beta\text{-Gluco-oligosaccharides} \xrightarrow{\;+\,\beta\text{-glucosidase}\;} \text{D-Glucose}$$
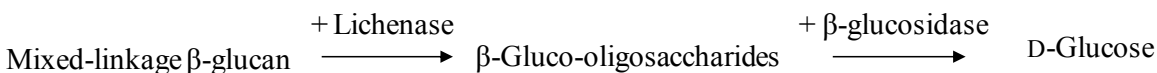
Procedure: Approximately 50 mg of samples were weighed into glass test tubes and 0.2 mL of 50% v/v aqueous ethanol added. 5 mL of 20 mM sodium phosphate buffer (pH 6.5) was added, stirred on a vortex mixer and then incubated at $\sim 100\ ^{\circ}\text{C}$ for 2 min. It was mixed again on a vortex mixer and incubated at $\sim 100\ ^{\circ}\text{C}$ for further 4 min. It was then cooled to $50\ ^{\circ}\text{C}$, and 0.2 mL of lichenase (100 U/mL) added, incubated in water bath at $50\ ^{\circ}\text{C}$ for 1 h. The volume was adjusted to 100 mL with 100 mM sodium acetate buffer (pH 4.0). The resulting solution was centrifuged at 1000 g for 10 min. 0.1 mL aliquots (in triplicate) were pipetted and two of these incubated with 0.1 mL *β*-glucosidase (2 U/mL) for 15 min. To the third, 0.1 mL of 100 mM sodium acetate buffer (pH 4.0) was added (sample blank). 3.0 mL of GOPOD reagent (glucose determination reagent) was added to the tubes and incubated at $50\ ^{\circ}\text{C}$ for 20 min. Absorbance was read at 510 nm against the reagent blank (i.e., 0.1 mL distilled water + 0.1 mL sodium acetate buffer + 3.0 mL GOPOD reagent) using a spectrophotometer (Shimazu UV-VIS 160A).

Control glucose solution was also run (in quadruplicate) concurrently. The β-glucan content was calculated using the Megazyme Mega-Calc^{TM} Software.

2.2.5 Bradford protein assay

The Bradford assay is a protein determination method that involves the binding of Coomassie Brilliant Blue G-250 dye to proteins (Bradford, 1976). The dye exists in three forms: cationic (red), neutral (green) and anionic (blue). Under acidic conditions, the dye is predominantly in the doubly protonated red cationic form (A_{max} = 470 nm). However, when the dye binds to a protein, it is converted to a stable unprotonated blue form (A_{max} = 595nm). It is this blue protein form that is detected in the assay using a spectrophotometer or microplate reader.

A standard calibration curve was generated with bovine serum albumin (BSA) standards (125 -1000 µg/ml) and used to estimate the protein content of samples. The blank (0 µg/mL) was made using distilled water and dye reagent. 100 µL of each standard, blank and unknown samples were pipetted into separate clean test tubes. 5 mL of the dye reagent was then added to each tube and vortexed. The resulting solution was incubated at room temperature for 10 min. Absorbance readings were then taken at 595 nm using a spectrophotometer (Shimazu UV-VIS 160A).

2.2.6 Nuclear magnetic resonance (NMR) spectroscopy

NMR spectroscopy is a nondestructive technique used to provide information on the chemical structure of high-molar mass molecules including polysaccharides (Dais and Perlin, 1982; Wood *et al.*, 1994b; Cui *et al.*, 2000; Duus *et al.*, 2000; Colleoni-Sirghie *et al.*, 2003; Lazaridou *et al.*, 2003; Johansson *et al.*, 2004; Brummer and Cui, 2006; Ghotra *et al.*, 2008).

It works on the principle that NMR active nuclei (such as ^{1}H and ^{13}C, which are used frequently) absorb at a frequency characteristic of the isotope when placed in a strong magnetic field. The resonant frequency, energy of the absorption and the intensity of the signal are proportional to the strength of the magnetic field. Different protons in a molecule (depending on the local chemical environment) will resonate at slightly different frequencies when placed in a magnetic field. The frequency shift is converted into a field-independent dimensionless value known as the *chemical shift*. The chemical shift is usually expressed in parts per million (ppm) and reported relative to a reference resonance frequency, e.g. tetramethylsilane (TMS, $Si(CH_3)_4$). ^{1}H-NMR signals are much more sensitive than ^{13}C signals due to their natural abundance. However, ^{13}C-NMR has significant advantages over ^{1}H-NMR spectroscopy in the analysis of polysaccharides because the chemical shifts in ^{13}C-NMR spectrum are spread out over a broad range, which helps to overcome the severe overlapping problems associated with the proton spectrum (Duus *et al.*, 2000; Friebolin, 2005; Keeler, 2005; Brummer and Cui, 2006).

By understanding different chemical environments, the NMR spectrum is assigned using the chemical shifts to obtain structural information about the molecule in a sample. In the proton spectrum, all chemical shifts derived from carbohydrates including mono-, oligo-, and polysaccharides are in the range of 1 to 6 ppm from TMS. The α-anomeric protons from each monosaccharide will appear in the region of 5-6 ppm while the *β*-anomeric protons will appear in the 4-5 ppm range. In the ^{13}C-NMR spectrum, signals from the anomeric carbons appear in the 90-110 ppm region while the nonanomeric carbons are between 60 and 85 ppm. Usually the α-anomeric carbons are known to appear in the region of 95-100 ppm while the *β*-anomeric carbons appear between 100 and 105 ppm. Uronic acid containing polysaccharides, however, give signals from the carboxyl carbons in a lower field between 170 and 180 ppm. The carbon

atoms with primary hydroxyl groups, such as C6 in pyranoses and C5 in furanoses, will give signals in the higher field between 60-64 ppm while carbon atoms with secondary hydroxyl groups (C2, 3, 4 in pyranoses and C2, 3 in furanoses) will appear in the region of 65-85 ppm. Signals from alkoylated carbons atoms (C5 in pyranoses and C4 in furanoses) will however shift 5-10 ppm to the lower field (Brummer and Cui, 2006).

One-dimensional liquid state ^{1}H- and ^{13}C-NMR spectra have been used to study anomeric protons and carbons of *β*-glucan and arabinoxylans and for comparison of *β*-glucans of different botanical sources (Dais and Perlin, 1982; Westerlund *et al.*, 1993; Wood *et al.*, 1994b; Colleoni-Sirghie *et al.*, 2003; Lazaridou *et al.*, 2003; Skendi *et al.*, 2003; Johansson *et al.*, 2004; Ghotra *et al.*, 2008). Two-dimensional NMR (2D-NMR) has also been used to provide detailed information on the structural features of *β*-glucan (Ensley *et al.*, 1994; Cui *et al.*, 2000; Johansson *et al.*, 2000; Lazaridou *et al.*, 2004). Complete assignments of both the ^{13}C and ^{1}H spectra has been achieved by the use of direct and long-range homo (^{1}H/^{1}H) and hetero (^{13}C /^{1}H) nuclear shift correlations to confirm sequences and linkage sites of cereal *β*-glucans (Cui *et al*., 2000).

2.2.6.1 ^{13}C- NMR spectroscopy

The ^{13}C–NMR spectroscopy was performed with a Bruker AV 500 Spectrometer at 125.76 MHz using a 5 mm BBO probe. The samples were dispersed (2 % w/v) in pure deuterated methylsulphoxide (d6-DMSO) by heating and continuous stirring at 90°C for 3 h. The proton-decoupled spectra were recorded at 70 ^{o}C overnight by applying 12800 pulses with a delay time of 2 s and a radio frequency tip angle of 30°. Chemical shifts were expressed in parts per million (ppm) relative to d6-DMSO at 39.5 ppm and reported relative to tetramethylsilane (TMS).

2.2.7 High-performance size-exclusion chromatography

High-performance liquid chromatography is a commonly used chromatographic technique for analyzing carbohydrates. A pump (high pressure) is used to move the mobile phase and the analyte through a column coated with a stationary phase. The concentration changes in the column effluent are translated into electrical signals by a detector. Thus the detector emits a response due to the eluting sample compound and subsequently signals a peak on the recorder or computer data system as a chromatogram. Both qualitative and quantitative information can be obtained from the chromatogram as each compound in the mixture has unique retention time (i.e. the time (in minutes) it takes for a compound to travel from the injection port to the detector) under a given set of conditions, and both the peak area and height are proportional to the amount of the corresponding analyte (Rounds and Gregory, 2003; Meyer, 2004).

Size-exclusion chromatography (SEC) unlike all other chromatographic methods separates molecules on the basis of size (i.e., according to the molecular mass) rather than an interaction process. The column packing is made up of a porous material whereby the larger molecules are *excluded* as the only space available for sample molecules that are too large to diffuse into the pores is that between the individual stationary phase particles. In other words, SEC works by trapping the smaller molecules in the pores of a particle while the larger molecules pass by the pores as they are too large to enter the pores. Therefore larger molecules will have a shorter retention time as they flow through the column faster than the smaller molecules. Thus the largest molecules are eluted first and smallest molecules last. High-performance size-exclusion chromatography (HPSEC) with hydrophilic polymeric size-exclusion packing or column is used for rapid determination of average molecular weights and degree of polydispersity of polysaccharides. When equipped with a light scattering detector, the molecular weight

distribution of polysaccharides can be determined directly from the HPSEC (Rounds and Gregory, 2003; Meyer, 2004).

2.2.7.1 Molecular weight determination

β-Glucan samples were solubilized (~1 mg/mL) in deionised water for 3 h at 90°C. Solutions were diluted with deionised water, filtered through a 0.45 μm filter, and the peak molecular weight (M_p) was measured by HPSEC. The sample was injected into a Shodex (Showa Denko K.K., Tokyo, Japan) OHpak SB-806 M column (with OHpak guard) followed by a Waters Ultrahydrogel linear column (40 °C) using a Waters 717plus autosampler and eluted at 1 mL/min in 0.1M Tris buffer (pH 8.0) with a Shimadzu model LC-20AT pump. A Shimadzu LC-10ATVP pump was used for post-column addition of Calcofluor (20 mg/L in 0.1M Tris buffer, pH 8.0, at 1 mL/min) (CalcofluorWhiteM2R New, C.I. 40622, fluorescent brightener 28, American Cyanamid Co., Bound Brook, NJ), enabling fluorescence detection in a Shimadzu RF-10Axl fluorescence detector (excitation, 360 nm; emission, 450nm). Fluorescence intensity was collected by a Viscotek DM 400 data manager and data integration was performed using TriSEC 3.0 (Viscotek, Houston, TX) software. Five β-glucan molecular weight standards (20,000-1,200,000 g/mol), both prepared in-house and obtained commercially (Megazyme International), were used to construct a calibration curve for β-glucan by plotting retention time versus log M_p.

2.3 Results and discussion

2.3.1 Purity and molecular weight of oat β-glucan isolates

Initially the purity and the molecular weight were determined for all the samples. The protein content of the β-glucan isolate (OBG) and the hydrolysates (H05, H10, H15) was about 13% whilst the β-glucan content was found to be in the range 78 − 86 % on a dry weight basis

(Table 2.1). The original oat β-glucan isolate (OBG) had a very high molecular weight (Mw) of 2.8 x 10^6 g/mol whilst the acid hydrolysis process yielded lower Mw samples varying between 142 – 252 x 10^3 g/mol (H05 > H10 > H15) (Table 2.1).

Controlled acid hydrolysis caused depolymerization of the initial β-glucan sample, thereby generating products of different Mw but with the same structural characteristics: the longer the acid hydrolysis treatment time employed, the lower the Mw of the resulting material. Similarly, other researchers also utilized acid hydrolysis to degrade oat gums and reported a reduction in the average Mw of the initial material (Doublier and Wood, 1995; Vaikousi *et al.*, 2004; Kontogiorgos *et al.*, 2009a).

Table 2.1: Content, molecular and structural features of oat β-glucan isolates on dry basis (d.b).

Sample	β-glucans (% d.b)	Protein (% d.b)	Mw[a] x 10^3 (g/mol)	$(1{\rightarrow}4)/$ $(1{\rightarrow}3)^b$
OBG	83	13.7	2800	2.15
H05	86	13.2	252	2.20
H10	78	13.0	172	2.18
H15	78	12.9	142	2.07

[a] Peak molecular weight obtained from the HPSEC chromatograms.

[b] From ^{13}C-NMR spectra (relative intensities of the two C-6 resonances).

Figure 2.2 presents the HPSEC chromatograms of oat β-glucan samples with different peak molecular weight.
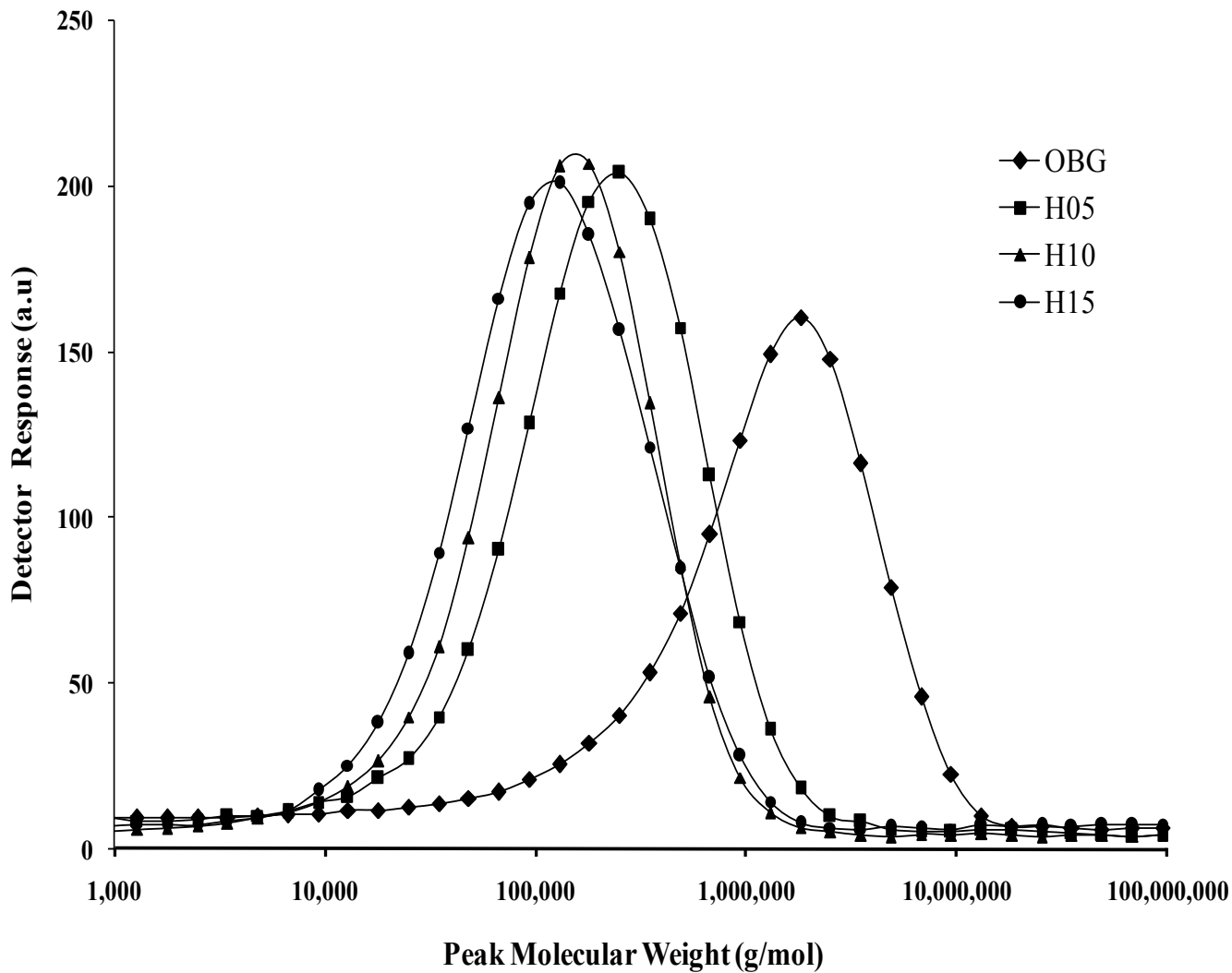
Figure 2.2: HPSEC chromatograms of oat *β*-glucan samples.

After isolation, purity and molecular weight determination of the samples, their structural

characteristics were investigated as described in the following section.

2.3.2 Structural features of oat *β*-glucan

The ^{13}C-NMR spectra obtained for all samples (Figure 2.3) were typical of a mixed linkage cereal *β*-glucan and the peaks were assigned (Figure 2.4; Table 2.2) using information previously reported in the literature (Dais and Perlin, 1982; Wood *et al.*, 1994b; Cui *et al.*, 2000; Colleoni-Sirghie *et al.*, 2003; Lazaridou *et al.*, 2003; Skendi *et al.*, 2003; Irakli *et al.*, 2004; Ghotra *et al.*, 2008).

The resonance at 102.3 ppm is due to C-1 carbon of the (1→3)-*β*-linkage and the resonance at 102.5 ppm has been assigned to the C-1 of the (1→4)-*β*-linkage. The single resonance at 86.9 ppm corresponds to the C-3 carbon of (1→3)-*β*-linkage whereas the resonances at 72.1, 68.2, 76.2 and 60.7 ppm has been assigned to the carbons C-2, C-4, C-5 and C-6 of the O-3-*β*-glucopyranosyl residue, respectively. For carbons C-2, C-3, C-4, C-5 and C-6 of the O-4-*β*-glucopyranosyl residue, the resonances appeared at 72.9, 74.5, 80.0, 74.8 and 60.3 ppm, respectively. Finally, carbons C-1, C-2, C-3, C-4, C-5 and C-6 of the O-4-*β*-glucospyranose-3-O residue resonated at 103.4, 73.4, 74.3, 79.8, 74.8 and 60.3 ppm, respectively for all isolates (Table 2.2).

Table 2.2: ^{13}C-NMR assignments for oat *β*-glucan spectra.

Glucopyranosyl residue (Glc p)	^{13}C Chemical shifts (ppm)					
	C-1	**C-2**	**C-3**	**C-4**	**C-5**	**C-6**
O-3-*β*-Glc p	102.3	72.1	86.9	68.2	76.2	60.7
O-4-*β*-Glc p	102.5	72.9	74.5	80.0	74.8	60.3
O-4-*β*-Glc p-3-O	103.4	73.4	74.3	79.8	74.8	60.3
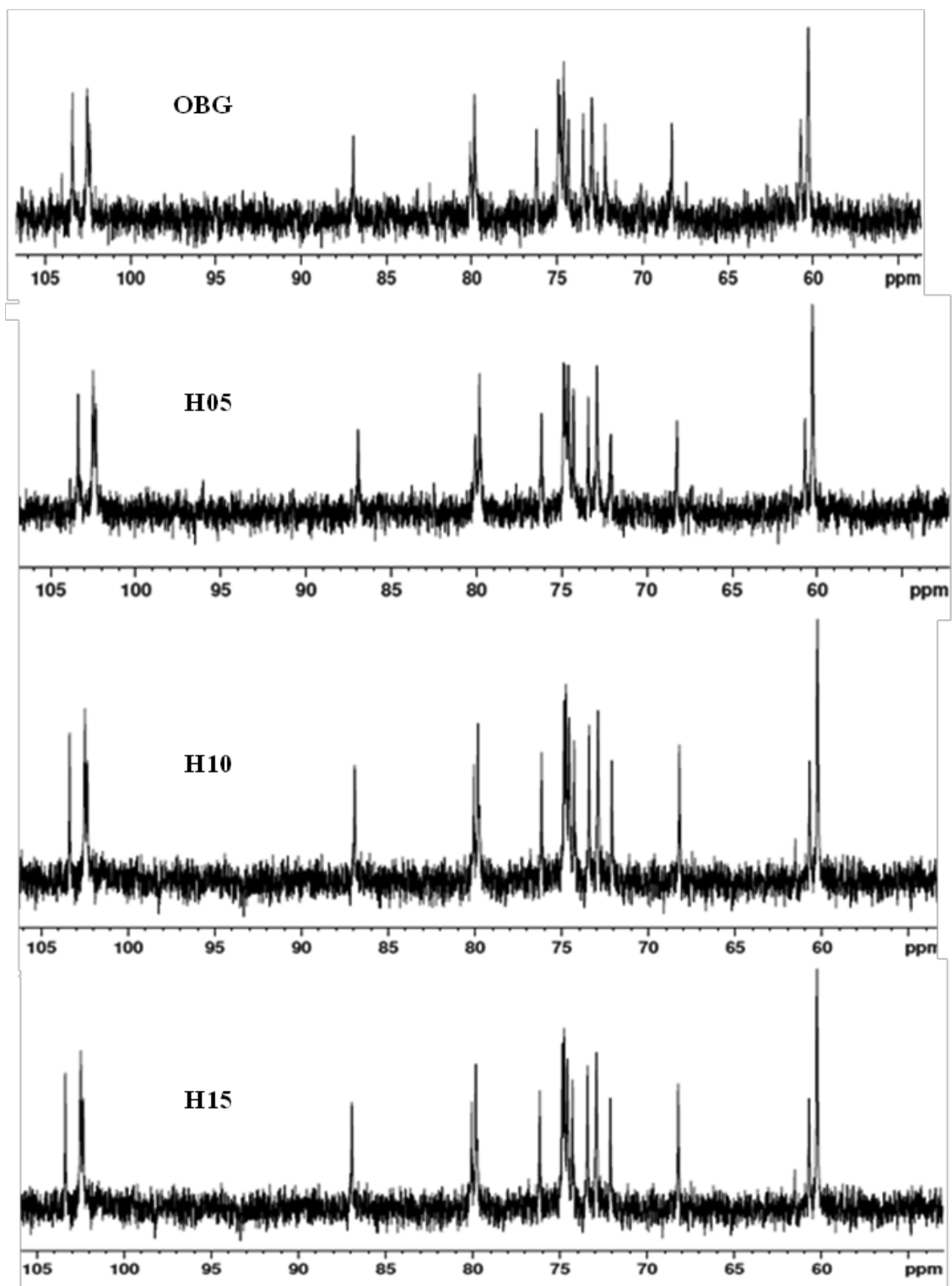
Figure 2.3: ^{13}C-NMR spectra of oat β-glucan isolates
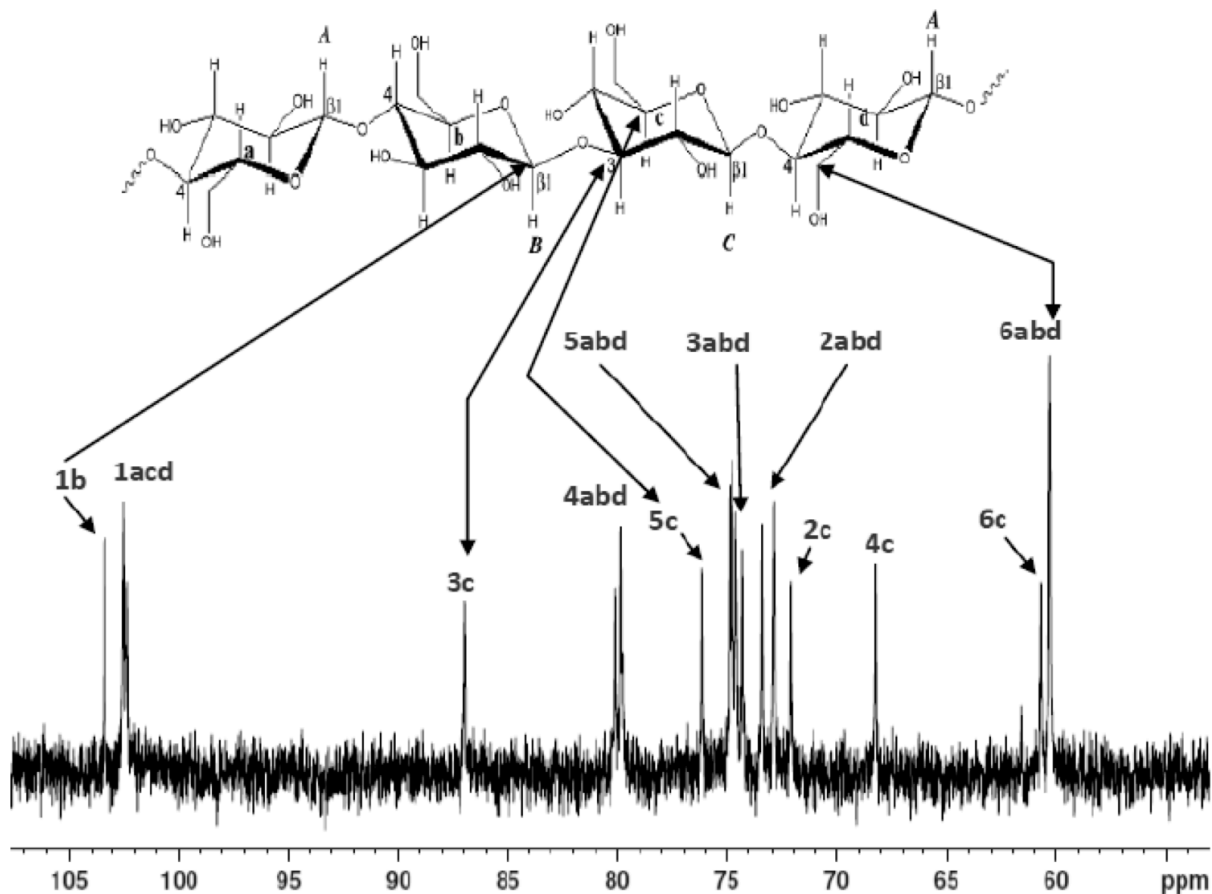
Figure 2.4: ^{13}C-NMR assignments for oat β-glucan spectra. Insertion on top is (1→3,1→4)-β-D-glucan structure to illustrate the carbon positions (1-6) of the glucopyranosyl residues (a, b, c, d).

The presence of only a single resonance for C-3 and C-4 of the O-3-β-glucopyranosyl residue (at 86.9 ppm and 68.2 ppm respectively) confirms that there is no consecutive β-(1→3)-linkages in the β-glucan chain (Dais and Perlin, 1982; Wood *et al.*, 1994b; Cui *et al.*, 2000; Colleoni-Sirghie *et al.*, 2003; Lazaridou *et al.*, 2003; Skendi *et al.*, 2003; Irakli *et al.*, 2004; Ghotra, 2008; Ghotra *et al.*, 2008). The non-consecutive occurrence of β-(1→3) linkages along the polymeric chain has been suggested to contribute to solubility and flexibility of (1→3),(1→4)-β-glucans whilst the regularity of the (1→4) linkages is considered to be responsible for insolubility and aggregation phenomena (Buliga *et al.*, 1986; Woodward *et al.*,

1988). The purity of the β-glucan is also confirmed by the presence of only three resonances for the C-1 carbons. Thus the absence of starch and arabinoxylan is indicated by the absence of resonances due to the alpha configuration of the anomeric carbons (α-Glc) which would resonate at ~ 100 ppm and the anomeric β-Glc carbon resonances slightly downfield (at ~104 ppm) (Colleoni-Sirghie $et\ al.$, 2003; Irakli $et\ al.$, 2004). Finally, the relative intensities of the two C-6 resonances at 60.3 ppm and 60.7 ppm gives an index of the ratio of the (1→4)/(1→3) linkages in the β-glucan chain (Skendi $et\ al.$, 2003) and this was found to be between 2.07 – 2.20 (Table 2.1).

2.4 Conclusion

The β-glucan isolate (OBG) and hydrolysates (H05, H10 and H15) were obtained by aqueous extraction from oat flour and controlled acid hydrolysis, respectively. The structural features of isolated β-glucan samples and molecular weights (Mw) were characterized by ^{13}C–NMR spectroscopy and high performance size-exclusion chromatography. The samples with β-glucan content between 78-86 % on a dry weight basis had Mw the range of 142 - 2800 x 10^3 g/mol. The ^{13}C-NMR spectra obtained for all samples were identical and typical of a mixed linkage cereal β-glucan. The results showed that controlled acid hydrolysis caused depolymerization of the initial β-glucan sample, thereby generating products of different molecular weight but with the same structural characteristics: the longer the acid hydrolysis treatment time employed, the lower the Mw of the resulting material.

CHAPTER 3

RHEOLOGICAL AND MICROSTRUCTURAL INVESTIGATION OF OAT β-GLUCAN ISOLATES VARYING IN MOLECULAR WEIGHT

3.1 Introduction

Solubility in water and the capacity to form highly viscous solutions is a fundamental characteristic of oat *β*-glucan due to its high molecular weight, conformation, and self-association characteristics (Lazaridou *et al.*, 2003; Brennan and Cleary, 2005). Fundamental studies on the rheological properties of *β*-glucan have been performed previously and the functionality of *β*-glucan was found to be highly dependent on polysaccharide structure, molecular weight and concentration (Lazaridou *et al.*, 2003; Skendi *et al.*, 2003; Tosh *et al.*, 2004b; Vaikousi *et al.*, 2004; Papageorgiou *et al.*, 2005). However, limited information exists on the link between the microstructure and the rheological properties of this polysaccharide. Application of atomic force microscopy (AFM) has enabled visualization of individual polysaccharide molecules and their interactions in solution (Kirby *et al.*, 1996; Round *et al.*, 1997; Capron *et al.*, 1998; Gunning *et al.*, 2000; Ikeda *et al.*, 2001; Morris *et al.*, 2001; Ikeda *et al.*, 2005; Dang *et al.*, 2006; Yang *et al.*, 2006; Funami *et al.*, 2007). Imaging biopolymers by AFM to characterize important factors such as molecular weight, morphology and the nature of self-association can provide useful information to explain functionality.

The objective of this investigation, therefore, is to find a relationship between rheological and microstructural properties of oat *β*-glucan as a function of molecular weight using rheometry and AFM.

3.2 Materials and methods

3.2.1 Materials

The oat *β*-glucan isolates (denoted as OBG, H05, H10 and H15) of different molecular weight (2800×10^3, 252×10^3, 172×10^3 and 142×10^3 g/mol, respectively) obtained as described in detail in Chapter 2 (refer to Section 2.1.2, 2.1.3; Figure 2.1) were used for the investigation.

3.2.2 Atomic force microscopy (AFM)

The atomic force microscope (AFM) is a type of probe microscope used for studying biological systems and ideally suited for imaging food biopolymers (Morris *et al.*, 2001; Morris, 2009). The AFM generates images by feeling a surface with a probe. The interaction between the probe and the sample surface is monitored to generate different images of the surface topography, adhesion, elasticity or charge. The sample is placed on top of a piezoelectric device (a tube scanner) which expands or contracts to move the sample in three dimensions (3D). The probe or tip (usually microfabricated from silicon nitride, pyramidal in shape, ~ 3 µm in height and ~30-50 nm radius of curvature) is used to feel the specimen. The tip is attached to a cantilever which bends or twists in response to the changes in force between the tip and the sample surface during scanning. The movement of the cantilever is detected using an optical lever. A low lever beam is reflected from the end of the cantilever onto a quadrant photodiode. As the cantilever bends or twists, the changes in position of the reflected beam on the photodiode maps the motion of the cantilever. The output from the photodiode, in the form of a potential difference is used to generate images of the sample (Morris, 2009).

Procedure: Prior to AFM imaging, *β*-glucan sample dispersions (0.1 % w/v) were treated with 1.0 mg/mL of proteinase κ-agarose (Sigma Chemicals, UK) at 37 °C for 48 h to further reduce

the protein content of the samples. The AFM used was manufactured by East Coast Scientific Ltd. (Cambridge, UK). The instrument was operated in contact mode under butanol and the cantilevers used were 100 μm 'SiNi Budget Sensors' (Innovative Solutions, Bulgaria Ltd.) with a quoted force constant of 0.27 N/m. The β-glucan samples were diluted in pure water Barnstead Nanopure (Triple Red, UK) to 2μg/mL. Heating to 90 °C in a sealed tube for 30 min was necessary to ensure complete dissolution of the samples. After returning to room temperature a pipette was used to deposit 3μL single droplets onto freshly cleaved mica (Agar Scientific, UK). The deposit was left for 10 min to dry before imaging.

3.2.3 Rheological measurements

β-Glucan samples were dispersed at 0.01-8.0 % w/v in distilled water in sealed glass-vials at 80 $^{\rm o}$C by continuous stirring to ensure complete solubilization. The intrinsic viscosity [η] of β-glucan solutions was determined at 20 $^{\rm o}$C with a Ubbelohde capillary viscometer and calculations made according to both the Huggins and Kraemer's equations. All rheological measurements (oscillatory and viscometry) were carried out at 20.0 $^{\rm o}$C using a Bohlin Gemini 200HR nano rotational rheometer (Malvern Instruments, Malvern, UK) equipped with cone-and-plate geometry (55 diameter, cone angle 2$^{\rm o}$). The oscillatory measurements were performed at a strain of 0.1%, which was found to be within the linear viscoelastic range of the material after strain sweep measurements, and a range of angular frequencies (ω) of 0.06 – 628 rad/s. The flow curves were measured at a range of shear rates in the range 0.01 – 1000 s^{-1}. The data were analyzed with the supporting rheometer software. All rheological measurements were carried out on freshly prepared samples.

3.3 Results and discussion

3.3.1 Rheological measurements

The viscosity of a polymer solution depends on the molecular weight (Mw), concentration and also on the interaction between the solvent and neighboring polymeric chains. The fractional increase in viscosity due to the presence of a polymer in solution is expressed as the specific viscosity (η_{sp}) whilst the intrinsic viscosity ([η]) is used to characterize the volume occupied by the individual polymer molecules in isolation. The intrinsic viscosities at 20 $^{\circ}$C were determined by the extrapolation of the experimental viscometric data to zero concentration according to both the Huggins and Kraemer equations (refer to equations 17 and 18 under section 1.5.1). Figure 3.1 shows the extrapolation of the data obtained for oat β-glucan sample H05.
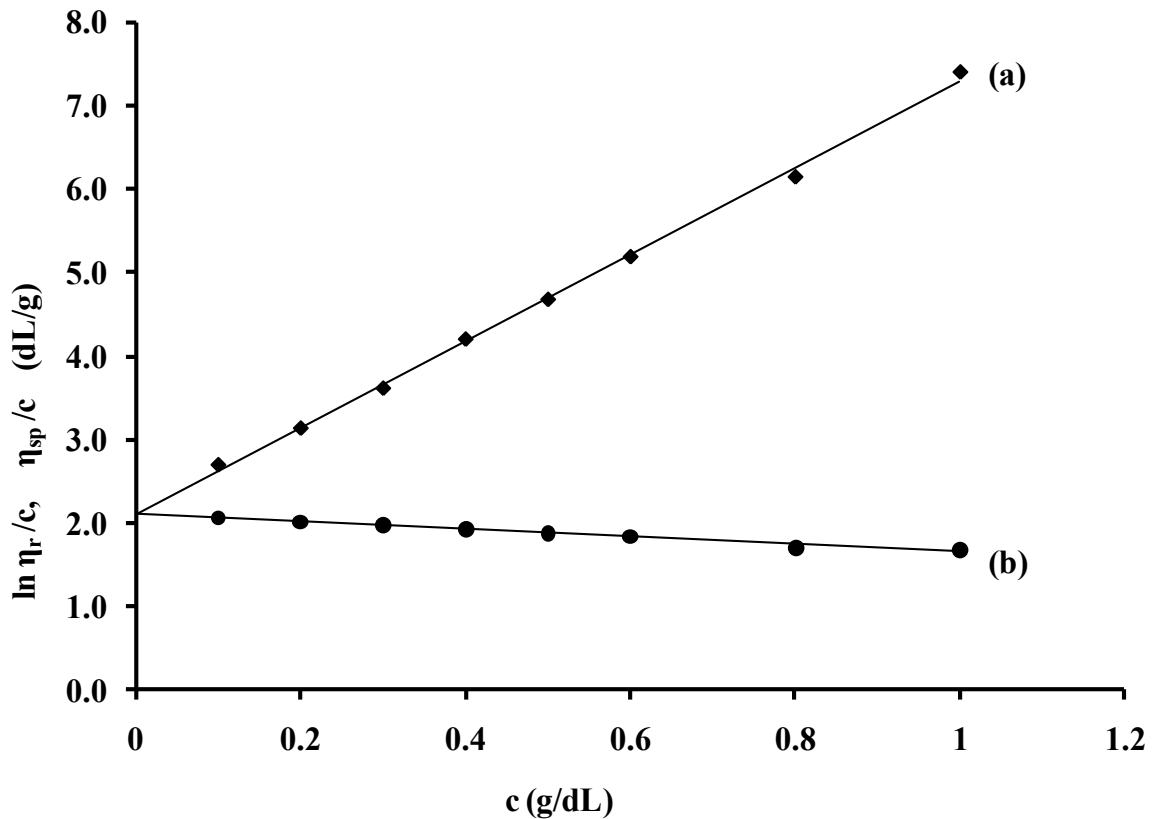
Figure 3.1: Determination of intrinsic viscosity of oat β-glucan (H05) by the (a) Huggins and (b) Kraemer extrapolation to zero concentration.

The calculated [η] values of *β*-glucan samples varied between 1.7 and 7.2 dL/g (Table 3.1) and noticeably increased with increasing Mw. Similar values of [η]; namely 0.67–3.83 dL/g (Mw between 35–350x10³ g/mol), 1.15–4.6 dL/g (Mw between 40 to 375x10³ g/mol), 4.9–6.4 dL/g (Mw between 0.27–0.78x10⁶ g/mol) and 2.58-9.63dL/g (Mw between 100 and 1200x10³ g/mol) have been reported previously for other *β*-glucan preparations (Vårum and Smidsrød, 1988; Doublier and Wood, 1995; Lazaridou *et al.*, 2003; Ren *et al.*, 2003; Skendi *et al.*, 2003).

Table 3.1: Slopes, intrinsic viscosity [η] and critical concentration (c*) values of *β*-glucan isolates

Sample	Slope 1	Slope 2	[η] (dL/g)	c* (g/dL)	c*[η]
OBG	1.00	3.97	7.2	0.25	1.80
H05	0.93	3.13	2.1	0.56	1.17
H10	0.69	3.38	1.8	0.97	1.74
H15	0.64	3.62	1.7	1.10	1.85

The product of intrinsic viscosity and concentration gives an index of the total degree of space-occupancy: the reduced concentration (c[η]). Figure 3.2 presents double logarithmic plots of η_{sp} *vs.* c[η] which illustrates the dependency of specific viscosity at zero shear rates on the reduced concentration – the coil overlap parameter of aqueous *β*-glucan solutions.
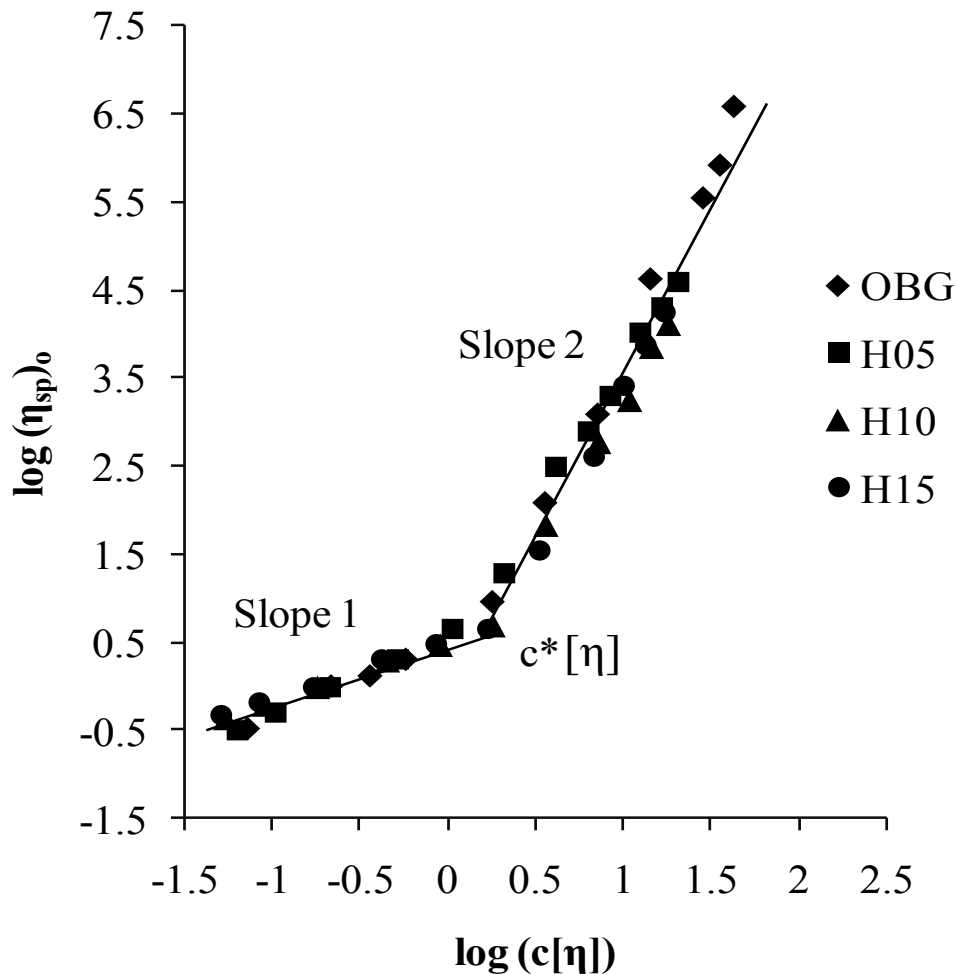
Figure 3.2: Zero shear specific viscosity $(\eta_{sp})_o$ versus the reduced concentration $c[\eta]$ for β-glucan isolates.

The results superimpose closely falling into two distinct linear regions for all samples studied, a behaviour that is typical for most disordered polysaccharide solutions. However, as the specific viscosity is directly related to Mw and strongly dependent on concentration, these plots are used to take into account the differences between hydrodynamic dimensions among different samples, and to estimate the transition from the dilute to the concentrated regime. The transition from dilute to concentrated solution behaviour at the interception between the two linear regions is designated as $c^*[\eta]$ (Figure 3.2). Thus at concentrations higher than c* the polymer chains become highly entangled and conformational dynamics are determined by intermolecular/chain-

chain interactions, whilst at concentrations less than c* individual molecules are separated from neighbouring molecules (Hwang and Shin, 2000; Zimeri and Kokini, 2003). The c* values varied between 0.25 g/dL and 1.10 g/dL for the different oat β-glucan dispersions due to the differences in the Mw of the samples (Table 3.1). Two linear regions with only one critical concentration c* varying between 0.5 and 2.0 % (g/dL) has also been observed previously for barley β-glucans in the Mw range between 375 and 40 x 10^3 g/mol (Böhm and Kulicke, 1999a). Comparatively, a critical concentration (c*) of 0.3 % (g/dL) has been reported for chitosan solutions (Hwang and Shin, 2000). Similarly, two distinct linear regimes of slopes that fit the results for β-glucans and disordered chains have been identified previously (Ren *et al*., 2003; Morris *et al*., 1981). Other researchers, however, observed an intermediate transition from dilute to semi-dilute and from semi-dilute to a concentrated regime giving rise to two critical concentrations, c* and c** respectively (hence three slopes instead of two as in our case) (Skendi *et al*., 2003; Irakli *et al*., 2004; Vaikousi *et al*., 2004). However, the estimates are in close agreement with their findings with respect to c* and c** values for samples with similar Mw. The c* values increased with decreasing Mw of the β-glucan samples which shows that coil overlap occurs at lower concentrations in the case of high molecular weight samples (OBG < H05 < H10 < H15) (Table 3.1). The results therefore are indicative of the fact that variation in concentration or Mw significantly affects the zero shear viscosity. The coil overlap parameter c*[η] ranged between 1.17-1.85 and was in close agreement with those reported previously (Doublier and Wood, 1995; Lazaridou *et al*., 2003). From the master plot (Figure 3.2) the slope 1 = 0.8 for the dilute regime whereas slope 2 = 3.8 for the concentrated regime and the calculated c*[η] = 1.8. According to Morris *et al*. (1981) the values for the slope are ~1.4 and ~3.3 for dilute and concentrated solutions, respectively, with c*[η] ≈ 4 for most disordered polysaccharides studied. However,

they also observed deviation from this behaviour (e.g., for solutions of locust bean gum, guar gum, and hyaluronate at low pH and high ionic strength) due to specific intermolecular/chain-chain interactions.

Using the Mark-Houwink equation (see equation 20), the plot of log [η] *versus* log Mw of the four *β*-glucan samples gave the Mark-Houwink exponent, α to be ~0.5 (i.e., the slope value = 0.49) which is in close agreement with literature that α value ranges between 0.5 and 0.8 for random coiled polymers (Harding, 1997; Böhm and Kulicke, 1999a; Rao, 2007). Böhm and Kulicke (1999a) found α = 0.71 for barley *β*-glucans varying in Mw from 40 to 375×10^3 g/mol indicating an expanded coil which was attributed to chain stiffness.

Following dilute solution rheology the flow behaviour of the samples was studied next as a function of Mw and concentration at 20 ^{o}C. Figure 3.3 illustrates the dependence of viscosity on shear rate for the *β*-glucan solutions differing in concentration and Mw.
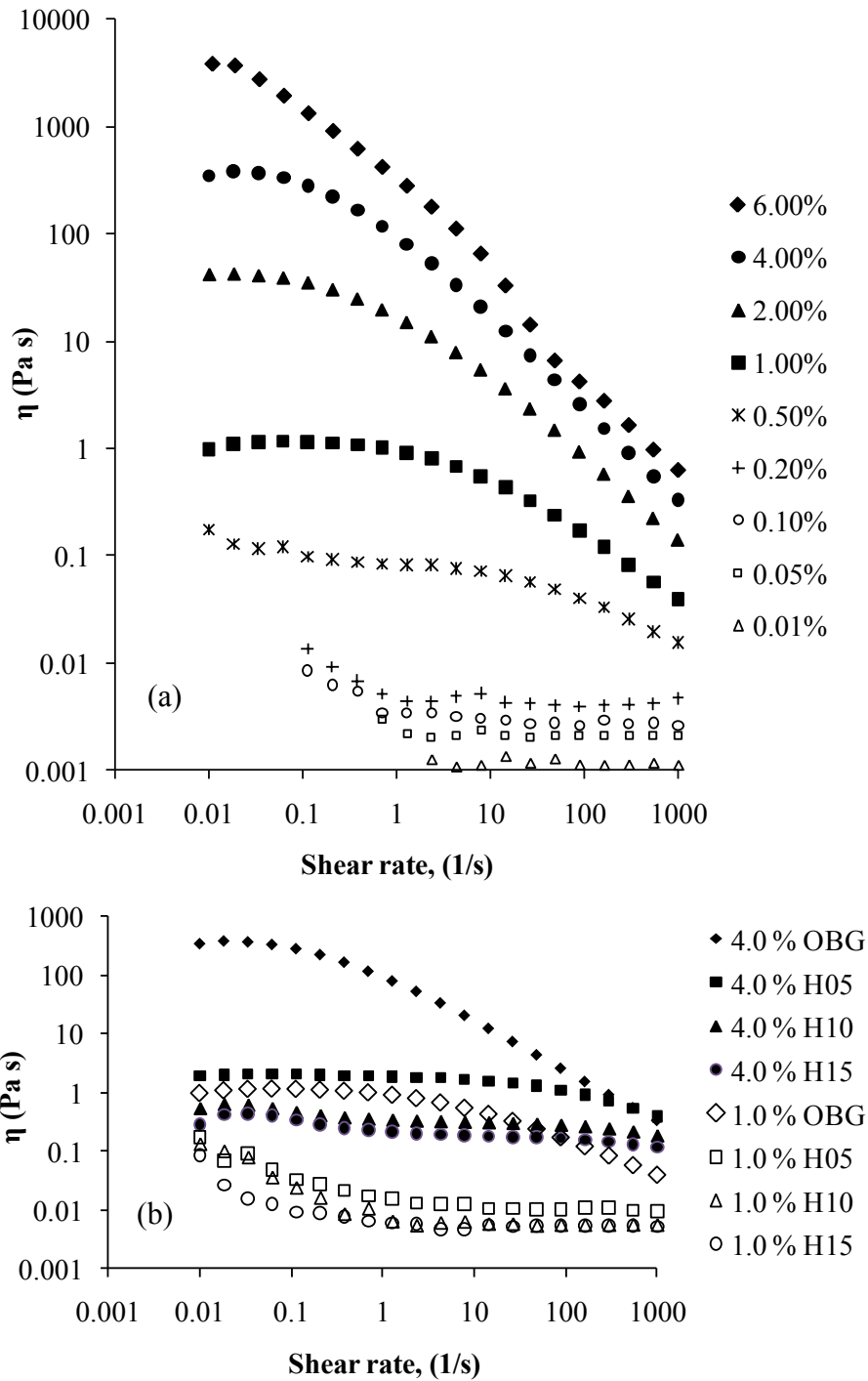
Figure 3.3: Viscosity dependence on shear rate for oat *β*-glucan solutions differing in (a) concentration (OBG) and (b) different molecular weights at 1 % and 4 % (w/v).

At higher concentrations, pseudoplastic behaviour was exhibited as the shear rate increased whereas, at lower concentrations, Newtonian behaviour was observed. The molecular weight

dependence of viscosity versus shear rate for the four oat β-glucan samples revealed that, at the same concentration, the viscosity was higher for higher Mw samples (OBG < H05 < H10 < H15)(Figure 3.3b). A similar trend has also been observed in previous studies involving β-glucan dispersions varying in Mw and concentration (Lazaridou *et al.*, 2003; Skendi *et al.*, 2003; Vaikousi *et al.*, 2004; Papageorgiou *et al.*, 2005).

The relationship between steady shear viscosity and complex viscosity was also studied for all β-glucan isolates. According to the Cox-Merz rule (as explained under section 1.6.2), the complex dynamic viscosity η^* (as a function of angular frequency, ω, rad/s) can be superimposed onto the plot of shear viscosity as a function of shear rate (1/s). Thus a direct relationship exists between the rheological response to non-destructive and destructive deformation whereby the oscillatory and shear flow curves should be identical if the polymer solutions are free from high-density entanglements or aggregates. Previous studies indicated that polymer solutions follow the Cox-Merz rule at low concentrations but deviations occur at high concentrations whereby η^* was higher than η at high frequencies or shear rates (Morris *et al.*, 1981; Jacon *et al.*, 1993; Böhm and Kulicke, 1999a; Lazaridou *et al.*, 2003; Skendi *et al.*, 2003; Vaikousi *et al.*, 2004).

At concentrations up to 1 % w/v, OBG followed the Cox-Merz relationship as there were no significant differences between η^* and η at equivalent rates of deformation, whereas OBG dispersions > 1% showed deviations from the rule (i.e., $\eta^* > \eta$) at high shear rates with an increasing difference as the concentration increased. In contrast, H05, H10 and H15 samples at 6 % w/v concentration all followed the Cox-Merz rule (Figure 3.4) whilst H10 and H15 exhibited Cox-Merz rule applicability even at 8 % concentration.
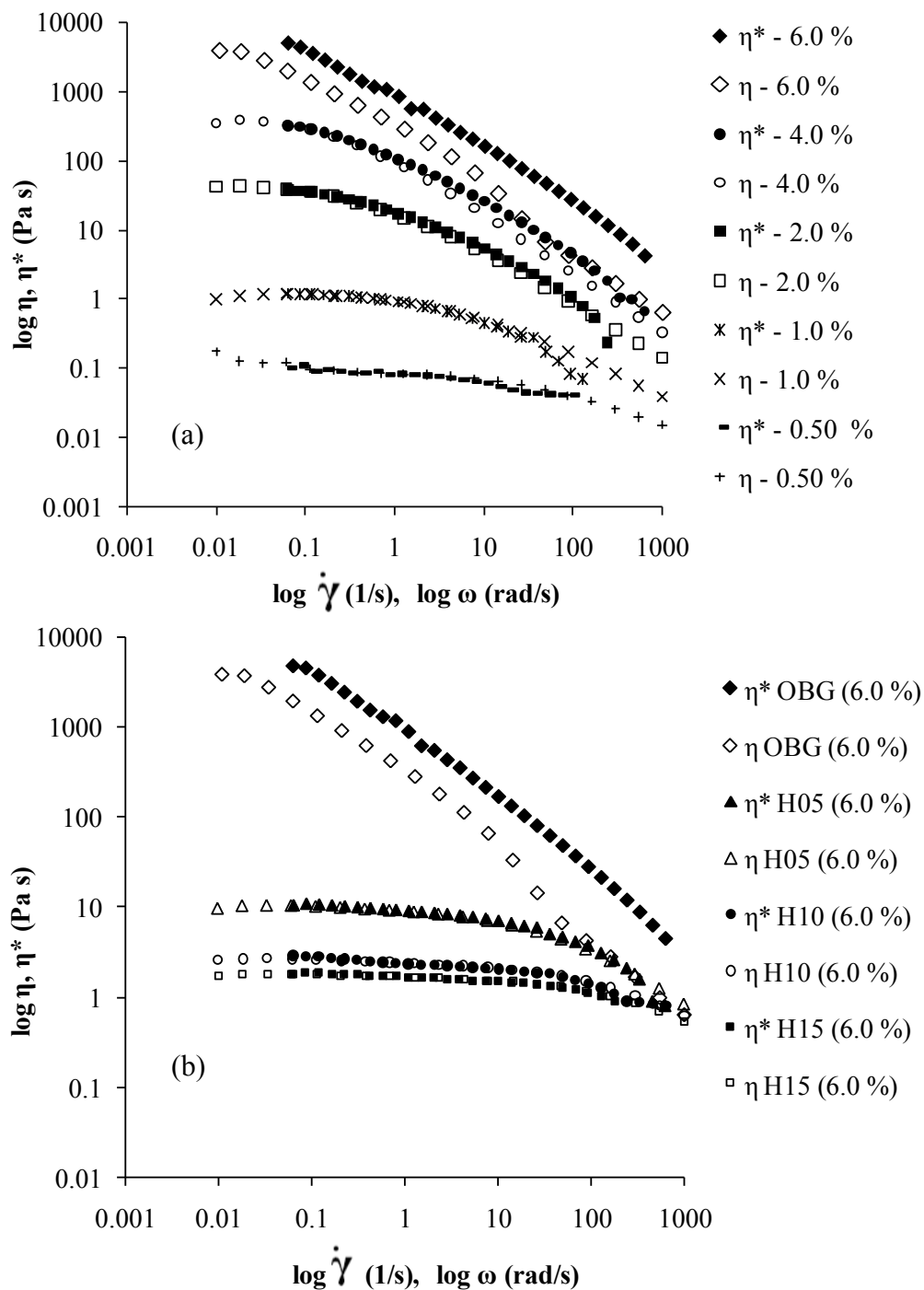
Figure 3.4: Cox-Merz rule applicability for oat β-glucan solutions at (a) different concentrations (OBG) and (b) with different molecular weights at 6 % (w/v).

Noticeably, OBG at 6 % concentration showed deviations with $\eta^* > \eta$ at all shear rates. The deviations may be due to the presence of high-intensity entanglements and/or intermolecular

chain aggregation of the system. These aggregates are more sensitive to shear forces than to the oscillatory perturbations where they have more time to reform in every cycle of oscillation. These aggregates exist and were visualized by AFM, as will be described in the next section. The results therefore indicate that Cox-Merz rule applicability for the oat β-glucan isolates is dependent on both Mw and concentration of the polysaccharides in solution.

Oscillatory measurements may provide indirect information on the conformation of polysaccharides in solution (Xu *et al*., 2008) and therefore dynamic measurements were performed for all the isolated samples. Figure 3.5 depicts the dependence of the mechanical spectra on concentration and Mw for various β-glucan solutions. At low concentrations (≤ 1.0 %) the loss modulus (G´´) was greater than storage modulus (G´) at all frequencies for the OBG dispersions, with the response corresponding to that of a non-entangled solution (Figure 3.5a). As the concentration increased (>2%) the G´-G´´ crossover, a characteristic of solutions with entangled polymeric chains, became evident. However, the entanglement plateau was more evident at high concentrations for the high molecular weight sample (Figure 3.5a). On the other hand, the G´-G´´ crossover was not observed for the low molecular weight solutions even at high concentrations (Figure 3.5b). This behaviour reflects the flexibility of the polysaccharide chain that is attributed to the β-(1→3) glycosidic linkage interrupting the continuity of the stiff cellulosic regions, thus imparting random coil conformation to the polysaccharide. Similar behaviour has been observed in previous studies for other polysaccharides such as locust bean gum (Lazaridou *et al*., 2001), levan (Kasapis *et al*., 1994), cactus mucilage (Cardenas *et al*., 1997), wheat arabinoxylans (Izydorczyk and Biliaderis, 1992) and cereal β-glucans (Doublier and Wood, 1995; Lazaridou *et al*., 2003; Vaikousi *et al*., 2004).
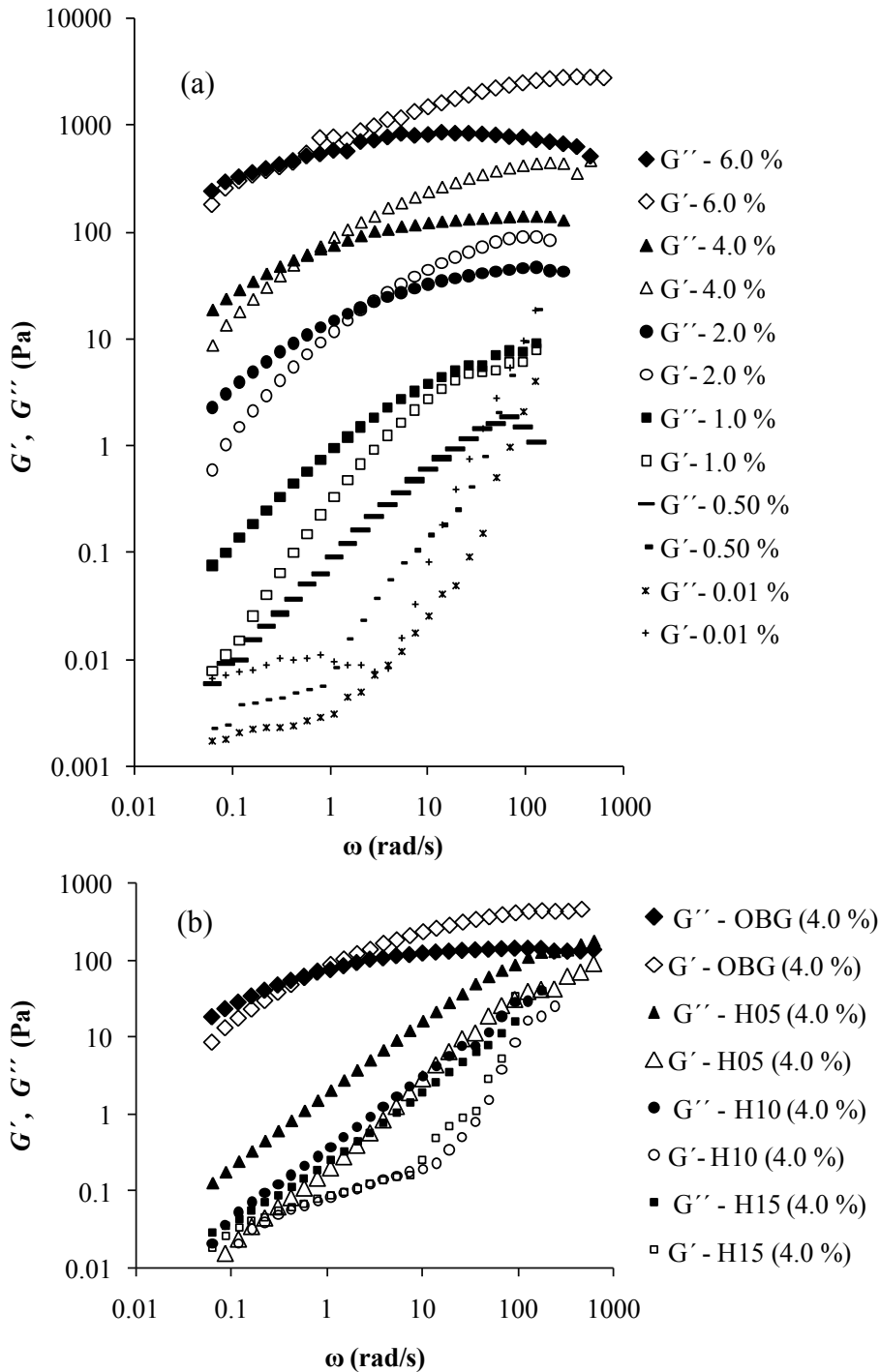
Figure 3.5: Frequency dependence of storage (G′) and loss (G″) moduli of oat *β*-glucan solutions at (a) different concentrations (OBG) and (b) with different molecular weights at 4 % (w/v).

The results clearly indicate that the rheological properties of the *β*-glucans depend on both molecular weight and concentration, which inevitably influence the interactions of the polysaccharide chains in solution. Therefore, the microstructure of *β*-glucans in solution was investigated by atomic force microscopy to identify any link between the rheological and microstructural properties as a function of molecular weight.

3.3.2 Microstructure of oat *β*-glucans by atomic force microscopy (AFM)

Polysaccharides including carrageenan (Ikeda *et al.*, 2001), xanthan (Capron *et al.*, 1998), gellan (Morris *et al.*, 2001), pectin (Löfgren *et al.*, 2002; Yang *et al.*, 2006), polygalacturonic acid (Alonso-Mougán *et al.*, 2003), psyllium polysaccharide (Guo *et al.*, 2009) and *β*-glucans (Vårum *et al.*, 1992; Grimm *et al.*, 1995; Li *et al.*, 2006b; Li *et al.*, 2011) form macromolecular aggregates when solubilized in water due to intermolecular hydrogen bonding.

Figure 3.6 depicts the typical microstructure of *β*-glucans of varying molecular weight indicating the formation of aggregates. Aggregate morphology was found to be highly dependent on the Mw of the sample. Generally, the size of the aggregates formed increased with increasing Mw of the sample in solution. Clusters of aggregates are seen with single molecules emerging from them, which are scattered heterogeneously throughout the system. It can be seen from the AFM images that the *β*-glucan clusters extend with thread-like polymer chains of variable thickness that join neighbouring molecules, short chain fragments or cluster of aggregates.
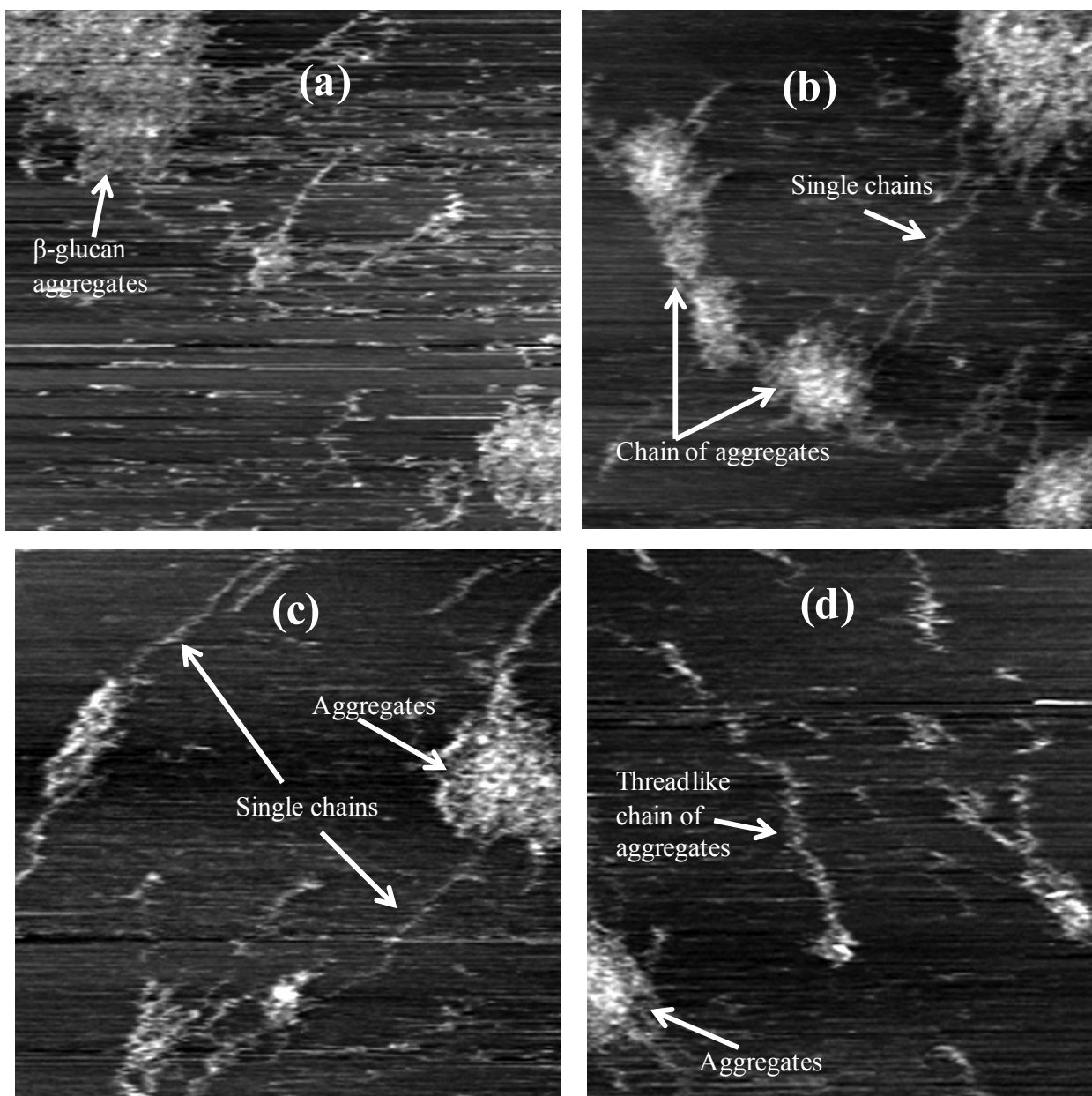
Figure 3.6: Topographical atomic force microscopy images of oat *β*-glucan isolates (a) OBG, (b) H05, (c) H10, and (d) H15 at 0.1 % (w/v) concentration. The scan sizes are 1μm x 1μm for all the images.

In a previous study, aggregates of oat β-glucan in aqueous solutions have been detected using static light scattering but not observed using osmotic pressure measurement for the same concentration range. It has been suggested that only a fraction of the molecules are involved in association to form large stabilized aggregates which has been described by a closed association model (Vårum *et al.*, 1992). Also, both static and dynamic light scattering techniques have been employed from which a fringed micelle model was proposed for barley β-glucan aggregates in dilute aqueous solution whereby formation of aggregates increased the measured chain stiffness (Grimm *et al.*, 1995). It has been shown that the aggregation behaviour of cereal β-glucans in aqueous solution is a fast dynamic process whereby the molecular association and dissociation are quick phenomenon. A cluster-cluster aggregation was suggested to be dominant whereby the average apparent diameter of β-glucans was also concentration dependent. As the Mw increased, the degree of aggregation decreased due to the lower diffusion rate of large molecules (Li *et al.*, 2011). Apparently, the nature of aggregation varies depending on the source and Mw of β-glucans, as well as the concentration in solution.

Formation of aggregates, therefore, is believed to have had an important influence on the rheological properties (Gómez *et al.*, 1997). The polydispersity of the aggregates increases with time (Alonso-Mougán *et al.*, 2003). It has been suggested that, when the system is at rest, the aggregates grow in size, possibly by means of diffusion (Li *et al.*, 2011). In contrast, under the force of deformation, aggregate breakdown occurs (Morris *et al.*, 2001) which also explains why η was generally lower than η^* at higher shear rates or frequencies in the steady shear and oscillatory measurements. Both η^* and η increased with increasing Mw at equivalent concentration and shear rate (Figure 3.4). The deviation from the Cox-Merz rule at even lower concentration for the high molecular weight sample (in comparison to the lower molecular

weight samples) may be due to the presence of high-intensity entanglements or big clusters of aggregates and their associated fragments, which are sensitive to shear forces. It is possible that it is the thread-like structures linking the aggregates which may rupture under shear. The viscoelastic behaviour of β-glucans (as shown by the mechanical spectra in Figure 3.5a) was also typical of entangled or aggregated solution for the OBG sample, which correlates well with the AFM images obtained. The beginning of the rubbery zone (i.e. the cross-over point when G´ > G´´) occurred at lower frequencies as the concentration of the polymer increases. This suggests that increased polysaccharide concentration enhances chain/aggregate interactions resulting in increase in the elasticity of the sample (Morris *et al.*, 2001).

3.4 Conclusion

In this investigation the rheological and microstructural properties of oat β-glucan isolates varying in molecular weight were examined by means of rheometry and atomic force microscopy. Results showed that the intrinsic viscosity, critical concentration, the flow and viscoelastic properties were highly dependent on the molecular weight of the samples. Pseudoplastic and Newtonian flow behaviour was exhibited depending on the concentration and molecular weight of the samples. The Cox-Merz rule was found to be applicable for the lower Mw samples at higher concentrations, whilst the high Mw samples showed a deviation at concentrations greater than 1.0 % w/v, suggesting the presence of aggregates. Atomic force microscopy revealed formation of clusters of aggregates linked via individual molecules scattered heterogeneously throughout the system. The aggregate size and morphology was also dependent on molecular weight of the samples and influences the rheological behaviour of β-glucan solutions.

CHAPTER 4

POLYSACCHARIDE DETERMINATION IN PROTEIN/ POLYSACCHARIDE MIXTURES FOR PHASE DIAGRAM CONSTRUCTION·

4.1 Introduction

Phase separated biopolymer systems are an active research area owning to their applications in food, nutraceutical and drug industry (Tolstoguzov, 2003; Kasapis, 2008). A first step to investigating such systems in the liquid state usually involves construction of phase diagrams of the constituent biopolymers at the specified conditions of interest in order to identify their compatibility region. Several methods can be used to construct a biopolymer phase diagram depending on the desired accuracy. Methods such as the phase-volume-ratio method (Polyakov *et al.*, 1980; Schorsch *et al.*, 1999) or simple visual observation of the separated phases (Hemar *et al.*, 2001; Thaiudom and Goff, 2003) are frequently used to construct phase diagrams of binary biopolymer mixtures. However, the most detailed phase diagram is obtained when the concentration of biopolymers in the separated phases is determined analytically. The polysaccharide concentration in the phases can be determined with methods such as refractometry (Bourriot et al., 1999b), or flow injection analysis (Kontogiorgos *et al*., 2009b), with the most popular apparently being the phenol-sulfuric method (Zhang and Foegeding, 2003; Antonov *et al.*, 2006; Kim *et al.*, 2006; Ercelebi and Ibanoglu, 2007; Lazaridou *et al.*, 2008; Lazaridou and Biliaderis, 2009; Perrechil *et al.*, 2009).

The phenol-sulphuric acid method is a simple and rapid colorimetric method for determining total carbohydrates, including mono-, di-, oligo- and polysaccharides. In this method, the concentrated sulfuric acid breaks down any polysaccharides, oligosaccharides, and disaccharides to monosaccharides. Pentoses then are dehydrated to furfural, and hexoses to hydroxymethyl furfural. These compounds (furan derivatives) then react with phenol to produce a yellow-gold colour that can be measured spectrophotometrically. The colour for this reaction is stable for hours, and the accuracy is within ±2% under proper conditions. The absorptivity of different carbohydrates, however, varies. For products high in hexose sugars, absorption is measured at 490 nm with glucose commonly used as standard. The absorbance is measured at 480 nm for pentoses and uronic acids (Brummer and Cui, 2006).

The original (Dubois *et al*., 1956) as well as the microplate format of the method (Masuko *et al*., 2005) for total sugar determination have been developed for pure sugar, oligosaccharide or polysaccharide solutions free of interferences. In mixed biopolymer systems, however, interferences resulting from the protein component may significantly affect the absorption measurements. Addition of sulphuric acid to proteins results in the production of various amounts of ammonium sulphate, sulphur and carbon dioxide. These products will interfere with the overall chemistry of the reactions making additionally dubious the use of the calibration curves. Furthermore, blank correction to alleviate signals that originate from sources other than the polysaccharide is also problematic since different blanks are needed as the protein concentration varies in the mixtures. Therefore, estimation of polysaccharide concentration is not a straightforward issue and removal of protein prior to analysis is required. The aforementioned reasons also create difficulties in other methods, such as total hydrolysis of the polysaccharide

followed by quantitative HPLC, making these techniques laborious and difficult to be used in practice.

Response surface methodology (RSM) to achieve optimization provides an effective way to visualize how the system's response changes when one or more of its factors change. RSM is advantageous as it reduces the number of experimental trials needed to evaluate multiple parameters and their interactions and provides sufficient information for statistically acceptable results. RSM has also been successfully demonstrated as useful in optimizing process variables and widely applied for optimizing conditions for polysaccharides in food and drug industry (Lee *et al.*, 2000; Kshirsagar and Singhal, 2007; Simsek *et al.*, 2007; XuJie and Wei, 2008 ; Gu *et al.*, 2009; Qiao *et al.*, 2009; Yongjiang *et al.*, 2009).

The objective of this investigation, therefore, is to explore the effect of protein removal from the mixtures on the determination of total sugar concentration for phase diagram construction in binary protein/polysaccharide mixtures using RSM and phenol-sulphuric method as an analytical tool and thus suggest the optimum parameter space that this method can be safely used.

4.2 Materials and methods

4.2.1 Materials and sample preparation

Guar gum, α-D-mannose, and sodium caseinate were purchased from Sigma (Sigma-Aldrich, St. Luis, MO). Distilled water and all chemicals used for the total sugar determination were of analytical grade.

Guar gum and sodium caseinate were dispersed in distilled water at 0.2% w/v and 2, 11 and 20 % w/v, respectively under continuous stirring and mild heating for several hours. After the end of the hydration period the stock solutions were centrifuged to remove any insoluble

material. Stock solutions were subsequently mixed in 1:1 ratio yielding binary mixtures with 0.1% w/v guar concentration and 1, 5.5, or 10 % w/v protein concentration as determined by the experimental design (Table 4.1).

4.2.2 Total sugar determination

TFA (0.1, 0.8, or 1.5 mL) was added in the mixtures and vortexed immediately. The resulting mixture was left to stand for 5, 32.5, or 60 min at room temperature and immediately centrifuged at 6000 rpm for 10 min (Beckman, TJ-6). The phenol-sulphuric acid method was then carried out on the supernatant (Dubois *et al*., 1956). A 0.5 mL aliquot of the supernatant was pipetted into a separate test tube and 0.5 mL of 5% phenol (in 0.1 M HCl) added. 2.5 mL of concentrated sulphuric acid was then added, vortexed and left to cool at room temperature. The absorbance readings of each tube were measured at 490 nm using a spectrophotometer (Shimazu UV-VIS 160A). A calibration curve was prepared using mannose as standard solution. All determinations were carried out in triplicate whereas the central point in the experimental design was repeated eighteen times (Table 4.1). The blank consists of all reagents used in their respective amounts excluding mannose or guar gum. Each run had a different blank solution according to the levels of the independent variables in the experimental design.

4.2.3 Experimental design and statistical analysis

For the investigation of the effect of TFA volume, time and protein concentration on the determination of total sugar concentration in protein-polysaccharide mixtures, response surface methodology with a full factorial face central composite design (FCCD) ($\alpha = 1$) was employed using Minitab Statistical Software (v. 15, Minitab Inc. US). FCCD consists of 20 base runs that

were performed in triplicate. This design yields 18 replicates of the central point and 42

replicates of the cube and axial points leading to a total of 60 replicates (Table 4.1).

Table 4.1: Experimental design and levels of factors in actual and coded values in the investigation of their effect on the determination of total sugar concentration in protein-polysaccharide mixtures.

Factors	Levels[a]		
	-1	0	1
TFA volume (mL) (X_1)	0.1	0.8	1.5
Time (min) (X_2)	5	32.5	60
Protein concentration (%w/v) (X_3)	1	5.5	10

		Factors	
Run	TFA volume (mL)	Time (min)	Protein concentration (% w/v)
1	0.1	5	1
2	0.1	60	1
3	0.1	32.5	5.5
4	0.1	5	10
5	0.1	60	10
6	0.8	32.5	1
7	0.8	5	5.5
8*	0.8	32.5	5.5
9	0.8	60	5.5
10	0.8	32.5	10
11	1.5	5	1
12	1.5	60	1
13	1.5	32.5	5.5
14	1.5	5	10
15	1.5	60	10

* This is the central point in the experimental design that was repeated 18 times in total.
[a] $X_1 = (X_1 - 0.8)/0.7$; $X_2 = (X_2 - 32.5)/27.5$; $X_3 = (X_3 - 5.5)/4.5$.

Experimental runs were randomized to minimize the effects of unexpected variability in the observed responses, allowing each experimental response to be optimized. The range and centre point values of three independent variables were selected on the basis of previously published data on guar-protein phase diagrams (Antonov *et al.*, 1999; Bourriot *et al.*, 1999a; Neirnyck *et al.*, 2007). A full second order polynomial response surface model was fitted to the experimental data that is given by the equation:

$$Y = \beta_o + \sum_{i=1}^{3} \beta_i X_i + \sum_{i=1}^{3} \beta_{ii} X_i^2 + \sum_{i<j}^{3} \beta_{ij} X_i X_j$$

where Y is the guar gum concentration, β_0, β_i β_{ii} and β_{ij} are the regression coefficients estimated by the model and X_i, X_j are levels of the independent variables. The model includes, from left to right, an intercept, linear terms, squared terms and quadratic interaction terms.

4.2.4 Fluorescence microscopy

Guar gum solution, pre-stained with 0.01% w/v solution of fluorescent brightener-28 (Sigma-Aldrich, St. Luis, MO) was mixed with pre-stained with rhodamine B (0.02% w/v) sodium caseinate solution at different ratios (1:1, 2:1, 1:2 guar:protein) yielding solutions with final biopolymer concentrations of 0.05-1, 0.05-2.5, 0.05-5, 0.1-1, 0.1-2.5 and 0.1-5% w/v (guar-protein). A drop of freshly prepared mixture was placed on a slide, covered with a cover slip and placed on the stage of the microscope at room temperature. Microscopy observations were carried out using an Olympus BX-41 epifluorescent microscope equipped with a mercury burner and an Olympus digital camera. Filter cubes with wide band UV excitation/emission filters, 350/440 nm and 555/595 nm, were used to observe the polysaccharide (fluorescent brightener 28) and the protein phase (rhodamine B), respectively. Images were captured with

both filter sets and brightness/contrast, highlights, shadows and midtones ("levels") were subsequently adjusted using Creative Suite 8 (Adobe Systems Inc, CA, US).

4.3 Results and discussions

4.3.1. Investigation of phenol-sulphuric method in protein-polysaccharide mixtures

Preliminary findings showed that, the estimated total sugar concentration in protein/polysaccharides mixtures varies depending on the protein content in the mixtures. In particular, a significant downward trend ($p < 0.05$) in polysaccharide recovery was observed as the protein concentration in the mixtures increased. This is indicative of interferences of the protein component on the phenol-sulphuric method that may affect the construction of phase diagrams. Therefore, the need for modification in the methodology seems necessary to optimize polysaccharide determination from the mixtures.

The actual guar concentration that could be determined with the phenol-sulphuric method in the stock solution was investigated first and compared with the nominal (dispersed polysaccharide powder). The actual guar concentration was estimated to be $0.094 \pm 0.007\%$ w/v when the nominal was 0.100% w/v indicating about a 6% deviation. This error is in close agreement with previously reported values on the phenol-sulphuric acid method in guar gum solutions (~5%) (Ng *et al*., 2009). These differences are attributed to the purity of the guar gum preparation and its hydration behaviour since it highly depends on the molecular weight and concentration of the dispersed galactomannan (Wang *et al.*, 2003; Parvathy *et al.*, 2007; Ng *et al.*, 2009). Therefore some material is removed after the centrifugation step that was employed resulting in actual concentration that is lower than the nominal. The following discussion is done in terms of the actual concentration (0.094% w/v), which was held constant for all mixtures throughout.

The effect of three parameters (TFA, time and protein concentration) on the estimation of total sugar concentration by the phenol-sulphuric method was investigated next by response surface methodology. The coefficient estimates of model equation, along with the corresponding *p*-values, are presented in Table 4.2.

Table 4.2: Estimated regression coefficients for the polynomial model used to describe the total sugar concentration (% w/v).

Factor	Coefficient
Constant	0.050***
TFA	- 0.003*
Time	0.004**
Protein	-0.0065***
TFA^2	0.0035 (NS)
$Time^2$	-0.004 (NS)
$Protein^2$	-0.003 (NS)
TFA × Time	-0.002 (NS)
TFA × Protein	0.002 (NS)
Time × Protein	0.005**
r^2	0.546
Probability of lack-of-fit	0.213 (NS)

* $p < 0.05$, ** $p < 0.01$, *** $p < 0.001$

(NS): not significant. Analysis was done using coded units.

The *p*-values were used as a tool to check the significance of each coefficient, which also indicate the interaction strength between each independent variable. The constant (0.050, Table 4.2) shows that about half of the guar gum concentration in the mixtures can be determined if there were no influence from the factors. All the factors (TFA volume, protein concentration, time) had a significant influence on the polysaccharide recovery from the mixtures. The results showed that TFA had a significant ($p < 0.05$) linear contribution on guar concentration with the negative coefficient value (Table 4.2) implying that the higher the TFA volume the lower the resulting guar gum that can be estimated with the present methodology. This however is counteracted by the quadratic effect implying the overall pattern is also subject to interactions with protein and time that samples were left in the presence of the acid in the systems (Table 4.2; Figure 4.1). TFA is not expected to play a direct role on the measurements since guar gum is a neutral polysaccharide and not influenced by changes of pH. Furthermore, polysaccharide hydrolysis usually occurs at high temperatures and is unlikely to take place at room temperature as in the present investigation (Phillips and Williams, 2009). Therefore, the significant effect ($p < 0.05$) of TFA on the determination of guar concentration could be attributed to the effect of acid on the protein. As TFA is added in the mixtures pH drops and proteins reach their isoelectric point thus precipitating. However, at increased protein concentration, precipitation results in polysaccharide removal due to entrapment of guar in the protein aggregates (Turgeon *et al.*, 2003) and therefore less sugar can be determined in the resulting supernatant. Therefore, as protein concentration increases in the mixtures less total sugars can be determined because more polysaccharide is co-precipitating entrapped in the protein matrix (de Kruif and Tuinier, 2001) (Figure 4.1). The linear effect of time as well as its interaction with protein concentration had both positive significant contributions to the total sugar concentration (Table 4.2).
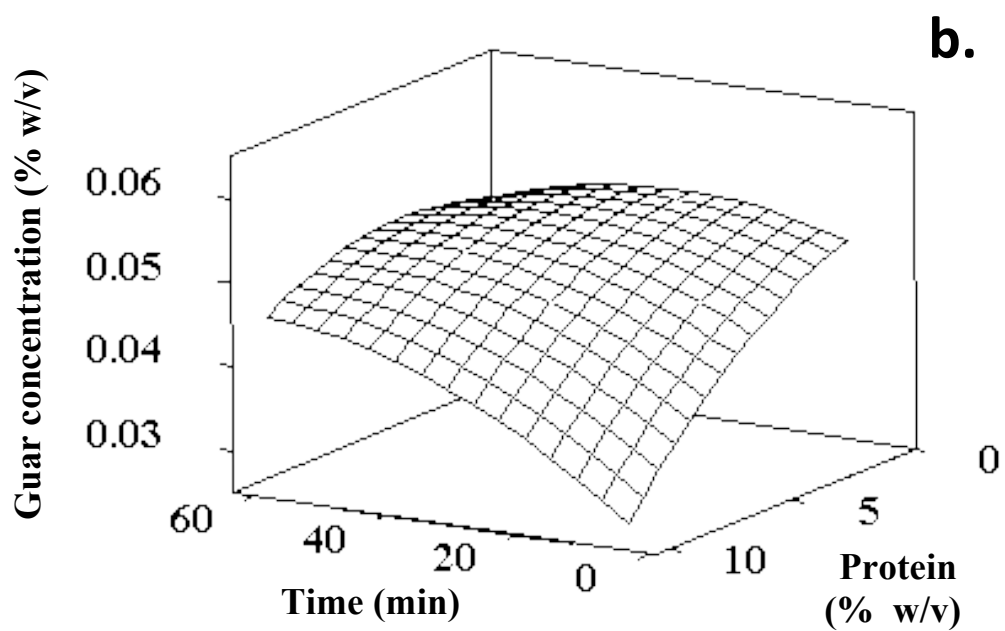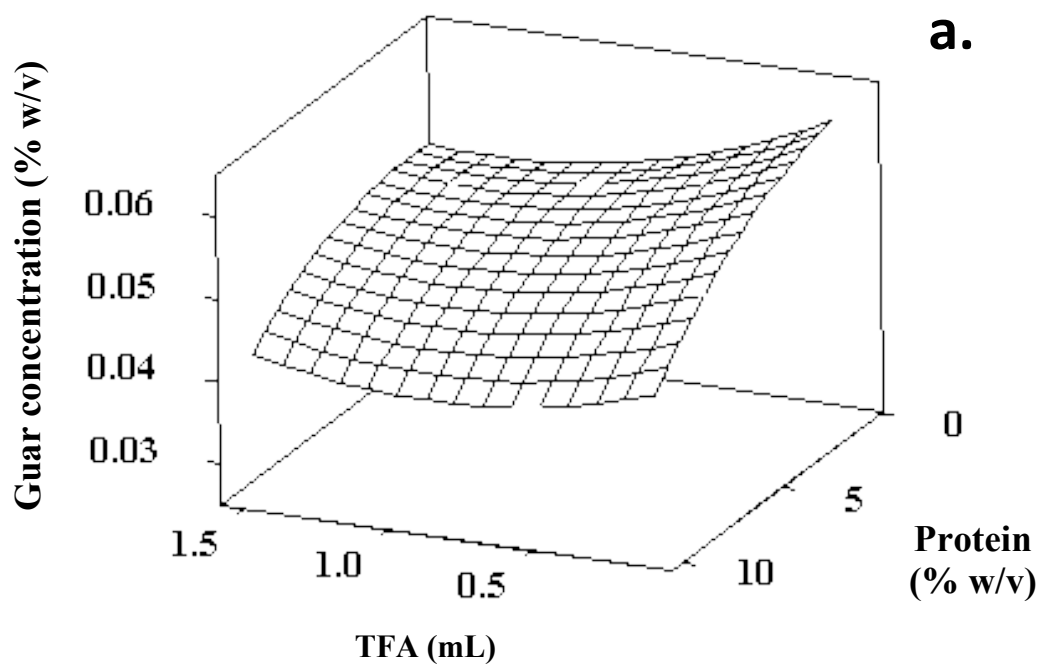
Figure 4.1: Surface plots of total sugar concentration (% w/v) versus (a) as a function of TFA and protein concentration and (b) as a function of time and protein concentration.

Figure 4.1b shows that guar gum concentration increases with increasing time that the samples were left in the presence of TFA before phenol-sulphuric analysis. This implies that the longer the time lapse more proteins precipitate and therefore more polysaccharide can be estimated in the supernatant. The overall effect of the factors is also subject to their quadratic effect and interactions. The quadratic effects of each factor (X_i^2) was not significant for all factors studied something that indicates that it is not expected curvature in the response surface, that is to say, there will not be an optimum polysaccharide concentration (either maximum or minimum) by varying these factors.

By using the estimated regression coefficients, the response variable, Y (total sugar concentration) and the test variables X_1, X_2 and X_3 (representing TFA volume, time and protein concentration, respectively) can be related by the following equation: $Y = 0.050 - 0.003X_1 + 0.004X_2 - 0.0065X_3 + 0.0035X_1^2 – 0.004X_2^2 - 0.003X_3^2 – 0.002X_1X_2 + 0.002X_1X_3 + 0.005X_2X_3.$ The lack-of-fit which is a measure failure of the model to represent the data in the experimental domain (Qiao *et al*., 2009). The lack-of-fit was not significant ($p > 0.05$) relative to the pure error; something that indicates that the fitted equation could describe the response under any combination of values of the variables tested. The obtained r^2 value (0.546) indicates the agreement between the experimental and predicted values of the determined guar gum concentration and although from analytical chemistry perspective seems to be low, it is satisfactory if we take into account the complexity of mixed biopolymer systems as well as the objective of the present investigation.

The mean maximum polysaccharide concentration that could be determined was about 0.06% w/v that represents about 64% of the mixture concentration. The unrecovered amounts can therefore be attributed to the negative effects of the test variables as well as losses possibly

due to polysaccharide co-precipitation and interferences from proteins that remained in the polysaccharide phase. However, the method can be reliably used to estimate the polysaccharide concentration in mixed biopolymer systems, as the percentage error ($\pm$ 6 %) is considered acceptable for the purposes of the present investigation. Taking all findings of the present investigation into consideration, it is possible to estimate about 60 % of the initial guar gum concentration in the mixtures (0.094 % w/v), when the protein content in the mixtures ranges between 5-10 % w/v, about 0.5 mL TFA is added and left for 30 min rest. For greater than 60 % guar gum determination, the protein content in the mixtures must be less than 5.5 %w/v with less than 0.5 mL TFA and more than 30 min rest. However, these suggestions could work best for biopolymer mixed systems involving neutral polysaccharides since the charged ones may form complexes with proteins (Antonov *et al*., 1999) that cannot be removed with TFA precipitation thus further increasing the complexity of the system. The results provide strong evidence that when attempting to construct phase diagram of mixed biopolymer systems the equilibrium phases must be diluted to a protein content < ~5 % w/v before TFA treatment if the maximum polysaccharide concentration is to be determined.

The incompatible nature of proteins and polysaccharide (Doublier *et al*., 2000; Tavares and da Silva, 2003; Turgeon *et al*., 2003; Neirynck *et al*., 2007) clearly influences the determination of the polysaccharide in the mixtures. Therefore, the microstructure of the mixtures was investigated next by fluorescence microscopy to seek further evidence of interferences in the determination of the total sugar concentration.

4.3.2 Morphology of mixed systems

The morphological features and topological arrangement of biopolymers in the mixtures were probed by means of fluorescent microscopy. Guar gum solutions revealed bright patterns

scattered homogeneously throughout the sample (Figure 4.2a). In contrast, sodium caseinate solutions in the absence of guar result in featureless patterns at all concentrations studied (1, 5 and 10 % w/v) (Figure 4.2b). Phase separation in the system was evident with addition of guar gum into the protein phase. Images taken at various mixture concentrations and with two different filter sets revealed a phase-separated system with the guar domains surrounded by a continuous protein phase (Figure 4.2c-f). Similar irregular-shaped morphological elements have been previously observed in high molecular weight *β*-glucan/whey protein mixtures (Kontogiorgos *et al*., 2009a; Kontogiorgos *et al*., 2009b), pea protein/κ-carrageenan (Musampa *et al*., 2007), *β*-lactoglobulin/pectin (Girard *et al*., 2004) or soy protein/κ-carrageenan (Li *et al*., 2008b). In contrast, mixtures of guar/micellar casein (Bourriot *et al*., 1999a; Schorsch *et al*., 1999; Norton & Frith, 2001), gelatin/maltodextrin (Kasapis, 2008), milk proteins/xanthan (Hemar *et al*., 2001) or low molecular weight *β*-glucan/whey protein mixtures (Kontogiorgos *et al*., 2009a) exhibited spherical morphology. Evidently, the morphological features of protein/polysaccharide mixtures vary depending on the properties of the solvent and constituent biopolymers. Visualization of mixtures using two different excitation/emission filter sets revealed new morphological characteristics as guar gum and protein concentration increases. Guar aggregates are able to entrap protein within the guar aggregates (Figure 4.3). Furthermore, as protein content in the mixture increases the protein that is entrapped in the polysaccharide aggregate also increase (Figure 4.3b). These protein inclusions are difficult to remove with TFA and may play important role on the polysaccharide quantification, as they will both interfere with absorption measurements and volume changes of the system leading to erroneous calculations.
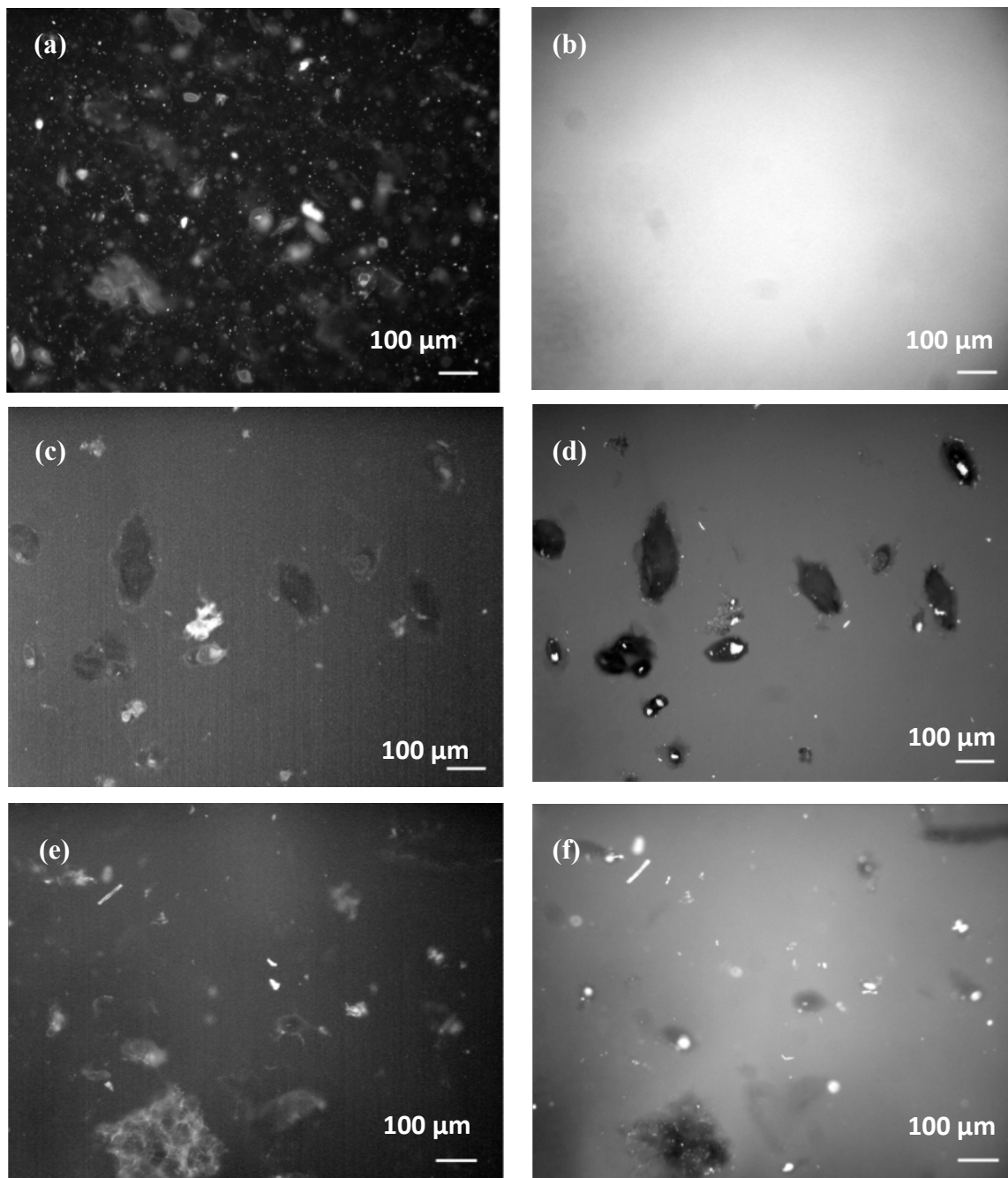
Figure 4.2: Fluorescent images of the mixtures at different guar/protein concentrations (a) 0.1% w/v guar gum (b) 5% w/v sodium caseinate, (c, d) 0.1–2 and (e, f) 0.05-1 (% w/v guar-protein). Images were taken using two different filter sets: left (a, c, e) for excitation of fluorescent brightener 28 (polysaccharide phase) and right (b, d, f) for excitation of rhodamine B (protein phase).
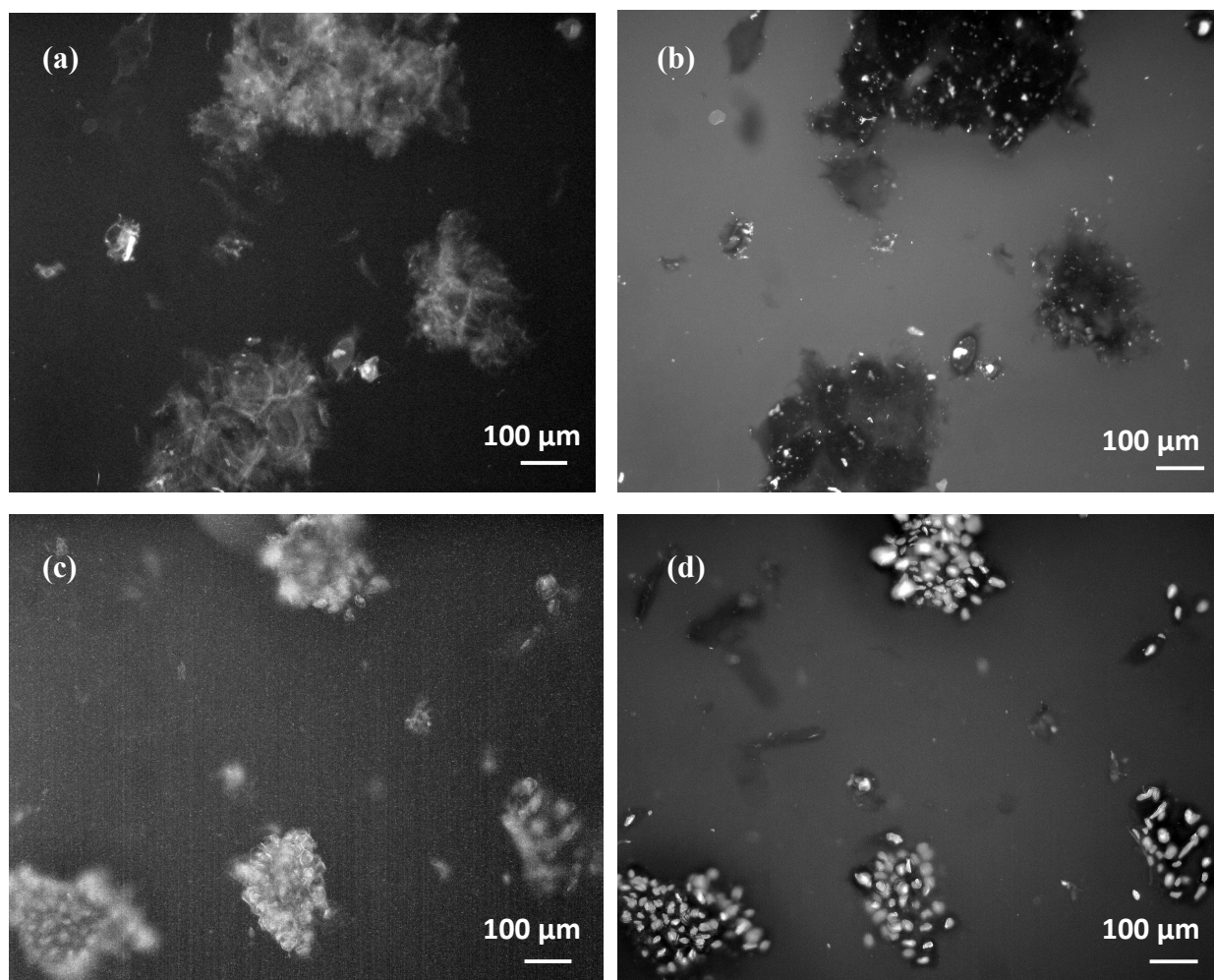
Figure 4.3: Fluorescent images of the mixtures at (a, b) 1% w/v and (c, d) 5% w/v protein concentrations at the same guar concentration (0.1 % w/v).

Taking everything into account, microscopical evidence as well as experimental measurements (Figure 4.1) show that for greater polysaccharide estimation the protein concentration must be low ($< \sim$5% w/v) before phenol-sulphuric method in mixed systems.

4.4 Conclusion

The effect of protein precipitation prior to phenol-sulphuric acid method in protein/polysaccharide mixtures was investigated by response surface methodology and fluorescent microscopy. Protein concentration, TFA volume as well as the time that the mixture was left in the presence of TFA, significantly influence the total sugar concentration that is estimated with this method. Fluorescence microscopy revealed a phase-separated system while some protein inclusions are formed within the polysaccharide phase, which provides further evidence of interferences in the determination of the total sugar concentration. Equilibrium phases must be diluted to a protein content $< \sim5\%$ w/v before TFA treatment for maximum total sugar concentration determination in phase-diagram construction of mixed biopolymer systems.

CHAPTER 5

PHASE BEHAVIOUR OF β-GLUCAN/SODIUM CASEINATE MIXTURES VARYING IN MOLECULAR WEIGHT

5.1 Introduction

The phase behaviour of protein-polysaccharide mixtures contributes significantly to the stability, structural, rheological and textural characteristics of food products. Phase separation is known to occur depending on the molecular characteristics of biopolymers (molecular weight, conformation, charge density) as well as the mixing conditions or factors such as pH, ionic strength, solvent quality, mixing ratio, relative concentration of both biopolymers, mixing temperature, cooling rate, etc. (Schmitt *et al.*, 1998; Doublier *et al.*, 2000; Tolstoguzov, 2000; de Kruif and Tuinier, 2001; Norton and Frith, 2001; Tolstoguzov, 2003; Turgeon *et al.*, 2003; Neirynck *et al.*, 2007; Perez *et al.*, 2009). In the mixed system involving nonionic (neutral) polysaccharide and protein, pH and ionic strength influence only the protein self association and incompatibility is linked to this phenomenon (Syrbe *et al.*, 1998). The criteria for thermodynamically favourable interactions have been discussed under Chapter 1 Section 1.4.3.

The approval of oat *β*-glucan as a functional bioactive ingredient has stimulated new product development activity over the years (Brennan and Cleary, 2005; Lazaridou and Biliaderis, 2007). Incorporation of *β*-glucans into milk and dairy products presents a potential application of this polysaccharide to confer the associated health benefits to consumers. However, the required amount (≥ 0.75 g/serving) for health claims makes it difficult in the development of food formulations as *β*-glucans exhibit thermodynamic incompatibility when mixed with milk proteins (Kontogiorgos *et al.*, 2009a; Kontogiorgos *et al.*, 2009b; Lazaridou and

Biliaderis, 2009). It is important, therefore, to understand the phase behaviour of β-glucans with food proteins in the attempt to make products with desired rheological properties.

Determination of phase diagrams is often employed to describe the thermodynamic compatibility of mixed biopolymer systems. In a previous study, the phase behaviour of high molecular weight β-glucan/whey protein isolate binary mixtures under different solvent conditions was investigated. It was shown that a decrease of pH from 7.0 to 3.0 and sucrose addition enhanced miscibility (Kontogiorgos *et al.*, 2009b). The molecular weight of the biopolymers is expected to influence the extent of miscibility and concentration levels at which phase separation occurs. Theoretically, a decrease in the molecular weight of the biopolymers is expected to increase the biopolymer compatibility in solution since this will increase the combinatorial entropy of mixing (Schmitt *et al.*, 1998).

This study, therefore, aims to investigate the phase behaviour of mixtures of sodium caseinate with β-glucan isolates varying in molecular weight by means of phase diagram construction, rheometry, electrophoresis and fluorescence microscopy.

5.2 Materials and methods

5.2.1 Materials and sample preparation

Sodium caseinate, fluorescent brightener-28, rhodamine B, sodium azide (NaN_3) and trifluoroacetic acid (TFA) were purchased from Sigma-Aldrich (Poole, Dorset, UK). All chemicals used were analytical grade reagents.

The initial β-glucan isolate (denoted as OBG) obtained by aqueous extraction from oat and three samples of lower molecular weights (H05, H10 and H15) produced from the initial isolate by controlled acid hydrolysis (for 0.5, 1.0 and 1.5 h respectively) as described in detail under

Chapter 2 (refer to Section 2.1.2, 2.1.3; Figure 2.1) were used for the investigation of the phase behaviour with sodium caseinate.

Stock dispersions of the biopolymers (14% w/v sodium caseinate, 1.0% w/v OBG, 1.2 % w/v H05, 1.8 % w/v H10, 1.8 % H15) were prepared in 0.1 M Sorensen's phosphate buffer (pH 7.0) with 0.02% w/v sodium azide (NaN_3) as preservative. Sodium caseinate was dispersed under mild heating at 40 ^{o}C in the buffer solution whereas β-glucan was dispersed in the pH 7.0 buffer solutions at 90 ^{o}C in a sealed vial under continuous stirring for 3 h. The concentrations of the β-glucan sample solutions differ because of the maximum concentration that could be prepared with each isolate; the higher the molecular weight the lower the maximum experimental concentration achieved. Higher concentrations yielded insoluble β-glucan agglomerates resulting in inhomogeneous dispersions. The dispersions were left to hydrate at 5 ^{o}C overnight followed by centrifugation (1500$\times$ g at 5 ^{o}C for 10 min) to remove insoluble particles. Subsequently, the stock dispersions were vortex-mixed at seven different volume ratios (95/5, 80/20, 65/35, 50/50, 40/60, 25/75, 95/5 % v/v (sodium caseinate/β-glucan)) in centrifuge tubes at constant volume (5 mL) yielding binary mixtures of different biopolymer concentrations.

5.2.2 Phase analysis and phase diagram construction

The mixed samples were centrifuged at 3000 $\times$ g for 30 min at 5 ^{o}C in order to accelerate equilibrium phase separation. Centrifugation of the mixtures under these conditions resulted in constant composition of the phases demonstrating that equilibrium was reached. After phase separation, the equilibrium phase was analyzed for the protein and β-glucan content.

The protein content was determined according to the Bradford protein assay (Bradford, 1976). The β-glucan concentration was determined using a modified phenol-sulphuric acid method for the phase-diagram construction (Agbenorhevi and Kontogiorgos, 2010). Briefly, 0.2

mL TFA was added in the 5 ml of diluted mixtures and vortexed immediately to precipitate the proteins out of solution. The resulting mixture was left to stand for 40 min at room temperature and immediately centrifuged at $6000 \times g$ for 10 min. An aliquot of the supernatant was taken and the phenol-sulphuric acid method was then carried out to determine the total polysaccharide concentration. A standard calibration curve was prepared using glucose. All samples were replicated at least twice and the biopolymer concentration in the phases analyzed in triplicates.

After the equilibrium phase analysis for the biopolymer concentration, values obtained were used to construct a phase diagram. GraphPadPrism v.5 (GraphPad Software, San Diego, USA) was used to create the final binodal curve.

5.2.3 Viscosity measurements

The flow behaviour (viscosity) of the mixed systems was determined at 20 ^{o}C using a Bohlin Gemini 200HR nano rotational rheometer (Malvern Instruments, Malvern, UK) equipped with cone-and-plate geometry (55 mm diameter, cone angle 2°). Flow curves were measured at a range of shear rates in the range 0.01–1000 s^{-1}. Data were analyzed with the supporting rheometer software. All rheological measurements were carried out on freshly prepared samples.

5.2.4 Fluorescence microscopy

A drop of freshly prepared β-glucan/sodium caseinate mixture (at different mixed ratios as previously described) pre-stained with fluorescent brightener-28 (0.01% w/v) and rhodamine B (0.02% w/v) was placed on a slide, covered with a cover slip and placed on the stage of the microscope at room temperature. Microscopy observations were carried out using an Olympus BX-41 epifluorescent microscope equipped with a mercury burner and an Olympus digital camera. Filter cubes with wide band UV excitation/emission filters 350/440 nm and 555/595 nm

were used to observe the polysaccharide (fluorescent brightener 28) and the protein phase (rhodamine B), respectively.

5.2.5 Sodium dodecyl sulfate polyacrylamide gel electrophoresis (SDS-PAGE)

All chemical reagents (MES SDS buffer kit) and gels (NuPAGE® Novex 12% Bis-Tris Gel 1.0mm, 10 well) used for SDS-PAGE analysis were purchased from Invitrogen Ltd. (Paisley, UK). The stock solutions of each pure casein subunit (α-, *β*-, κ-casein), sodium caseinate and the various mixtures of sodium caseinate and *β*-glucans were prepared using a phosphate buffer pH 7.0 as in all other experiments.

Into an eppendorf tube, 5 µL of sample (stock) solution, 5 µL of NuPAGE® LDS sample buffer (4X), 2 µL of NuPAGE® reducing agent (10x) and 8 µL of deionised water were added and well mixed. The samples were then heated at 70 °C for 10 min to denature the proteins.

The electrophoresis was performed using the XCell *SureLock*™ Mini-Cell (Invitrogen Ltd., Paisley, UK) according to the NuPAGE® Bis-Tris Mini Gel protocol. A continuous buffer system (prepared by adding 50 mL of 20x NuPAGE MES SDS running buffer to 950 mL of deionised water) was used. The inner and outer buffer chambers were filled with the appropriate amount of the running buffer. The various treated samples, standards and the protein molecular weight marker were then loaded (10 µL) into separate wells of the gel and electrophoresis was run for 35 min at 200 V. The Novex® Sharp Protein Standard prestained molecular weight marker was used comprising a mix of proteins ranging from 3.5 to 260 kDa.

After the electrophoresis was completed, gels were removed from the plates, washed with deionised water and then stained using SimplyBlue™ Safe-Stain. After staining, the gels were then washed several times with changes of deionised water. Images of the bands on the gel were taken using a digital camera.

5.3 Results and discussion

5.3.1 Phase diagram

To investigate the concentration levels at which sodium caseinate in mixtures with β-glucan of different molecular weights may exhibit compatibility (co-solubility) or incompatibilty (phase-separation), phase diagrams were constructed (Figure 5.1) following the analytical determination of the biopolymer concentrations in the equilibrium phase at 5 $^{\circ}$C.

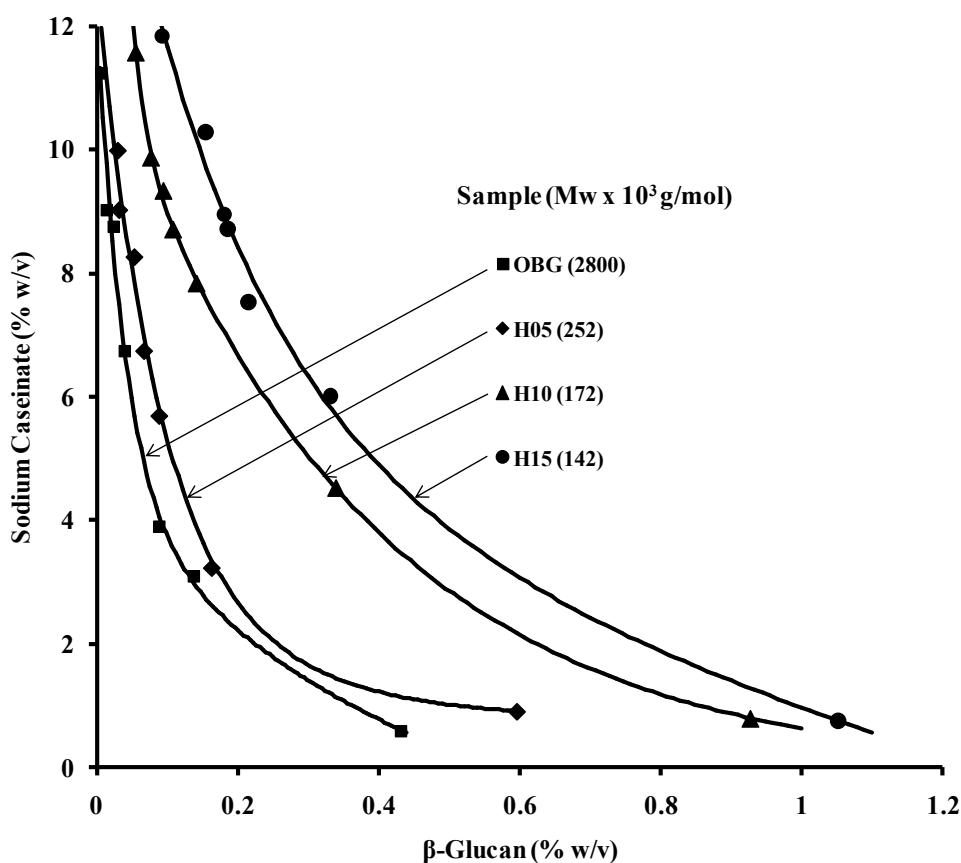**Figure 5.1:** Phase diagram of binary mixtures of sodium caseinate and β-glucans varying in molecular weight.

The solid curve represents the binodal, which demarcates the compatible (one phase) from the incompatible (two phase) region. Thus the area below the binodal shows the concentration levels at which the β-glucan/sodium caseinate mixtures are at equilibrium (i.e., stable) whereas

the area above the binodal represent the concentration zones where phase separation occurs. Therefore, the results clearly indicate that the compatibility region increases significantly as the molecular weight of β-glucan decreases (i.e., OBG < H05 < H10 < H15). This shows that the molecular weight of β-glucan samples has a significant effect on miscibility with proteins. Since the experiments were performed at neutral pH, which otherwise would influence the protein, and β-glucan is a neutral linear polysaccharide, variation in the thermodynamic compatibility with sodium caseinate as a function of molecular weight could be explained by the excluded volume effect. High molecular weight β-glucan yields a large excluded volume, which is inaccessible to sodium caseinate. In contrast, low molecular weight samples (obtained through depolymerisation by controlled acid hydrolysis) have increased molecular flexibility and reduced hydrodynamic volume thereby creating free volume for the protein molecules even at relatively high β-glucan concentrations, resulting in extensive thermodynamic compatibility. In other words, the smaller molecular weight/size of β-glucan chains in the system will possibly give rise to increased entropy of mixing and consequently enhance the mixing stability (Tolstoguzov, 1997; Syrbe *et al.*, 1998; Doublier *et al.*, 2000; Semenova, 2007).

5.3.2 Microstructure of mixtures

Following the phase analysis, the microstructure of biopolymers in mixtures was probed by means of fluorescence microscopy. Sodium caseinate solutions in the absence of β-glucan exhibited featureless patterns at all concentrations studied (Figure 5.2a) whereas β-glucan solutions without sodium caseinate showed bright spots distributed homogeneously throughout the sample (Figure 5.2b). At various combinations in the mixed system, images taken with two different filter sets revealed phase separated domains (Figure 5.2).
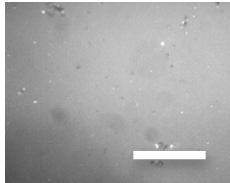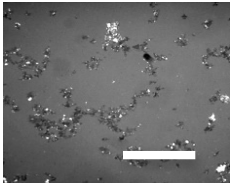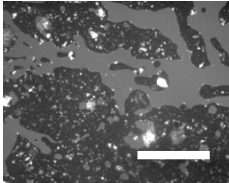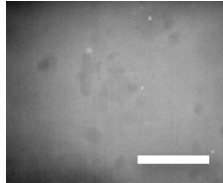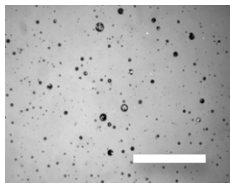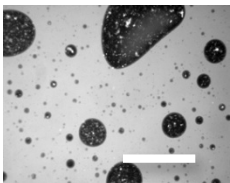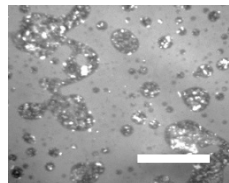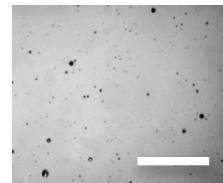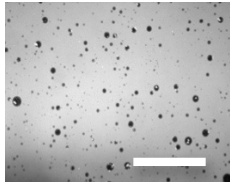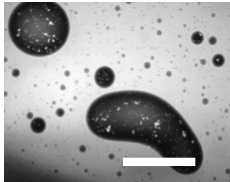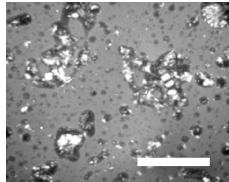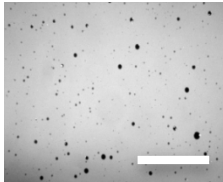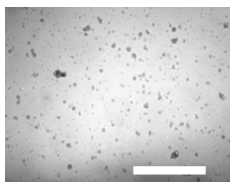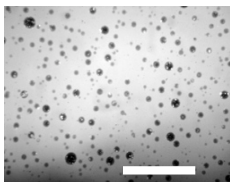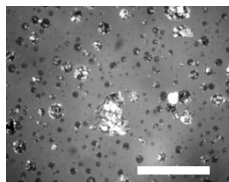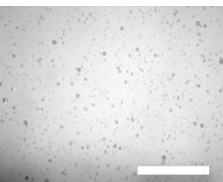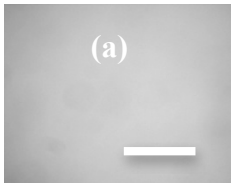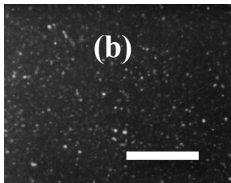
Figure 5.2: Typical fluorescence microscopic images of *β*-glucan/sodium caseinate mixtures at different regions of the phase diagram. (a) protein (sodium caseinate) only (b) β-glucan only. Scale bar: 100 μm.

Biopolymer morphology varied depending on the concentration and molecular weight. In the protein-rich phase, β-glucans appear as droplets whereas in the bicontinuous phase, β-glucan droplets increase in number especially for the lower molecular weight samples. In the polysaccharide-rich phase, β-glucan aggregates become more pronounced in size and irregularity especially for the higher molecular weight materials. As can be seen, the high Mw sample (OBG) showed distinct morphology from the low Mw counterparts in the bicontinuous and polysaccharide-rich phases. Such morphology suggests that apart from the thermodynamic considerations aforementioned, the state of aggregation also influences the phase behaviour of the mixtures through density differences. It was interesting to note that mixed systems at equilibrium comparatively had lesser or no β-glucan aggregates present. At equivalent concentration levels in mixture with sodium caseinate, it was observed that lower Mw samples become more dispersed in the protein domain, form small aggregates and achieve homogeneity in the equilibrium phase. This confirms that a reduction in the excluded volume effect of small macromolecules gives rise to improved thermodynamic compatibility.

5.3.3 Flow behaviour of mixtures

The viscosity of sodium caseinate solutions, increases as the concentration increases, with the flow behaviour being mainly Newtonian at all shear rates for the concentrations (0.1 – 14% w/v) studied (Figure 5.3). For β-glucan solutions, viscosity also rises with increasing concentration, and at equivalent concentration levels, viscosity was higher for the higher molecular weight samples (Agbenorhevi *et al.*, 2011). In the sodium caseinate/β-glucan mixed systems, however, the viscosity also varied depending on the concentration of the two biopolymers.
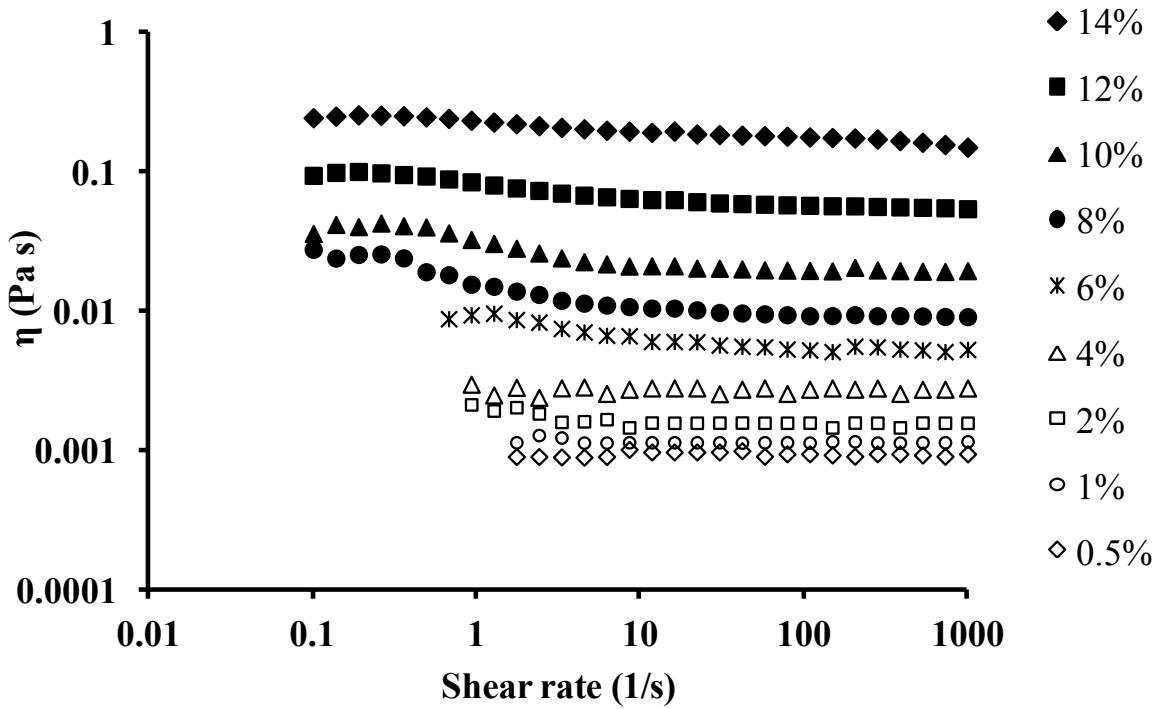
Figure 5.3: Flow behaviour of sodium caseinate at different concentrations (0.5–14 %w/v).

Figure 5.4 shows typical flow curves of the *β*-glucan/sodium caseinate mixtures at different mixed ratios (i.e., varying biopolymer concentrations). In the protein-rich phase, the flow behaviour was mainly influenced by the sodium caseinate whereas in the polysaccharide-rich phase, the flow behaviour was largely determined by *β*-glucan. At intermediate biopolymer concentrations, a mixed flow pattern was evident as previously reported (Kontogiorgos *et al.*, 2009b).
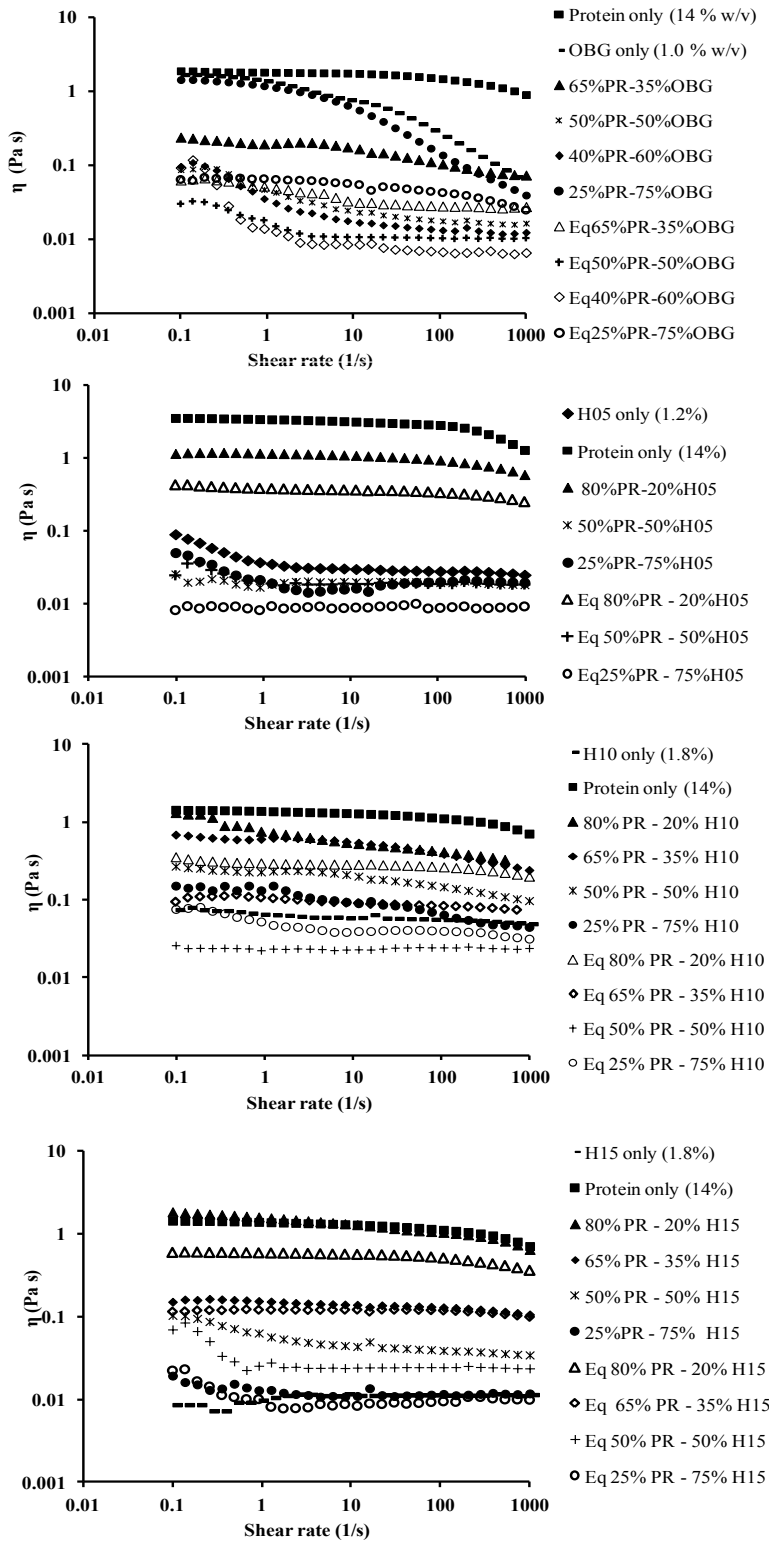
Figure 5.4: Flow curve of *β*-glucan/sodium caseinate mixtures at different biopolymer concentrations. The percentage values represent the mixing ratio of the stock solutions. Eq denotes the mixtures at equilibrium phase.

Noticeably, the flow pattern remains the same but the viscosity of the binary mixtures at equilibrium (one-phase regime) was lower than that after mixing (two-phase regime) when the system was under kinetic control. This is because centrifugation caused some protein and polysaccharide to precipitate resulting in less total biopolymer concentration in the final one-phase system, hence yielding lower viscosity. As confirmed by the microscopic images (Figure 5.2), mixed systems at equilibrium have smoother or lesser β-glucan aggregates present, which influence flow behaviour.

At the same protein concentration in the mixtures, the viscosity increases with increasing Mw and concentration of β-glucans (Figure 5.5a). This is attributed to the higher entanglement of the molecules and larger aggregates formation as the Mw and concentration of β-glucans increase (Figure 5.2; Figure 5.8). However, it was interesting to note that at equilibrium phase, comparing mixtures with similar levels of β-glucan samples varying in Mw, the lower Mw samples yielded identical or higher viscosity (Figure 5.5b). This is also in agreement with the microscopic observations as the lower Mw samples were more dispersed in the protein domain with smaller aggregates and achieve better homogeneity in the equilibrium phase. In other words, the centrifugation caused more of the aggregates of the higher Mw β-glucans to sediment out resulting in a lower viscosity.
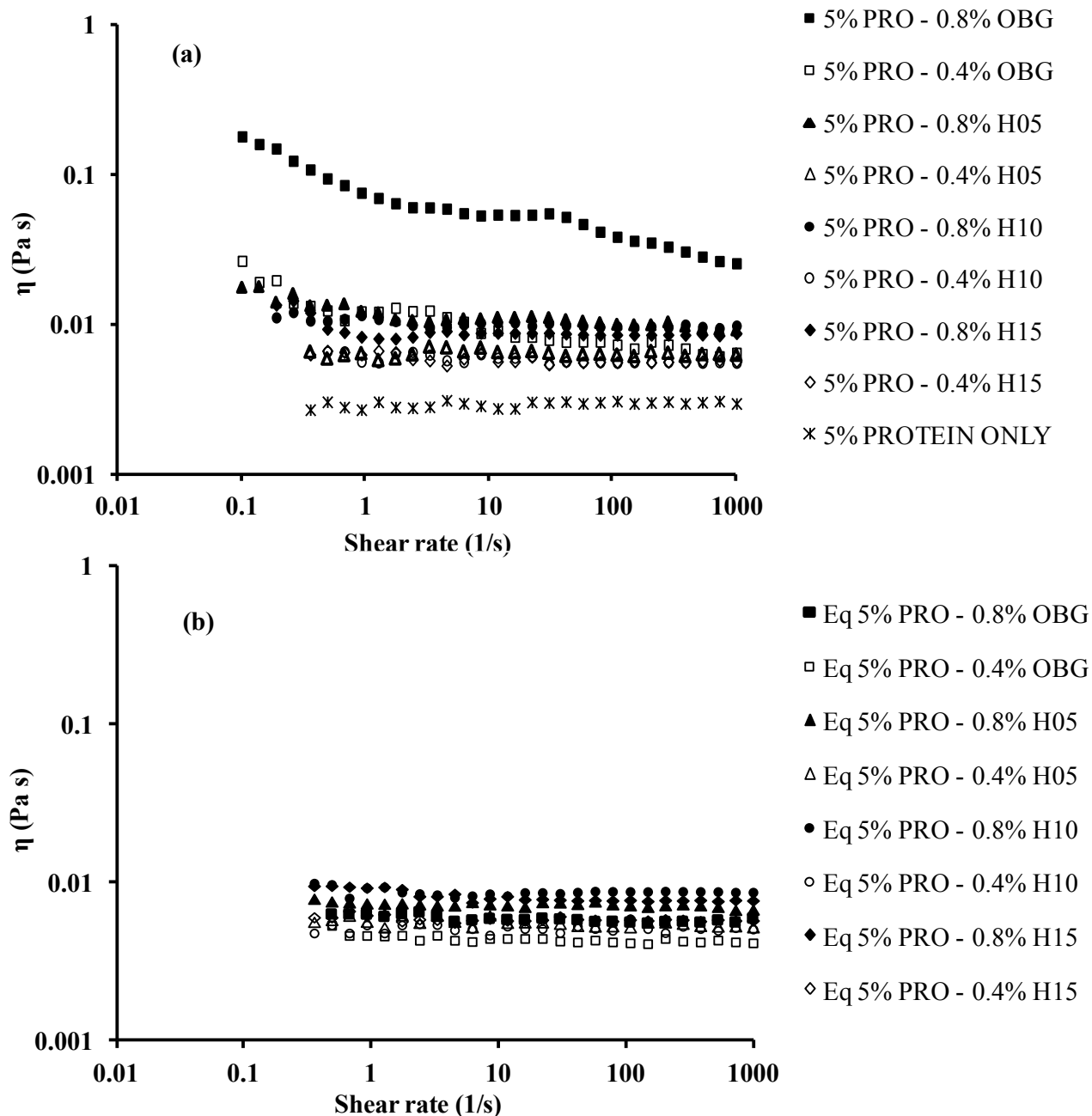
Figure 5.5: Flow behaviour of mixed systems at same protein level with varying concentration and Mw of β-glucans. Percentage values represent the mixing ratio of the stock solutions. (a) After mixing, (b) equilibrium phase after centrifugation. PRO: Protein (sodium caseinate). Eq denotes the mixtures at equilibrium phase.

5.3.4 Effect of hydrodynamic volume

The intrinsic viscosity, [η] of the *β*-glucan isolates increases with increasing molecular weight, and at the same concentration levels, the viscosity of the solutions also increase with increasing molecular weight. From a previous study, [η] values of the β-glucan samples; OBG, H05, H10 and H15 are known to be 7.2, 2.1, 1.8 and 1.7 dL/g, respectively (Chapter 3; Agbenorhevi *et al.*, 2011). The viscosity of the mixed systems was also higher for the higher molecular weight samples (OBG < H05 < H10 < H15) at the same concentration levels (Figure 5.5). Therefore, the flow behaviour was investigated at the same hydrodynamic volume (the volume of the polymer coil when in solution) to ascertain whether a similar trend is observed. Such a treatment will negate the effect of variable *β*-glucan Mw and reveal if there is any specific structure-function relationship of the polysaccharide that influences the viscosity of the mixtures. The product of intrinsic viscosity and concentration (c[η]) gives the coil overlap parameter, an index of the total degree of space-occupancy of the polymer in solution. The experiments were therefore performed at concentration levels of the *β*-glucan that will yield equivalent hydrodynamic volume.

At the concentration levels in mixture with sodium caseinate where c[η] = 1 (i.e., at the same hydrodynamic volume where the concentration is below their respective critical concentration; c < c* for each *β*-glucan sample), the viscosity was similar at all shear rates for all the samples despite the variation in molecular weight (with marginal difference for OBG at higher shear rates) (Figure 5.6).
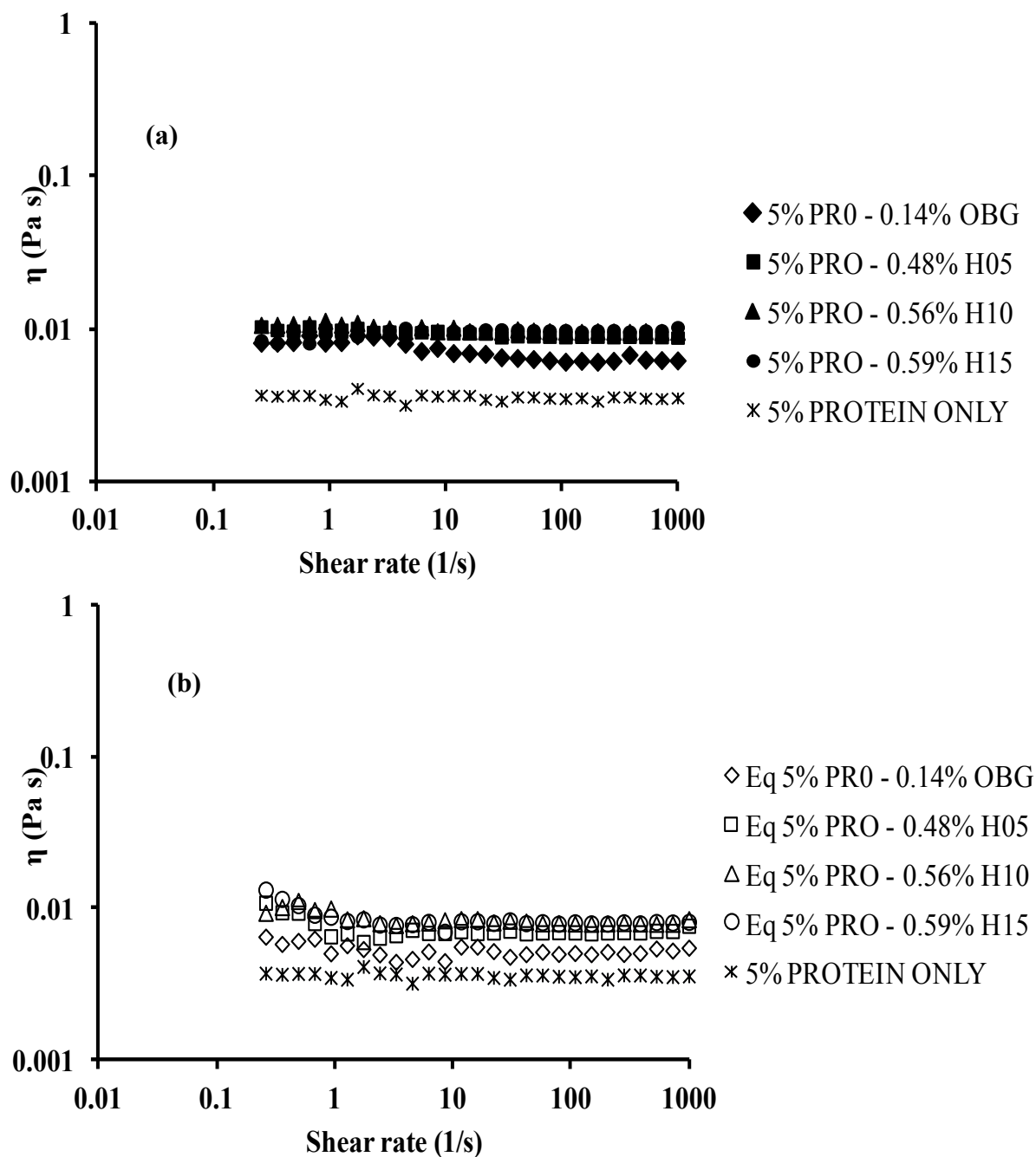
Figure 5.6: The flow curve of mixtures of sodium caseinate (protein) and *β*-glucan isolates at concentration levels of equivalent hydrodynamic volume, c[η] = 1. (a) After mixing, (b) equilibrium phase after centrifugation. Eq denotes the mixtures at equilibrium phase.

However, when the hydrodynamic volume was increased to $c[\eta] = 3$ (i.e., at $c > c^*$), the viscosity also increased but similarly for the lower molecular weight samples (H05, H10 and H15) with Newtonian-like flow behaviour. In contrast, OBG showed shear thinning behaviour at shear rates greater than 10 s^{-1} (Figure 5.7). The deviation from the flow pattern can be attributed to the size of the macromolecules/β-glucan aggregates. As can be seen in Figure 5.9, the size of the aggregates formed increase with increasing molecular weight (which also correlates with the microstructure of pure β-glucan solutions previously examined by atomic force microscopy (Figure 3.6). As the size of the macromolecules and their aggregates differ, the viscosity of the mixed system will be influenced differently. Under force of deformation or shear stress, the larger aggregates will progressively breakdown with increasing shear rate and hence account for the decreasing viscosity (shear thinning behaviour) exhibited. It can therefore be postulated that the macromolecular/aggregate size and morphology was mainly responsible for the variation in the rheological behaviour of the mixtures. That was the case even at constant protein concentration and equivalent hydrodynamic volume of β-glucans of different molecular weights.
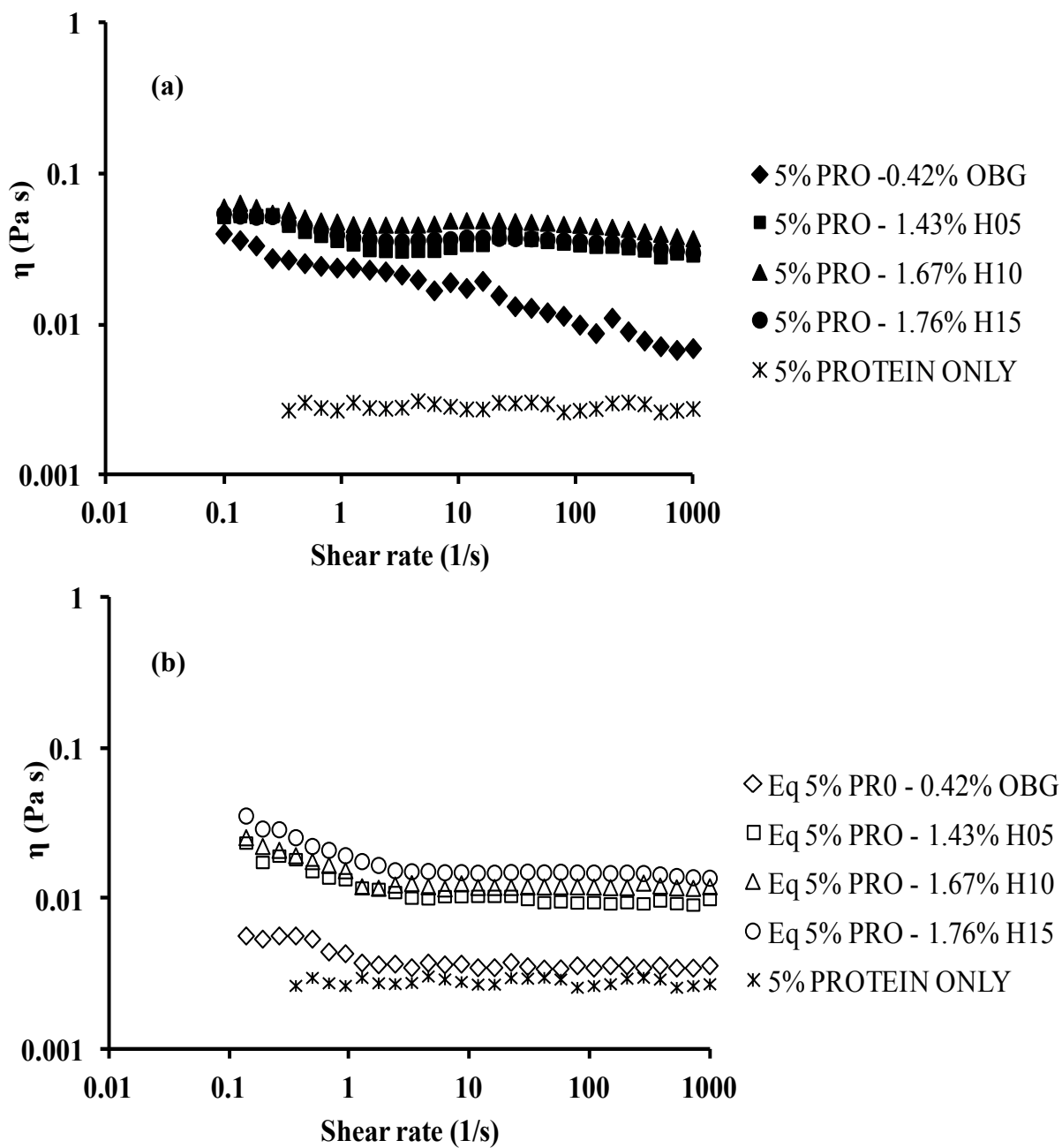
Figure 5.7: The flow curve of mixtures of sodium caseinate (protein) and *β*-glucan isolates at concentration levels of equivalent hydrodynamic volume, c[η] = 3. (a) After mixing, (b) equilibrium phase after centrifugation. Eq denotes the mixtures at equilibrium phase.
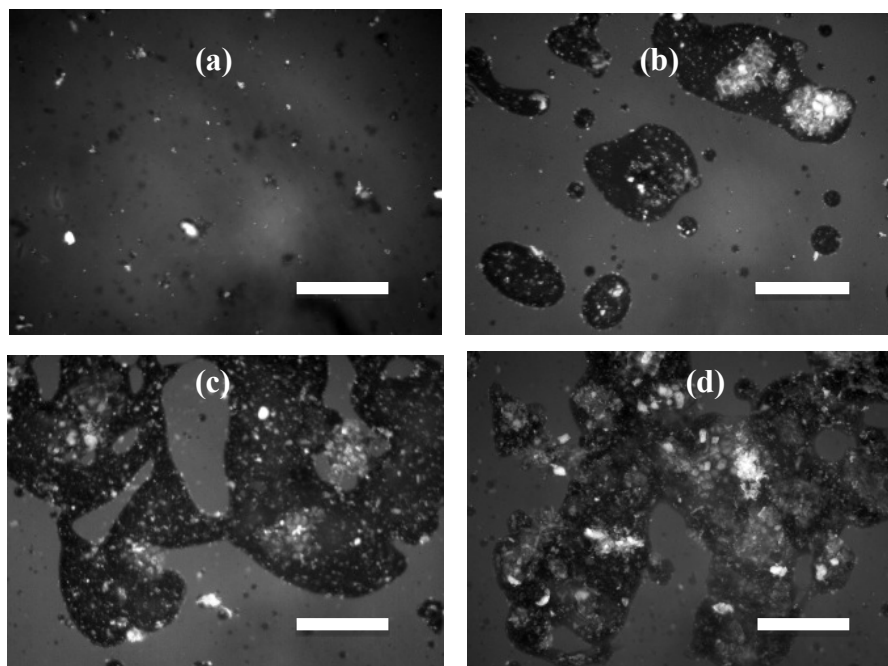
Figure 5.8: Fluorescence microscopic images of mixtures of sodium caseinate (5% w/v) with different β-glucan concentrations. (a) 5–0.2, (b) 5–0.6, (c) 5–0.8, (d) 5–1.0 (% w/v protein–β-glucan). Larger aggregates are formed as the concentration increases. Scale bar: 100 μm.
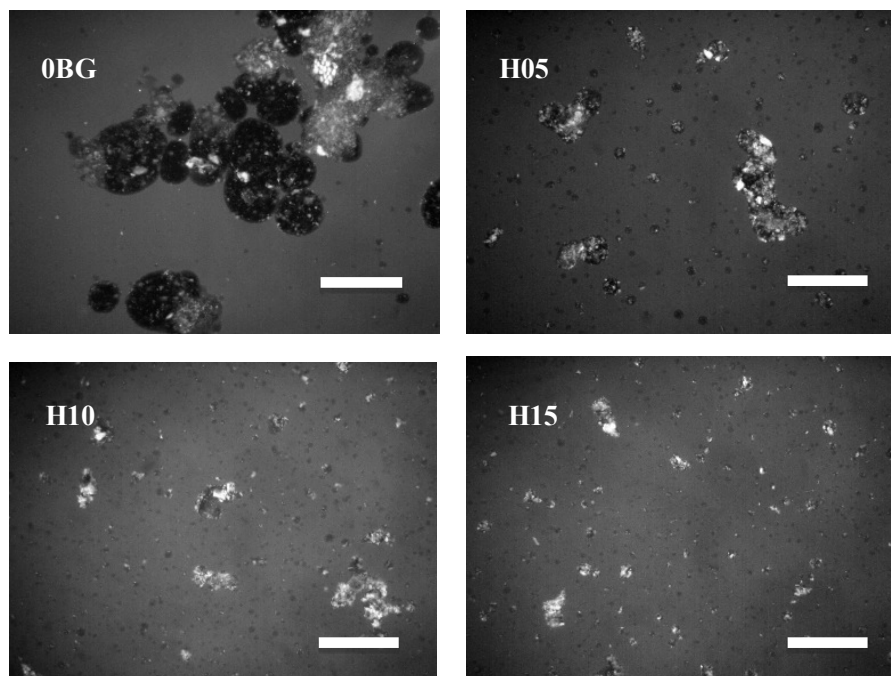
Figure 5.9: Fluorescence microscopic images of mixtures sodium caseinate with *β*-glucan samples varying in molecular weight at concentrations of equivalent hydrodynamic volume (c[η] = 1). Scale bar: 100 μm.

It was interesting to note also that in keeping the hydrodynamic volume of β-glucans constant while the protein concentration varies the viscosity was higher for the respective mixtures with higher protein concentration. Figure 5.10 illustrates the comparison of typical flow curves of mixtures with β-glucan isolates at concentration levels of equivalent hydrodynamic volume, $c[\eta] = 3$ but varying percentage protein (sodium caseinate). For instance, it can be seen that viscosity of mixtures with 5% w/v protein was higher than that with 2.5% w/v protein, other things being equal. It was also noticeable that the viscosity/flow behaviour was similar (Newtonian-like) for the mixtures with lower molecular weight β-glucan samples (H05, H10 and H15) whereas mixture 5% PRO–0.42% OBG exhibited shear thinning behaviour at higher shear rates in contrast to Newtonian flow behaviour shown by mixture 2.5% PRO–0.42% OBG. This suggests a synergistic contribution of the concentration of both biopolymers on the flow behaviour of the mixed system. Thus, the higher concentration of both sodium caseinate and β-glucans, the more viscous the resulting mixture and limited mobility of the biopolymer components/aggregates.
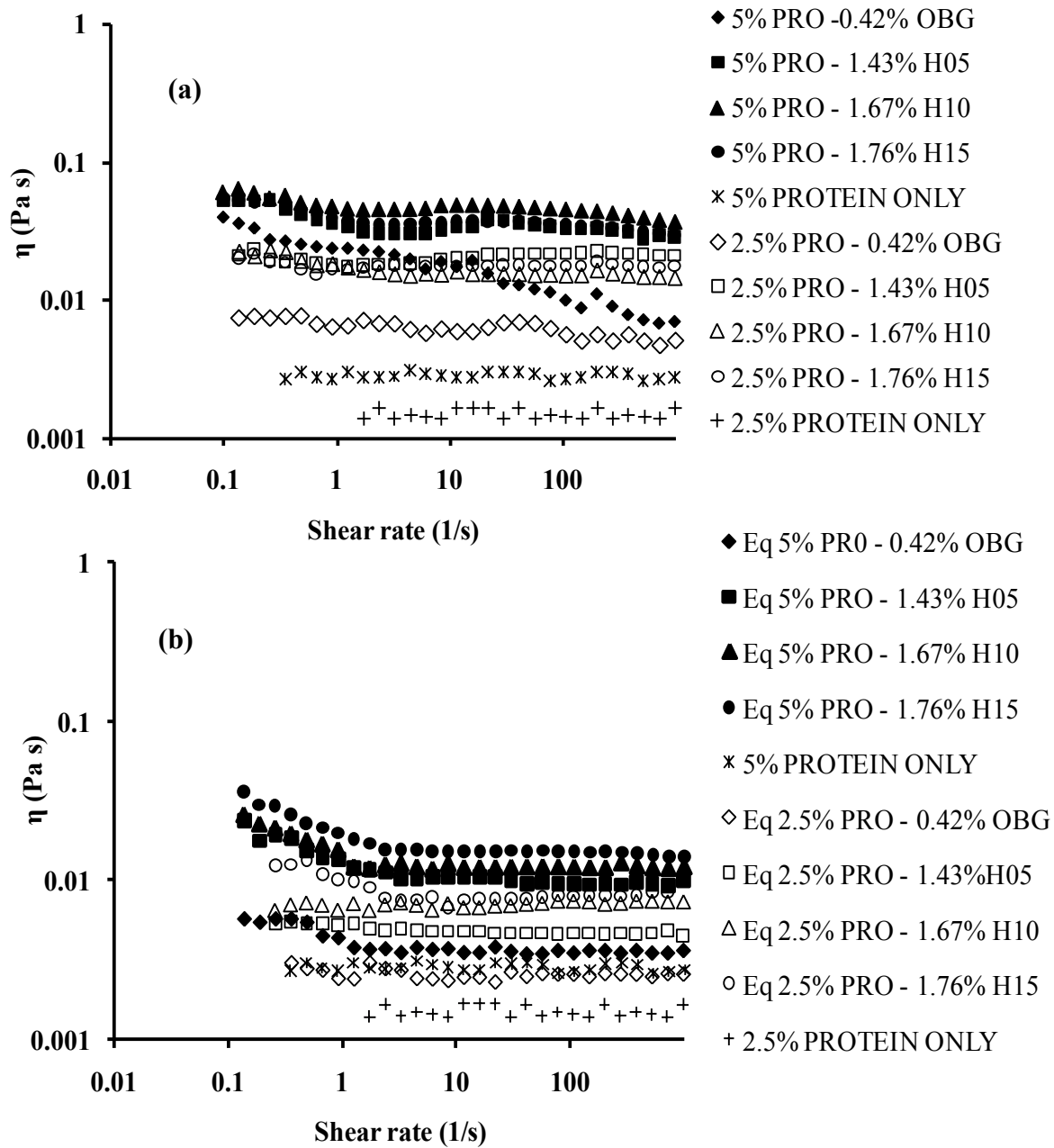
Figure 5.10: The comparison of flow curves of mixtures with *β*-glucan isolates at concentration levels of equivalent hydrodynamic volume, c[η] = 3 but varying percentage sodium caseinate (protein). (a) After mixing, (b) equilibrium phase after centrifugation. Eq denotes the mixtures at equilibrium phase.

5.3.5 Electrophoretic observations

An electrophoretic pattern of sodium caseinate revealed the presence of all the casein subunits (α-, *β*-, and κ-casein) when compared with the standards run (Figure 5.11; Figure 5.12) and as previously reported in literature (Macierzanka *et al.*, 2011). The bands appear between ~20 and ~30 kDa markers which is also in agreement with their molecular weight values (Table 1.1). However, high molecular weight protein band around 60 kDa and the faint bands around 80 kDa are probably due to unreduced disulphide linked casein aggregates or contaminants that have been also previously observed (Macierzanka, et al., 2011). Mixed systems, keeping the *β*-glucan concentration constant while varying the sodium caseinate concentration, showed that the bands become more prominent for the respective mixtures with higher protein concentration as expected, since the thicker bands simply indicate more proteins/subunits available to bind with the dye during staining (Figure 5.11). However, constant sodium caseinate concentration, but varying the concentration of the *β*-glucan, did not reveal any significant difference in electrophoretic pattern of the protein compositions. This may imply that changing the concentration of *β*-glucans will not influence the protein compositions while the experimental conditions (pH, temperature e.t.c.) are maintained.

At the same concentration levels in the mixture, the electrophoretic pattern of both the mixed state and equilibrium phase of sodium caseinate/*β*-glucans mixtures varying in Mw were identical (Figure 5.12). This indicates that varying the Mw of *β*-glucans in the mixture did not induce any significant changes to the structure/composition of the proteins under the experimental conditions studied. Furthermore, it is probable that the centrifugation of the mixtures did not cause any significant precipitation of the protein subunits since the resulting equilibrium phase exhibited similar pattern/bands as the initial mixed state.
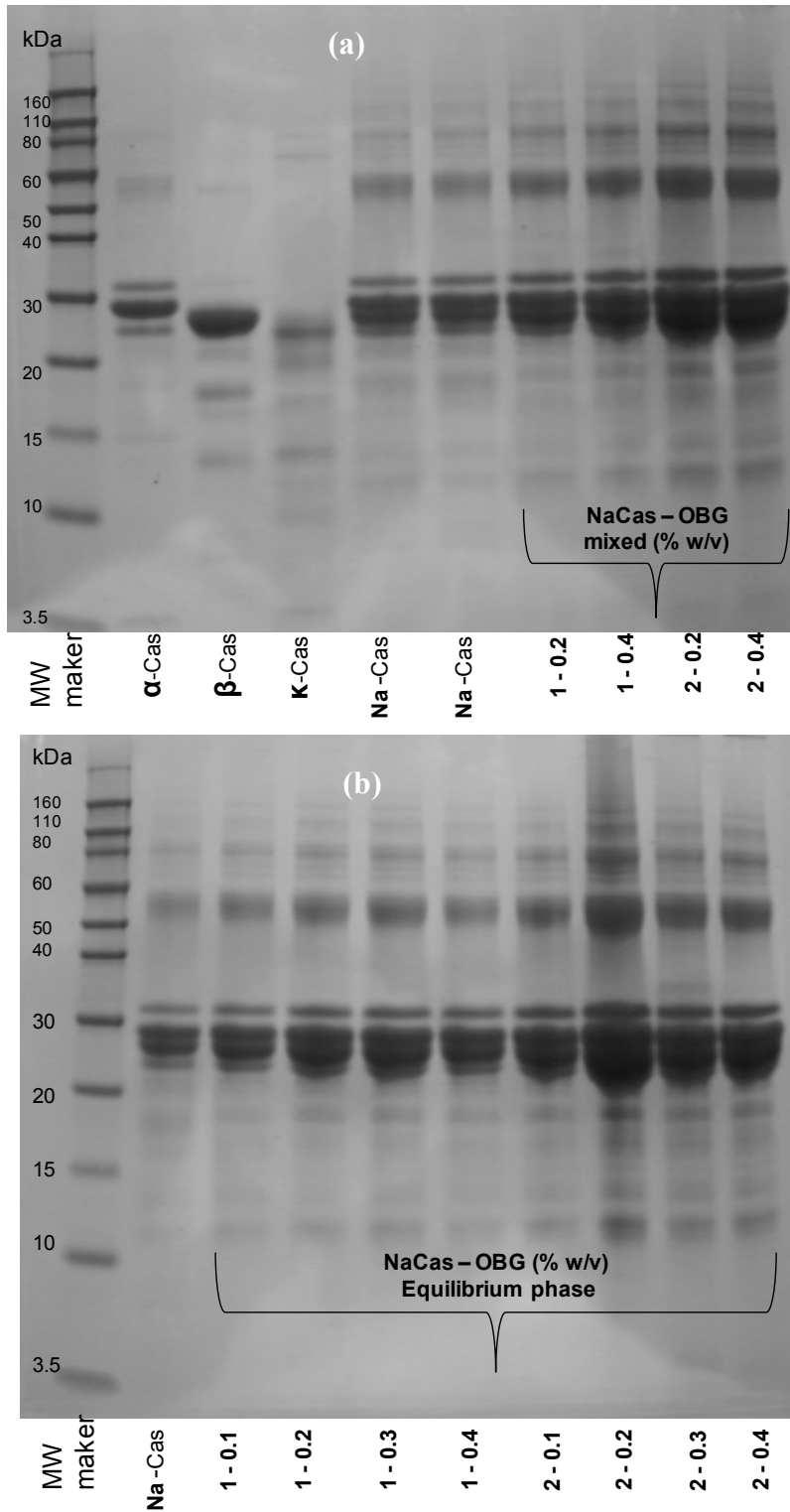
Figure 5.11: Typical electrophoretic patterns of sodium caseinate/*β*-glucan mixtures varying in concentration. Na-Cas denotes sodium caseinate whereas α-,β-, and κ-Cas denote α-,β-, and κ-casein samples, respectively.
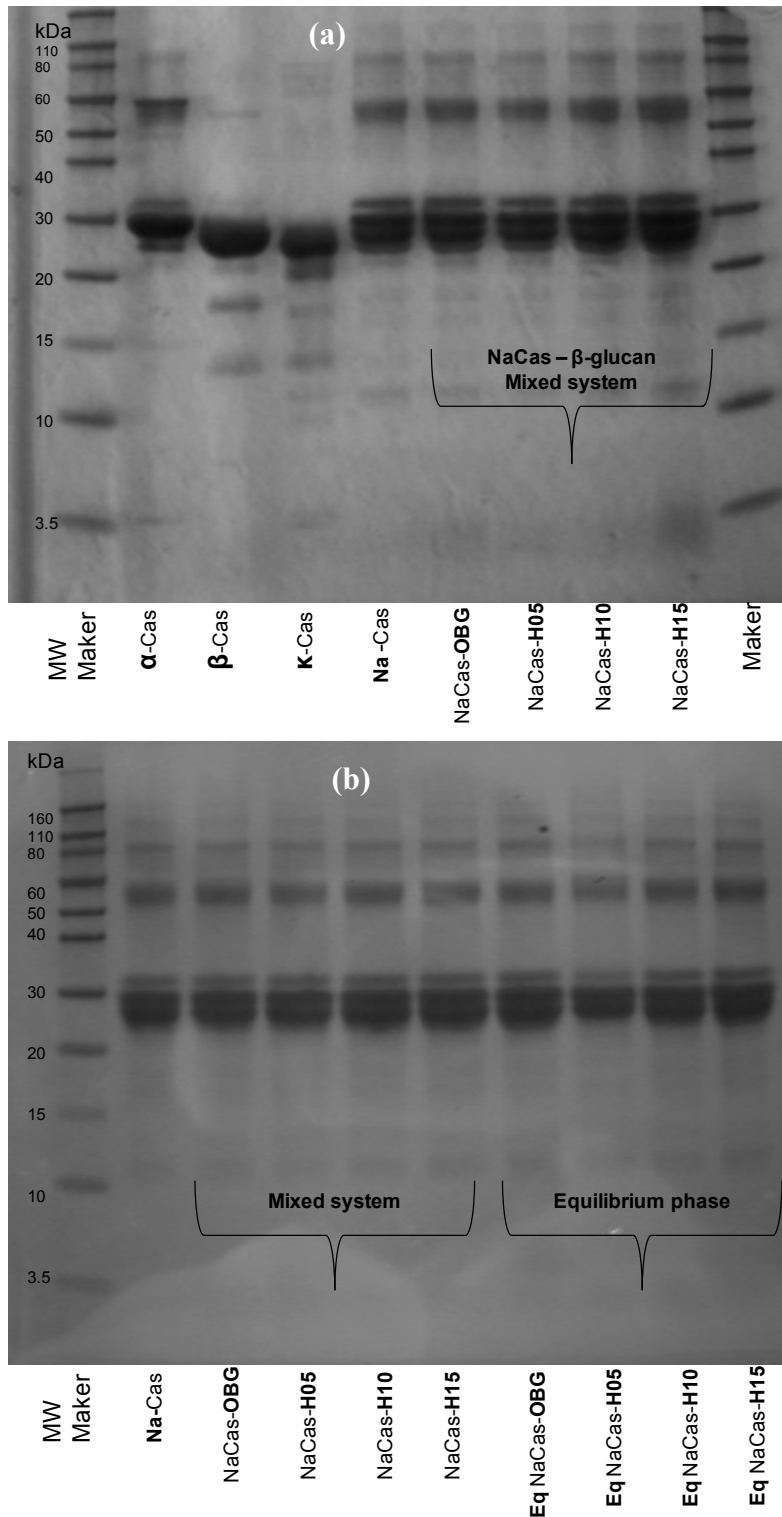
Figure 5.12: Typical electrophoretic patterns of sodium caseinate/β-glucan mixtures varying in molecular weight. NaCas denotes sodium caseinate whereas α-,β-, and κ-Cas denote α-,β-, and κ-casein samples, respectively.

5.4 Conclusion

In the present investigation, the isothermal phase behaviour at 5 ^{o}C of mixtures of sodium caseinate with oat *β*-glucan isolates varying in molecular weight was investigated. Results showed distinct phase behaviour with variable biopolymer concentration in mixtures. Phase diagrams indicated that the compatibility of the *β*-glucan/sodium caseinate system increases as the Mw decreases. Images of the mixtures taken at various biopolymer concentrations revealed phase separation, with the presence of *β*-glucan aggregates whose size depend on Mw and concentration. Mixed systems at equilibrium were comparatively smoother with lesser or no *β*-glucan aggregates present. The viscosity of the binary mixtures at equilibrium was also lower than that after mixing when the system was under kinetic control. At the same protein concentration in the mixtures, the viscosity increases with increasing Mw and concentration of *β*-glucans. However, the results also revealed that in the equilibrium phase with comparable polymer concentrations in mixture, the lower Mw samples yielded identical or higher viscosity. At equivalent hydrodynamic volume of *β*-glucans in the mixture, all the samples exhibited similar flow behaviour. A deviation dependent on the protein concentration was observed for the very high Mw sample in the concentrated regime due to the size of the *β*-glucans aggregates formed. Electrophoretic separation of the mixtures did not reveal any significant difference among the samples varying in concentration and Mw of *β*-glucans indicating no significant precipitation of the protein components under the experimental conditions studied.

CHAPTER 6

GENERAL CONCLUSIONS AND FUTURE WORK

6.1 Conclusions

In this thesis, the physical characteristics (molecular, structural and rheological properties) of oat β-glucan and the phase behaviour when mixed with sodium caseinate were investigated. The β-glucan isolate (OBG) and hydrolysates (H05, H10 and H15) were obtained by aqueous extraction from oat flour and controlled acid hydrolysis, respectively. The structural features of isolated β-glucan samples and molecular weights (Mw) were characterized by ^{13}C-NMR spectroscopy and high performance size-exclusion chromatography. The samples with β-glucan content between 78-86 % on a dry weight basis had Mw in the range of 142 - 2800 x 10^3 g/mol. The ^{13}C-NMR spectra obtained for all samples were identical and typical of a mixed linkage cereal β-glucan. The results showed that controlled acid hydrolysis caused depolymerization of the initial β-glucan sample, thereby generating products of different molecular weight but with the same structural characteristics: the longer the acid hydrolysis treatment time employed, the lower the Mw of the resulting material.

The rheological and microstructural properties of oat β-glucan isolates varying in molecular weight were examined by means of rheometry and atomic force microscopy. It was shown that the intrinsic viscosity, critical concentration, the flow and viscoelastic properties were highly dependent on the molecular weight of the samples. Pseudoplastic and Newtonian flow behaviour was exhibited depending on the concentration and molecular weight of the samples. The Cox-Merz rule was found to be applicable for the lower Mw samples at higher concentrations, whilst the high Mw samples showed a deviation at concentrations greater than

1.0 % w/v, suggesting the presence of aggregates. Atomic force microscopy revealed formation of clusters of aggregates linked via individual molecules scattered heterogeneously throughout the system. The aggregate size and morphology was also dependent on molecular weight of the samples and influences the rheological behaviour of β-glucan solutions.

The effect of protein precipitation prior to phenol-sulphuric acid method in protein/polysaccharide mixtures was investigated by response surface methodology and fluorescent microscopy. It was found that protein concentration, TFA volume as well as the time that the mixture was left in the presence of TFA, significantly influence the total sugar concentration that is estimated with this method. Experimental measurements as well as microscopical evidence suggests that for optimum polysaccharide determination ($\pm$ 6 % error), the protein content in the mixtures should be less than $\sim$ 5.5% w/v with less than 0.5 mL TFA combined with more than 30 min rest under the influence of TFA. It was suggested that the equilibrium phases must be diluted to protein content less than $\sim$5% w/v before TFA treatment for maximum determination of polysaccharide content in phase-diagram construction of mixed biopolymer systems.

The phase behaviour of oat β-glucan/ sodium caseinate with isolates varying in molecular weight was investigated by means of phase diagram construction, rheometry, electrophoresis and fluorescence microscopy. Phase diagrams showed that with decreasing Mw of β-glucan component, the thermodynamic compatibility with sodium caseinate increases. Images of the mixtures taken at various biopolymer concentrations revealed phase separation with the presence of β-glucan aggregates whose size depends on Mw and concentration. Mixed systems at equilibrium were comparatively smoother with fewer or no β-glucan aggregates present. Viscosity of the binary mixtures at equilibrium was also lower than that after mixing when the

system was under kinetic control. It was shown that at the same protein concentration in the mixtures, the viscosity increases with increasing Mw and concentration of β-glucan. However, the results also revealed that in the equilibrium phase from same levels in mixture, the lower Mw samples yielded similar or higher viscosity. At equivalent hydrodynamic volume of β-glucan in the mixtures, all the samples varying in molecular weight exhibited similar viscosity/flow behaviour. A deviation dependent on the protein concentration was observed for the very high Mw sample in the concentrated regime due to the size of the β-glucan aggregates formed. Electrophoretic separation of the mixtures did not reveal any significant difference among the samples varying in concentration and Mw of β-glucans. That indicated no significant precipitation of the protein components under the experimental conditions studied.

Results demonstrate that by controlling the structural features of β-glucans in mixture with sodium caseinate, informed manipulation of rheological properties in these systems can be achieved. The study suggests that it is possible to maximize thermodynamic compatibility of the β-glucan/sodium caseinate mixed system by using lower Mw β-glucan samples and controlling the hydrodynamic volume of the polysaccharide. It is hoped that such an approach should meet the recommended amount required to make health claims of a product while still achieving suitable viscosity/bulking effect.

6.2 Future work

The present investigations involving oat β-glucan/sodium caseinate mixed systems were carried out in the liquid state. Further work can be done at the gel state (by using higher β-glucan concentrations and or inducing gelation of the milk proteins). The molecular weight/structure is

known to influence the degree of gel formation, which also influences the phase separation kinetics by reducing or restricting mobility of the biopolymer components.

The mixed systems could also be investigated at acidic pH as this is expected to influence the protein self-association and thus the phase separation phenomenon, the macro- and micro-structure of the mixture as well as the rheological properties. It would also be useful to investigate the combinations of Mw, concentration of the biopolymers, pH of the system and addition of sucrose to the mixtures in a design possibly by means of response surface methodology to determine the conditions that would yield optimum thermodynamic compatibility as well as the desired viscosity of the mixture. This may be useful in the selection of multiple factors when creating food formulations.

The low Mw samples in the present investigation were obtained by controlled acid hydrolysis. A different approach perhaps by enzymatic hydrolysis e.g., using lichenase which specifically cleaves the β-(1→4)-glycosidic linkages of the three-substituted glucopyranosyl residues or using cellulase which cleaves only sections of the polymer with two or more consecutive β-(1→4)-linkages. Thus cellulase reduces the number of cellulose-like regions, whereas lichenase is more likely to disrupt the cellotriosyl units. Therefore, the method of hydrolysis will also influence the extent aggregation or gelation behaviour of the β-glucan in solution.

7. REFERENCES

Agbenorhevi, J. K. and Kontogiorgos, V. (2010). Polysaccharide determination in protein/ polysaccharide mixtures for phase diagram construction. *Carbohydrate Polymers,* 81**,** 849-854.

Agbenorhevi, J. K., Kontogiorgos, V., Kirby, A. R., Morris, V. J. and Tosh, S. M. (2011). Rheological and microstructural investigation of oat *β*-glucan isolates varying in molecular weight. *International Journal of Biological Macromolecules,* 49**,** 369-377.

Alonso-Mougán, M., Fraga, F., Meijide, F., Rodríguez-Nú Ez, E. and Vázquez-Tato, J. (2003). Aggregation behaviour of polygalacturonic acid in aqueous solution. *Carbohydrate Polymers,* 51**,** 37-45.

Andersson, A. A. M. and Börjesdotter, D. (2011). Effects of environment and variety on content and molecular weight of *β*-glucan in oats. *Journal of Cereal Science,* 54, 122-128.

Antonov, A. Y., Dmitrochenko, A. P. and Leontiev, A. L. (2006). Interactions and compatibility of 11S globulin from *Vicia faba* seeds and sodium salt of carboxymethylcellulose in an aqueous medium. *International Journal of Biological Macromolecules,* 38**,** 18-24.

Antonov, A. Y. and Goncalves, M. P. (1999). Phase separation in aqueous gelatin-κ-carrageenan systems. *Food Hydrocolloids,* 13**,** 517-524.

Antonov, A. Y., Lefebvre, J. and Doublier, J.-L. (1999). On the one-phase state of aqueous protein-uncharged polymer systems: casein-guar gum system. *Journal of Applied Polymer Sciences,* 71**,** 471-482.

Bae, I. Y., Kim, S. M., Lee, S. and Lee, H. G. (2010). Effect of enzymatic hydrolysis on cholesterol-lowering activity of oat *β*-glucan. *New Biotechnology,* 27**,** 85-88.

Bae, I. Y., Lee, S., Kim, S. M. and Lee, H. G. (2009). Effect of partially hydrolyzed oat *β*-glucan on the weight gain and lipid profile of mice. *Food Hydrocolloids,* 23**,** 2016-2021.

Barnes, H. A. (2000). *A Handbook of Elementary Rheology,* Aberystwyth, University of Wales Institute of Non-Newtonian Fluid Mechanics.

Beer, M. U., Arrigoni, E. and Amado, R. (1996). Extraction of oat gum from oat bran: effects of process on yield, molecular weight distribution, viscosity and (1→3)(1→4)-*β*-D-glucan content of the gum. *Cereal Chemistry,* 73**,** 58-62.

Beer, M. U., Wood, P. J. and Weisz, J. (1997). Molecular weight distribution and (1→3)(1→4)-*β*-D-glucan content of consecutive extracts of various Oat and Barley Cultivars 1. *Cereal Chemistry,* 74**,** 476-480.

Behall, K. M., Scholfield, D. J. and Hallfrisch, J. (2004). Diets containing barley significantly reduce lipids in mildly hypercholesterolemic men and women. *American Journal of Clinical Nutrition,* 80**,** 1185-1193.

Bhatty, R. S. (1993). Extraction and enrichment of (1→3)(1→4)-*β*-D-glucan from barley and oat brans. *Cereal Chemistry***,** 70, 73–77.

Böhm, N. and Kulicke, W. M. (1999a). Rheological studies of barley (1→3)(1→4)-*β*-glucan in concentrated solution: investigation of the viscoelastic flow behaviour in the sol-state. *Carbohydrate Research,* 315**,** 293-301.

Böhm, N. and Kulicke, W. M. (1999b). Rheological studies of barley (1→3)(1→4)-*β*-glucan in concentrated solution: mechanistic and kinetic investigation of the gel formation. *Carbohydrate Research,* 315**,** 302-311.

Bourdon, I., Yokohama, W., Davis, P., Hudson, C., Backus, R., Richter, D., Knuckles, B. and Schneeman, B. O. (1999). Postprandial lipid, glucose, insulin, and cholecystokinin responses in men fed barley pasta enriched with *β*-glucan. *American Journal of Clinical Nutrition,* 69**,** 55-63.

Bourriot, S., Garnier, C. and Doublier, J.-L. (1999a). Phase separation, rheology and microstructure of micellar casein-guar gum mixtures. *Food Hydrocolloids,* 13**,** 43-49.

Bourriot, S., Garnier, C. and Doublier, J.-L. (1999b). Phase separation, rheology and structure of micellar casein-galactomannan mixtures. *International Dairy Journal,* 9**,** 353-357.

Braaten, J. T., Scott, F. W., Wood, P. J., Riedel, K. D., Wolynetz, M. S., Brulé, D. and Collins, M. W. (1994a). High *β*-glucan oat bran and oat gum reduce postprandial blood glucose and insulin in subjects with and without type 2 diabetes. *Diabetes Medicine,* 11**,** 312-318.

Braaten, J. T., Wood, P. J., Scott, F. W., Wolynetz, M. S., Lowe, M. K., Bradley-White, P. and Collins, M. W. (1994b). Oat *β*-glucan reduces blood cholesterol concentration in hyperchole-sterolemic subjects. *Journal of Clinical Nutrition,* 48, 465-474.

Bradford, M. M. (1976). A rapid and sensitive method for the quantitation of microgram quantities of protein utilizing the principle of protein-dye binding. *Analytical Biochemistry,* 72**,** 248-254.

Brennan, C. S. and Cleary, L. J. (2005). The potential use of cereal (1→3)(1→4)-*β*-D-glucans as functional food ingredients. *Journal of Cereal Science,* 42**,** 1-13.

Brummer, Y. and Cui, S. W. (2006). Detection and determination of polysaccharides in foods. *In:* Stephen, A. M., Phillips, G. O. & Williams, P. A. (eds.) *Food Polysaccharides and Their Applications.* Second ed. Boca Raton: CRC Press, 675-712.

Buliga, G. S., Brant, D. A. and Fincher, G. B. (1986). The sequence statistics and solution conformation of a barley (1→3)(1→4)-*β*-D-glucan. *Carbohydrate Research,* 157**,** 139 - 156.

Capron, I., Alexandre, S. and Muller, G. (1998). An atomic force microscopy study of the molecular organisation of xanthan. *Polymer,* 39**,** 5725-5730.

Cardenas, A., Higuera-Ciapara, I. and Goycoolea, F. (1997). Rheology and aggregation of cactus (Opuntia ficus-indica) mucilage in solution. *Journal of the Professional Association* of *Cactus Development,* 2**,** 152-159.

Carr, J. M., Glatter, S., Jeraci, J. L. and Lewis, B. A. (1990). Enzymatic determination of beta-glucan in cereal-based food products. *Cereal Chemistry,* 67**,** 226-229.

Cavallero, A., Empilli, S., Brighenti, F. and Stanca, A. M. (2002). High $(1{\rightarrow}3)(1{\rightarrow}4)$-*β*-D-glucan barley fractions in breadmaking and their effects on human glycemic response. *Journal of Cereal Science,* 36**,** 59–66.

Cayot, P. and Lorient, D. (1997). Structure-function relationships of whey proteins. In: Damodaran, S. & Paraf, A. (eds.) *Food Proteins and Their Applications.* New York: Marcel Dekker, Inc., 225-256.

Clark, A. H. and Ross-Murphy, S. B. (2009). Biopolymer Network Assembly: Measurement and Theory. *In:* Kasapis, S., Norton, I. T. & Ubbink, J. B. (eds.) *Modern Biopolymer Science: Bridging the Divide between Fundamental Treatise and Industrial Application.* London: Academic Press, 1-27.

Colleoni-Sirghie, M., Fulton, D. B. and White, P. J. (2003). Structural features of water soluble $(1{\rightarrow}3)(1{\rightarrow}4)$-*β*-D-glucans from high-*β*-glucan and traditional oat lines. *Carbohydrate Polymers,* 54**,** 237-249.

Cox, W. P. And Merz, E. H. (1958). Correlation of dynamic and steady flow viscosities. *Journal of Polymer Science,* 28, 618-622.

Corredig, M., Sharafbafi, N. and Kristo, E. (2011). Polysaccharide–protein interactions in dairy matrices, control and design of structures. *Food Hydrocolloids,* 25**,** 1833-1841.

Cui, S. W. (2000). *Polysaccharide Gums from Agricultural Products: Processing, Structures & Functionality,* Lancaster: CRC Press.

Cui, S. W. and Roberts, K. T. (2009). Dietary Fiber: Fulfilling the Promise of Added-Value Formulations. *In:* Kasapis, S., Norton, I. T. & Ubbink, J. B. (eds.) *Modern Biopolymer Science: Bridging the Divide Between Fundamental Treatise and Industrial Application.* London: Academic Press, 399-448.

Cui, W. and Wood, P. J. (2000). Relationships between structural features, molecular weight and rheological properties of cereal *β*-D-glucans. *In:* Nishinari, K. (ed.) *Hydrocolloids— Part 1.* Amsterdam: Elsevier Science BV.

Cui, W., Wood, P. J., Blackwell, B. and Nikiforuk, J. (2000). Physicochemical properties and structural characterization by two-dimensional NMR spectroscopy of wheat *β*-D-glucan—comparison with other cereal *β*-D-glucans. *Carbohydrate Polymers,* 41**,** 249-258.

Dais, P. and Perlin, A. S. (1982). High-field, 13C-NMR spectroscopy of *β*-D-glucans, amylopectin, and glycogen. *Carbohydrate Research,* 100**,** 103-116.

Dalgleish, D. G. (1997). Structure-function relationships of caseins. *In:* Damodaran, S. & Paraf, A. (eds.) *Food Proteins and Their Applications.* New York: Marcel Dekker, Inc.,199-223.

Dang, J. M. C., Braet, F. and Copeland, L. (2006). Nanostructural analysis of starch components by atomic force microscopy. *Journal of Microscopy,* 224**,** 181-186.

De Kruif, C. G. and Tuinier, R. (2001). Polysaccharide protein interactions. *Food Hydrocolloids,* 15**,** 555-563.

Dickinson, E. (1995). Emulsion stabilization by polysaccharides and protein-polysaccaride complexes. *In:* Stephen, A. M. (ed.) *Food Polysaccharides and Their Applications.* New York: Marcel Dekker, Inc., 501-515.

Dikeman, C. L. and Fahey, G. C. (2006). Viscosity as related to dietary fiber: a review. *Critical Reviews in Food Science and Nutrition,* 46**,** 649-663.

Dogan, H. and Kokini, J. L. (2007). Rheological Properties of Foods. *In:* Heldman, D. R. & Lund, D. B. (eds.) *Food Engineering.* Second ed. Boca Raton: Taylor & Francis Group, 1-124.

Doublier, J.-L., Garnier, C., Renard, D. and Sanchez, C. (2000). Protein-polysaccharide interactions. *Current Opinion in Colloid and Interface Science,* 5**,** 202-214.

Doublier, J. L. and Wood, P. J. (1995). Rheological Properties of Aqueous Solutions of (1→3)(1→4)-*β*-D-Glucan from Oats (Avena sativa L.). *Cereal Chemistry,* 72**,** 335-340.

Dubois, M., Gilles, K. A., Hamilton, J. K., Rebers, P. A. and Smith, F. (1956). Colorimetric method for determination of sugars and related substances. *Analytical Chemistry,* 28**,** 350-356.

Duss, R. (2005). Oatwell® oat bran: proven and advanced nutrition for your heart. *Innovations in Food Technology***,** 94-98.

Duss, R. and Nyberg, L. (2004). Oat Soluble Fibers (*β*-Glucans) as a Source for Healthy Snack and Breakfast Foods. *Cereal Foods World,* 49**,** 320-325.

Duus, J. O., Gotfredsen, C. H. and Bock, K. (2000). Carbohydrate Structural Determination by NMR Spectroscopy: Modern Methods and Limitations. *Chemical Reviews,* 100**,** 4589-4614.

Edelman, M. W., Tromp, R. H. and van der Linden, E. (2003) Phase-separation-induced fractionation in molar mass in aqueous mixtures of gelatin and dextran. *Physical Review E,* 67**,** 021404.

Einhorn-Stoll, U., Guyot, C. and Rittweger, C. (2010). Milk proteins and pectins–compatibility and conjugation. *In:* Williams, P. A. & Phillips, G. O. (eds.) *Gums and Stabilisers for the Food Industry 15.* Glyndwr University, Wrexham, UK: The Royal Society of Chemistry, 223-229.

Eliasson, A-C. (2006). *Carbohydrates in Food*. Second ed. Boca Raton: CRC Press.

Ensley, H. E., Tobias, B., Pretus, H. A., McNamee, R. B., Jones, E. L., Browder, I. W. and Williams, D. L. (1994). NMR spectral analysis of a water-insoluble $(1 \rightarrow 3)(1 \rightarrow 4)$-$\beta$-D-glucan isolated from Saccharomyces cerevisiae. *Carbohydrate Research,* 258**,** 307-311.

Ercelebi, E.-A. and Ibanoglu, E. (2007). Influence of hydrocolloids on phase separtion and emulsion properties of whey protein isolate. *Journal of Food Engineering,* 80**,** 454-459.

FDA (1997). 21 CFR Part 101. Food labeling, health claims: soluble dietary fiber from certain foods and coronary heart disease. *Federal Register,* 15**,** 3584-3601.

Foster, T and Wolf, B. (2011). Hydrocolloid Gums – Their Role and Interactions in Foods. *In:* Norton, I. T., Spyropoulos, F. & Cox, P. (eds.) *Practical Food Rheology: An Interpretive Approach.* Oxford: Wiley-Blackwell, 61-84.

Fox, P. F. and Kelly, A. L. (2006). Chemistry and Biochemistry of Milk Constituents. *In:* Hui, Y. H. (ed.) *Food Biochemistry and Food Processing.* Oxford: Blackwel Publishers Ltd., 425-452.

Friebolin, H. (2005). *Basic one-and two-dimensional NMR-spectroscopy,* Weiheinm: Wiley-VCH.

Frith, W. J. (2010). Mixed biopolymer aqueous solutions-phase behaviour and rheology. *Advances in Colloid and Interface Science,* 161**,** 48-60.

Funami, T., Hiroe, M., Noda, S., Asai, I., Ikeda, S. and Nishinari, K. (2007). Influence of molecular structure imaged with atomic force microscopy on the rheological behavior of carrageenan aqueous systems in the presence or absence of cations. *Food Hydrocolloids,* 21**,** 617-629.

Ghotra, B. S., Vasanthan, T. And Temelli, F. (2008). Structural characterization of barley *β*-glucan extracted using a novel fractionation technique. *Food Research International,* 41**,** 957–963.

Girard, M., Sanchez, C., Laneuville, S. I., Turgeon, S. L. and Gauthier, S. F. (2004). Associative phase separation of *β*-lactoglobulic/pectin solutions: a kinetic study by small angle static light scattering. *Colloids and Surfaces B: Biointerfaces,* 35**,** 15-22.

Goff, D. (1995). Casein micelle structure. [Online] Available at < http://www.foodsci.uoguelph.ca /deicon/casein.html > [Accessed 10 June 2011].

Gómez, C., Navarro, A., Gamier, C., Horta, A. and Carbonell, J. V. (1997). Physical and structural properties of barley (1→3)(1→4)-*β*-D-glucan-III. Formation of aggregates analysed through its viscoelastic and flow behaviour. *Carbohydrate Polymers,* 34**,** 141-148.

Grimm, A., Krüger, E. and Burchard, W. (1995). Solution properties of *β*-D-(1→3)(1→4)-glucan isolated from beer. *Carbohydrate Polymers,* 27**,** 205-214.

Grinberg, V. Y. and Tolstoguzov, V. (1997). Thermodynamic incompatibility of proteins and polysaccharides in solutions. *Food Hydrocolloids,* 11**,** 145-158.

Gu, F., S., A. and Zhang, X. (2009). Optimization of Maillard reaction products from casein–glucose using response surface methodology. *LWT - Food Science and Technology,* 42**,** 1374–1379.

Gunning, A. P., Mackie, A. R., Kirby, A. R., Kroon, P., Williamson, G. and Morris, V. J. (2000). Motion of a cell wall polysaccharide observed by atomic force microscopy. *Macromolecules,* 33**,** 5680-5685.

Guo, Q., Cui, S. W., Wang, Q., Goff, H. D. and Smith, A. (2009). Microstructure and rheological properties of psyllium polysaccharide gel. *Food Hydrocolloids,* 23**,** 1542-1547.

Harding, S. E. (1997). The intrinsic viscosity of biological macromolecules. Progress in measurement, interpretation and application to structure in dilute solution. *Progress in Biophysics and Molecular Biology,* 68**,** 207-262.

Hemar, Y., Tamehana, M., Munro, P. A. and Singh, H. (2001). Viscosity, microstructure and phase behavior of aqueous mixtures of commercial milk protein products and xanthan gum. *Food Hydrocolloids,* 15**,** 565-574.

Huggins, M.L. (1942). The viscosity of long-chain molecules. IV. Dependence on concentration. *Journal of the American Chemical Society,* 64, 2716-2718.

Hwang, J. K. and Shin, H. H. (2000). Rheological properties of chitosan solutions. *Korea-Australia Rheology Journal,* 12**,** 175-179.

Ikeda, S., Funami, T. and Zhang, G. (2005). Visualizing surface active hydrocolloids by atomic force microscopy. *Carbohydrate Polymers,* 62**,** 192-196.

Ikeda, S., Morris, V. J. and Nishinari, K. (2001). Microstructure of aggregated and nonaggregated κ-carrageenan helices visualized by atomic force microscopy. *Biomacromolecules,* 2**,** 1331-1337.

Immerstrand, T., Andersson, K. E., Wange, C., Rascon, A., Hellstrand, P., Nyman, M., Cui, S. W., Bergenståhl, B., Trägårdh, C. and Oste, R. (2010). Effects of oat bran, processed to different molecular weights of *β*-glucan, on plasma lipids and caecal formation of SCFA in mice. *British Journal of Nutrition,* 104**,** 364-373.

Inglett, G. E. (1990). USDA's oatrim replaces fat in many food products. *Food Technology,* 44, 100.

Irakli, M., Biliaderis, C. G., Izydorczyk, M. S. and Papadoyannis, I. N. (2004). Isolation, structural features and rheological properties of water-extractable *β*-glucans from different Greek barley cultivars. *Journal of the Science of Food and Agriculture,* 84, 1170-1178.

Izydorczyk, M. S. and Biliaderis, C. G. (1992). Effect of molecular size on physical properties of wheat arabinoxylan. *Journal of Agricultural and Food Chemistry,* 40**,** 561-568.

Izydorczyk, M. S. and Biliaderis, C. G. (2000). Structural and Functional Aspects of Cereal Arabinoxylans and *β*-Glucans. *In*: Doxastakis, G., Kiosseoglou, V. (Eds.), *Novel Macromolecules in Food Systems*. Amsterdam: Elsevier Science B.V., 361–384.

Izydorczyk, M. S., Lagasse, S. L., Hatcher, D. W., Dexter, J. E. and Rossnagel, B. G. (2005). The enrichment of Asian noodles with fiber rich fractions derived from roller milling of hull-less barley *Journal of Agricultural and Food Chemistry,* 85**,** 2094–2104.

Izydorczyk, M. S., Macri, L. J. and Macgregor, A. W. (1998). Structure and physicochemical properties of barley non-starch polysaccharides—I. Water-extractable *β*-glucans and arabinoxylans. *Carbohydrate Polymers,* 35**,** 249-258.

Jacon, S. A., Rao, M. A., Cooley, H. J. and Walter, R. H. (1993). The isolation and characterization of a water extract of konjac flour gum. *Carbohydrate Polymers,* 20**,** 35-41.

JHCI (2004). Final report on a generic health claim for oats and reduction of blood cholesterol. [Online] Available at < http://www.jhci.org.uk/approv/oats.htm > [Accessed 10 June 2011].

Johansson, L., Tuomainen, P., Ylinen, M., Ekholm, P. and Virkki, L. (2004). Structural analysis of water-soluble and-insoluble *β*-glucans of whole-grain oats and barley. *Carbohydrate Polymers,* 58**,** 267-274.

Johansson, L., Virkki, L., Maunu, S., Lehto, M., Ekholm, P. and Varo, P. (2000). Structural characterization of water soluble *β*-glucan of oat bran. *Carbohydrate Polymers,* 42**,** 143-148.

Kahlon, T., Chow, F., Knuckles, B. and Chiu, M. (1993). Cholesterol-lowering effects in hamsters of *β*-glucan-enriched barley fraction, dehulled whole barley, rice bran, and oat bran and their combinations. *Cereal Chemistry,* 70**,** 435-440.

Kalra, S. and Jood, S. (2000). Effect of Dietary Barley *β*-Glucan on Cholesterol and Lipoprotein Fractions in Rat. *Journal of Cereal Science,* 31**,** 141-145.

Kasapis, S. (2008). Phase Separation in Biopolymer Gels: A Low- to High-Solid Exploration of Structural Morphology and Functionality. *Critical Reviews in Food Science and Nutrition,* 48:**,** 341–359.

Kasapis, S., Morris, E. R., Gross, M. and Rudolph, K. (1994). Solution properties of levan polysaccharide from *Pseudomonas syringae pv. phaseolicola,* and its possible primary role as a blocker of recognition during pathogenesis. *Carbohydrate Polymers,* 23**,** 55-64.

Keeler, J. (2005). *Understanding NMR Spectroscopy*. Sussex: John Wiley & Sons.

Kerckhoffs, D. A. J. M., Hornstra, G. and Mensink, R. P. (2003). Cholesterol-lowering effect of *β*-glucan -glucan from oat bran in mildly hypercholesterolemic subjects may decrease when *β*-glucan glucan is incorporated into bread and cookies. *The American Journal of Clinical Nutrition,* 78**,** 221-227.

Kim, H.-J., Decker, A. E. and McClements, D. J. (2006). Preparation of multiple emulsions based on thermodynamic incopatibility of heat-denatured whey protein and pectin solutions. *Food Hydrocolloids,* 20**,** 586-595.

Kinsella, J. E. and Morr, C. V. (1984). Milk proteins: physicochemical and functional properties. *Critical Reviews in Food Science and Nutrition,* 21**,** 197-262.

Kirby, A. R., Gunning, A. P. and Morris, V. J. (1996). Imaging polysaccharides by atomic force microscopy. *Biopolymers,* 38**,** 355-366.

Knuckles, B. E., Yokoyama, W. H. and Chiu, M. M. (1997). Molecular characterization of barley *β*-glucans by size-exclusion chromatography with multiple-angle laser light scattering and other detectors. *Cereal Chemistry,* 74**,** 599-604.

Kontogiorgos, V., Tosh, S. M. and Wood, P. J. (2009a). Kinetics of phase separation of oat *β*-glucan/whey protein isolate binary mixtures. *Food Biophysics,* 4**,** 240-247.

Kontogiorgos, V., Tosh, S. M. and Wood, P. J. (2009b). Phase behaviour of high molecular weight oat *β*-glucan/whey protein isolate binary mixtures. *Food Hydrocolloids,* 23**,** 949–956.

Kraemer, E. O. (1938). Molecular weights of celluloses and cellulose derivatives. *Industrial and Engineering Chemistry,* 30, 1200-1203.

Kshirsagar, A. C. and Singhal, R. S. (2007). Optimization of starch oleate derivatives from native corn and hydrolyzed corn starch by response surface methodology. *Carbohydrate Polymers,* 69**,** 455–461.

Lazaridou, A. and Biliaderis, C. G. (2007). Molecular aspects of cereal *ß*-glucan functionality: Physical properties thechnological applications and physiological effects. *Journal of Cereal Science,* 46**,** 101-118.

Lazaridou, A. and Biliaderis, C. G. (2009). Concurrent phase separation and gelation in mixed oat *ß*-glucans/sodium caseinate and oat *ß*-glucans/pullulan aqueous dispersions. *Food Hydrocolloids,* 23**,** 886–895.

Lazaridou, A., Biliaderis, C. G. and Izydorczyk, M. S. (2001). Structural characteristics and rheological properties of locust bean galactomannans: a comparison of samples from different carob tree populations. *Journal of the Science of Food and Agriculture,* 81**,** 68-75.

Lazaridou, A., Biliaderis, C. G. and Izydorczyk, M. S. (2003). Molecular size effects on rheological properties of oat *ß*-glucans in solution and gels. *Food Hydrocolloids,* 17**,** 693-712.

Lazaridou, A., Biliaderis, C. G., Micha-Screttas, M. and Steele, B. R. (2004). A comparative study on structure-function relations of mixed-linkage (1→3), (1→4) linear *ß*-D-glucans. *Food Hydrocolloids,* 18**,** 837-855.

Lazaridou, A., Vaikousi, H. and Biliaderis, C. G. (2008). Impact of mixed linkage (1→3,1→4) *ß*-glucans on physical properties of acid-set skim milk gels. *International Dairy Journal,* 18**,** 312-322.

Lee, J., Lin Ye, L., Landen, J. W. O. and Eitenmiller, R. R. (2000). Optimization of an Extraction Procedure for the Quantificationof Vitamin E in Tomato and Broccoli using Response Surface Methodology. *Food Composition And Analysis,* 13**,** 45-57.

Lee, S., Kim, S. and Inglett, G. E. (2005). Effect of shortening replacement with oatrim on the physical and rheological properties of cakes. *Cereal Chemistry,* 82**,** 120-124.

Li, W., Cui, S. W. and Kakuda, Y. (2006). Extraction, fractionation, structural and physical characterization of wheat *β*-D-glucans. *Carbohydrate Polymers,* 63**,** 408-416.

Li, W., Cui, S. W., Wang, Q. and Yada, R. Y. (2011). Studies of Aggregation Behaviours of Cereal *β*-Glucans in Dilute Aqueous Solutions by Light Scattering: Part I. Structure Effects. *Food Hydrocolloids,* 25**,** 189 -195.

Li, W., Wang, Q., Cui, S. W., Huang, X. and Kakuda, Y. (2006b). Elimination of aggregates of (1→3)(1→4)-*β*-D-glucan in dilute solutions for light scattering and size exclusion chromatography study. *Food Hydrocolloids,* 20**,** 361-368.

Li, X., Hua, Y., Qiu, A., Yang, C. and Cui, S. (2008). Phase behavior and microstructure of preheated soy proteins and κ-carrageenan mixtures. *Food Hydrocolloids,* 22**,** 845-853.

Löfgren, C., Walkenström, P. and Hermansson, A. M. (2002). Microstructure and rheological behavior of pure and mixed pectin gels. *Biomacromolecules,* 3**,** 1144-1153.

Loret, C., Schumm, S., Pudney, P. D. A., Frith, W. J. and Fryer, P. J. (2005) Phase separation and molecular weight fractionation behavior of maltodextrin/agarose mixtures. *Food Hydrocolloids,* 19, 557–565.

Lucey, J. A., Munro, P. A. and Singh, H. (1998). Whey separation in acid skim milk gels made with glucono-δ-lactone: effect of heat treatment and gelation temperature. *Journal of Textural Studies,* 29, 413-426.

Lucey, J. A., Srinivasan, M., Singh, H. and Munro, P. A. (2000). Characterization of commercial and experimental sodium caseinates by multiangle laser light scattering and size-exclusion chromatography. *Journal of Agricultural and Food Chemistry,* 48**,** 1610-1616.

Macierzanka, A., Bordron, F., Rigby, N. M., Mills, E. N. C., Lille, M., Poutanen, K. and Mackie, A. R. (2011). Transglutaminase cross-linking kinetics of sodium caseinate is changed after emulsification. *Food Hydrocolloids,* 25**,** 843-850.

Mälkki, Y. and Virtanen, E. (2001). Gastrointestinal effects of oat bran and oat gum: A review. *Lebensmittel-Wissenschaft und-Technologie,* 34**,** 337-347.

Maroziene, A. and De Kruif, C. G. (2000). Interaction of pectin and casein micelles. *Food Hydrocolloids,* 14**,** 391-394.

Masuko, T., Minami, A., Iwasaki, N., Majima, T., Nishimura, S.-I. and Lee, Y. C. (2005). Carbohydrate analysis by a phonol-sulfuric method in microplate format. *Analytical Biochemistry,* 339**,** 69-72.

McCleary, B. V. (1988). Purification of $(1{\to}3)(1{\to}4)$-*β*-D-glucan from barley flour. *In:* Wood, W. A. & Kellogg, S. T. (eds.). *Methods in Enzymology.* San Diego, CA: Academic Press, 511–514.

McCleary, B. V. and Glennie-Holmes, M. (1985). Enzymic modification of $(1{\to}3)(1{\to}4)$-*β*-D-glucan in barley and malt. *Journal of the Institute of Brewing,* 91**,** 285-295.

Meyer, V. (2004). *Practical High-Performance Liquid Chromatography.* Chichester: John Wiley & Sons, Inc.

Miri, T. (2011). Viscosity and Oscillatory Rheology. *In:* Norton, I. T., Spyropoulos, F. & Cox, P. (eds.) *Practical Food Rheology: An Interpretive Approach.* Oxford: Wiley-Blackwell, 7-28.

Morgan, K. R. and Ofman, D. J. (1998). Rapid Communication: Glucagel, A Gelling *β*-Glucan from Barley. *Cereal Chemistry,* 75**,** 879-881.

Morris, E. R., Cutler, A. N., Ross-Murphy, S. B., Rees, D. A. and Price, J. (1981). Concentration and shear rate dependence of viscosity in random coil polysaccharide solutions. *Carbohydrate Polymers,* 1**,** 5-21.

Morris, V. J. (2009). Single Molecule Techniques: Atomic Force Microscopy and Optical Tweezers. *In:* Kasapis, S., Norton, I. T. & Ubbink, J. B. (eds.) *Modern Biopolymer Science: Bridging the Divide between Fundamental Treatise and Industrial Application.* London: Academic Press, 365-397.

Morris, V. J., Mackie, A. R., Wilde, P. J., Kirby, A. R., Mills, E. C. N. and Gunning, P. A. (2001). Atomic force microscopy as a tool for interpreting the rheology of food biopolymers at the molecular level. *Lebensmittel-Wissenschaft und-Technologie,* 34**,** 3-10.

Musampa, R. M., Alves, M. M. and Maia, J. M. (2007). Phase separation, rheology and microstructure of pea protein-kappa-carrageenan mixtures. *Food Hydrocolloids,* 21**,** 92-99.

Neirynck, N., Van Lent, K., Dewettinck, K. and Van Der Meeren, P. (2007). Influence of pH and biopolymer ratio on sodium caseinate-guar gum interactions in aqueous solutions and in o/w emulsions. *Food Hydrocolloids,* 21**,** 862-869.

Ng, D., Coventry, K., Lim, P., Wiltshire, J., Qiao, G. G., Boulton, A. and Senior, G. (2009). An improved technique for concentration measurement of galactomannan solutions by differential refractive index. *Carbohydrate Polymers,* 77**,** 150-153.

Norton, I. T. and Frith, W. J. (2001). Microstructure design in mixed biopolymer composites. *Food Hydrocolloids,* 15**,** 543-553.

Oats and Health, (2007). Composition of oat: *β*-glucan [online] Available at < http://www.oatsandhealth.org/index.php?option=com_content&view=article&id=14&Ite mid=38 > [Accessed 20 November 2011].

Othman, R. A., Moghadasian, M. H. and Jones, P.J.H. (2011). Cholesterol-lowering effects of oat *β*-glucan. *Nutrition Reviews,* 69, 299-309.

Papageorgiou, M., Lakhdara, N., Lazaridou, A., Biliaderis, C. G. and Izydorczyk, M. S. (2005). Water extractable (1→3)(1→4)-*β*-D-glucans from barley and oats: An intervarietal study on their structural features and rheological behaviour. *Journal of Cereal Science,* 42**,** 213-224.

Parvathy, K. S., Susheelamma, N. S. and Tharanathan, R. N. (2007). Hydration characteristics of guar gum samples and their fractions. *Food Hydrocolloids,* 21**,** 630-637.

Perez, A. A., Carrara, C. R., Sanchez, C. C., Patino, R. J .M. and Santiago, L. G. (2009). Interactions between milk whey protein and polysaccharide in solution. *Food Chemistry,* 116**,** 104 -113.

Perrechil, F. A., Braga, A. L. M. and Cunha, R. L. (2009). Interactions between sodium caseinate and LBG in acidified systems: Rheology and phase behavior. *Food Hydrocolloids***,** 23, 2085-2093.

Phillips, G. O. and Williams, P. A. (2009). *Handbook of Hydrocolloids*. Oxford: Woodhead Publishing Ltd.

Polyakov, V. I., Grinberg, V. Y. and Tolstoguzov, V. B. (1980). Application of phase-volume-ratio method for determining the phase diagram of water-casein-soybean globulins system. *Polymer Bulletin,* 2**,** 757-760.

Qiao, D., Hu, B., Gan, D., Sun, Y., Ye, H. and Zeng, X. (2009). Extraction optimized by using response surface methodology, purification and preliminary characterization of polysaccharides from *Hyriopsis cumingii. Carbohydrate Polymers,* 76**,** 422–429.

Rao, M. A. (2007). *Rheology of Fluid and Semisolid Foods: Principles and Application.* Second ed. New York: Springer.

Rediguieri, C. F., De Freitas, O., Lettinga, M. P. and Tuinier, R. (2007). Thermodynamic incompatibility and complex formation in pectin/caseinate mixtures. *Biomacromolecules,* 8**,** 3345-3354.

Ren, Y., Ellis, P. R., Ross-Murphy, S. B., Wang, Q. and Wood, P. J. (2003). Dilute and semi-dilute solution properties of (1→3)(1→4)-*β*-D-glucan, the endosperm cell wall polysaccharide of oats (*Avena sativa L.). Carbohydrate Polymers,* 53**,** 401-408.

Ripsin, C. M., Keenan, J. M., Jacobs, D. R., Elmer, P. J., Welch, R. R., Horn, L. V., Liu, K., Turnbull, W. H., Thye, F. W. and Kestin, M. (1992). Oat products and lipid lowering. *JAMA: The Journal of the American Medical Association,* 267**,** 3317.

Rodríguez Patino, J. M. and Pilosof, A. M. R. (2011). Protein-Polysaccharide Interactions, At Fluid Interfaces. *Food Hydrocolloids*, 25, 1925-1937.

Round, A. N., Macdougall, A. J., Ring, S. G. and Morris, V. J. (1997). Unexpected branching in pectin observed by atomic force microscopy. *Carbohydrate Research,* 303**,** 251-253.

Rounds, M. A. and Gregory, J. F. (2003). High Performance Liquid Chromatograhpy. *In:* Nielsen, S. S. (ed.) *Food Analysis.* Third ed. New York: Kluwer Academic, 461-478.

Rubinstein, M. and Colby, R. H. (2003). *Polymer Physics.* New York: Oxford University Press Inc.

Russo, P. S. (2008). Intrinsic Viscosity [online] Available at < http://macro.lsu.edu/howto/ IntrinsicVisc.doc > [Accessed 8 December 2009].

Saulnier, L., Gevaudan, S. and Thibault, J. F. (1994). Extraction and partial characterisation of *β*-glucan from the endosperms of two barley cultivars. *Journal of Cereal Science,* 19**,** 171-178.

Schmitt, C., Sanchez, C., Desobry-Banon, S. and Hardy, J. (1998). Structure and technofunctional properties of protein-polysaccharide complexes: a review. *Critical Reviews in Food Science and Nutrition,* 38**,** 689-753.

Schmitt, C., Sanchez, C., Thomas, F. and Hardy, J. (1999). Complex coacervation between *β*-lactoglobulin and acacia gum in aqueous medium. *Food Hydrocolloids,* 13**,** 483-496.

Schorsch, C., Clark, A. H., Jones, M. G. and Norton, I. T. (1999). Behaviour of milk protein/polysaccharide systems in high sucrose. *Colloids and Surfaces B: Biointerfaces,* 12**,** 317-329.

Schorsch, C., Wilkins, D. K., Jones, M. G. And Norton, I. T. (2001). Gelation of casein-whey mixtures: effect of whey protein alone or in the presence of casein micelles. *Journal of Dairy Research,* 68, 471-481.

Semenova, M. G. (2007). Thermodynamic analysis of the impact of molecular interactions on the functionality of food biopolymers in solution and in colloidal systems. *Food Hydrocolloids,* 21**,** 23-45.

Simsek, A., Poyrazoglu, E. S., Karacan, S. and Velioglu, Y. S. (2007). Response surface methodological study on HMF and fluorescent accumulation in red and white grape juices and concentrates. *Food Chemistry,* 101**,** 987-994.

Skendi, A., Biliaderis, C. G., Lazaridou, A. and Izydorczyk, M. S. (2003). Structure and rheological properties of water soluble *β*-glucans from oat cultivars of *Avena sativa* and *Avena bysantina*. *Journal of Cereal Science,* 38**,** 15-31.

Sperling, L. H. (2006). *Introduction to Physical Polymer Science.* New Jersey: John Willet & Sons, Inc.

Storsley, J. M., Izydorczyk, M. S., You, S., Biliaderis, C. G. and Rossnagel, B. (2003). Structure and physicochemical properties of *β*-glucans and arabinoxylans isolated from hull-less barley. *Food Hydrocolloids,* 17**,** 831-844.

Symons, L. J. and Brennan, C. S. (2004). The effect of barley *β*-glucan fiber fractions on starch gelatinization and pasting characteristics. *Journal of Food Science,* 69, 257-261.

Syrbe, A., Bauer, W. J. and Klostermeyer, H. (1998). Polymer science concepts in dairy systems-An overview of milk protein and food hydrocolloid interaction. *International Dairy Journal,* 8**,** 179-193.

Tappy, L., Gügolz, E. and Würsch, P. (1996). Effects of breakfast cereals containing various amounts of *β*-glucan fibers on plasma glucose and insulin responses in NIDDM subjects. *Diabetes Care* 19**,** 831-834.

Temelli, F. (1997). Extraction and functional properties of barley *β*-glucan as affected by temperature and pH. *Journal of Food Science,* 62**,** 1194-1201.

Thaiudom, S. and Goff, H. D. (2003). Effect of κ-carrageenan on milk protein polysaccharide mixtures. *International Dairy Journal,* 13**,** 763-771.

Tolstoguzov, V. (1997). Protein-Polysaccharide Interactions. *In:* Damodaran, S. & Paraf, A. (eds.) *Food Proteins and Their Applications.* New York: Marcel Dekker, Inc., 171-198.

Tolstoguzov, V. (2006). Phase behaviour in mixed polysaccharide systems. *In:* Stephen, A. M., Phillips, G. O. & Williams, P. A. (eds.) *Food Polysaccharides and Their Applications.* Second ed. Boca Raton: CRC Press, 589-627.

Tolstoguzov, V. B. (2000). Phase behavior of macromolecular components in biological and food systems. *Nahrung,* 44**,** 299-308.

Tolstoguzov, V. B. (2003). Some thermodynamic considerations in food formulation. *Food Hydrocolloids,* 17**,** 1-23.

Tosh, S. M., Brummer, Y., Wolever, T. M. and Wood, P. J. (2008). Glycemic response to oat bran muffins treated to vary molecular weight of *β*-glucan. *Cereal Chemistry,* 85**,** 211-217.

Tosh, S. M., Brummer, Y., Wood, P. J., Wang, Q. and Weisz, J. (2004a). Evaluation of structure in the formation of gels by structurally diverse (1→3)(1→4)-*β*-D-glucans from four cereal and one lichen species. *Carbohydrate Polymers,* 57**,** 249–259.

Tosh, S. M., Wood, P. J., Wang, Q. and Weisz, J. (2004b). Structural characteristics and rheological properties of partially hydrolyzed oat *β*-glucan: the effects of molecular weight and hydrolysis method. *Carbohydrate Polymers,* 55**,** 425-436.

Tuinier, R. and De Kruif, C. (1999). Phase behavior of casein micelles/exocellular polysaccharide mixtures: Experiment and theory. *The Journal of Chemical Physics,* 110**,** 9296-9304.

Tuinier, R., Ten Grotenhuis, E. and De Kruif, C. (2000). The effect of depolymerised guar gum on the stability of skim milk. *Food Hydrocolloids,* 14**,** 1-7.

Tuinier, R., Ten Grotenhuis, E., Holt, C., Timmins, P. and De Kruif, C. (1999). Depletion interaction of casein micelles and an exocellular polysaccharide. *Physical Review E,* 60**,** 848-856.

Turgeon, S. L., Beaulieu, M., Schmitt, C. and Sanchez, C. (2003). Protein-polyssacharide interactions: phase-ordering kinetics, thermodynamic and structural aspects. *Current Opinion in Colloid and Interface Science,* 8**,** 401-414.

Vaikousi, H., Biliaderis, C. G. and Izydorczyk, M. S. (2004). Solution flow behavior and gelling properties of water-soluble barley (1→3)(1→4)-*β*-glucans varying in molecular size. *Journal of Cereal Science,* 39**,** 119–137.

Vårum, K. M. and Smidsrød, O. (1988). Partial chemical and physical characterisation of (1→3)(1→4)-*β*-D-glucans from oat (*Avena sativa L.)* aleurone. *Carbohydrate Polymers,* 9**,** 103-117.

Vårum, K. M., Smidsrød, O. and Brant, D. A. (1992). Light scattering reveals micelle-like aggregation in the (1→3)(1→4)-*β*-D-glucans from oat aleurone. *Food Hydrocolloids,* 5**,** 497-511.

Volikakis, P., Biliaderis, C. G., Vamvakas, C. and Zerfiridis, G. K. (2004). Effect of a commercial oat *β*-glucan concentrate on the chemical, physicochemical and sensory attributes of a low-fat white brined cheese product. *Food Research International,* 37, 83-94.

Wang, Q., Wood, P. J., Huang, X. and Cui, W. (2003). Preparation and characterization of molecular weight standards of low polydispersity from oat and barley (1→3)(1→4)-*β*-D-glucan. *Food Hydrocolloids,* 17**,** 845-853.

Warrand, J. (2006). Healthy polysaccharides. *Food Technology and Biotechnology,* 44**,** 355–370.

Webster, F.H. (1986). *Oats: Chemistry and Technology.* St. Paul, MN, USA: AACC, 433.

Westerlund, E., Andersson, R. and Aman, P. (1993). Isolation and chemical characterization of water-soluble mixed-linked *β*-glucans and arabinoxylans in oat milling fractions. *Carbohydrate Polymers,* 20**,** 115-123.

Wong, D. W. S., Camirand, W. M., Pavlath, A. E., Parris, N. and Friedman, M. (1996). Structures and functionalities of milk proteins. *Critical Reviews in Food Science and Nutrition,* 36**,** 807-844.

Wood, P., Beer, M. and Butler, G. (2000). Evaluation of role of concentration and molecular weight of oat *β*-glucan in determining effect of viscosity on plasma glucose and insulin following an oral glucose load. *British Journal of Nutrition,* 84**,** 19-23.

Wood, P. J. (2007). Cereal *β*-glucans in diet and health. *Journal of Cereal Science,* 46**,** 230-238.

Wood, P. J., Braaten, J. T., Scott, F. W., Riedel, D. and Poste, L. M. (1990). Comparisons of viscous properties of oat and guar gum and the effects of these and oat bran on glycemic index. *Journal of Agricultural and Food Chemistry,* 38**,** 753-757.

Wood, P. J., Braaten, J. T., Scott, F. W., Riedel, K. D., Wolynetz, M. S. and Collins, M. W. (1994a). Effect of dose and modification of viscous properties of oat gum on plasma glucose and insulin following an oral glucose load. *British Journal of Nutrition,* 72**,** 731–743.

Wood, P. J., Weisz, J. and Blackwell, B. A. (1994b). Structural studies of (1→3)(1→4)-*β*-D-glucans by 13 C-NMR and by rapid analysis of cellulose-like regions using high-performance anion-exchange chromatography of oligosaccharides released by lichenase. *Cereal Chemistry,* 71**,** 301-307.

Wood, P. J., Weisz, J., Fedec, P. and Burrows, V. D. (1989). Large scale preparation and properties of oat fractions enriched in (1→3)(1→4)-*β*-D-glucan. *Cereal Chemistry,* 66**,** 97-103.

Woodward, J. R., Phillips, D. R. and Fincher, G. B. (1988). Water-soluble (1→3,1→4)-*β*-D-glucans from barley (*Hordeum vulgare*) endosperm. IV. Comparison of 40°C and 65°C soluble fractions. *Carbohydrate Polymers,* 8**,** 85-97.

Xu, C., Willför, S. and Holmbom, B. (2008). Rheological properties of mixtures of spruce galactoglucomannans and konjac glucomannan or some other polysaccharides. *BioResources,* 3**,** 713-730.

Xujie, H. and Wei, C. (2008). Optimization of extraction process of crude polysaccharides from wild edible BaChu mushroom by response surface methodology *Carbohydrate Polymers,* 72**,** 67– 74.

Yang, H. S., Feng, G. P., An, H. J. and Li, Y. F. (2006). Microstructure changes of sodium carbonate-soluble pectin of peach by AFM during controlled atmosphere storage. *Food Chemistry,* 94**,** 179-192.

Yongjiang, W., Zhong, C., Jianwei, M., Minger, F. and Xueqian, W. (2009). Optimization of ultrasonic-assisted extraction process of Poria cocos polysaccharides by response surface methodology. *Carbohydrate Polymers,* 77**,** 713–717.

Zhang, G. and Foegeding, E. A. (2003). Heat-induced phase behavior of *β*-lactoglobulin/polysaccharide mixtures. *Food Hydrocolloids,* 17**,** 785-792.

Zimeri, J. E. and Kokini, J. L. (2003). Rheological properties of inulin-waxy maize starch systems. *Carbohydrate Polymers,* 52**,** 67-85.